TOPOGRAPHIC AND CHEMICAL PATTERNING OF CELL-SURFACE INTERFACES TO INFLUENCE CELLULAR FUNCTIONS

A Dissertation
Presented to
The Academic Faculty

by

Joseph L. Charest

In Partial Fulfillment
of the Requirements for the Degree
Doctor of Philosophy in the
Woodruff School of Mechanical Engineering

Georgia Institute of Technology
August, 2007

TOPOGRAPHIC AND CHEMICAL PATTERNING OF CELL-SURFACE INTERFACES TO INFLUENCE CELLULAR FUNCTIONS

Approved by:

Dr. William P. King, Advisor
Woodruff School of Mechanical Engineering
Georgia Institute of Technology

Dr. F. Levent Degertekin
Woodruff School of Mechanical Engineering
Georgia Institute of Technology

Dr. Andrés J. García
Woodruff School of Mechanical Engineering
Georgia Institute of Technology

Dr. Hang Lu
School of Chemical and Biomolecular Engineering
Georgia Institute of Technology

Dr. Todd C. McDevitt
Wallace H. Coulter Department of Biomedical Engineering
Georgia Institute of Technology

Date Approved: May 10, 2007

To those who have challenged, encouraged, and supported me

ACKNOWLEDGEMENTS

I would like to thank all of those who have made my earning my PhD possible. My advisor, Dr. Bill King, took a chance on my project and supported it through to the end. He pushed me to achieve, and allowed me flexibility in my work. My committee members have all contributed significantly. Dr. Andrés García, who welcomed me into his lab, provided me much advice both technical and personal, and served as great example of a researcher and teacher, kept me motivated with encouragement and his famous stories. Dr. Degertekin inspired me with his ideas and creative energy, every discussion with him was enjoyable and productive. Dr. Lu provided advice and well-thought out ideas and encouragement. Dr. McDevitt was a fine example of a sharp researcher, providing precise and accurate comment on my work. Faculty and staff of the Mechanical Engineering graduate office, past and present, have always supported me. Dr. Wepfer, Dr. Whiteman, Cosetta Williams, Trudy Allen, Norma Frank, Glenda Johnson all played a part in making the process work. A special thanks to Theresa Keita, for being a fantastic administrative assistant and keeping me smiling and laughing. The MiRC cleanroom staff maintained a great facility, with Devin Brown providing much help with electron beam lithography. From Emory University, Dr. Kowalczyk and his lab technician Jean Marie Jennings offered me cells, support, and time in their lab and Dr. Pavlath has given her recommendations for myoblast culture.

Many students have helped me along the way as well. My original officemates, Brent Nelson, Harry Rowland, and Tanya Wright, have been colleagues, friends, and family to me, and I treasure the time spent with them. Fabian Goericke has truly impressed me as an engineer, and always lent a hand regardless of how busy he was. Jay

Lee has impressed me with his work ethic and knowledge, and has helped with everything from assembling computers to microfabrication. Marcus Eliason cultured cells with me in the bioengineering lab and creatively documented the embossing equipment. Friendship and assistance has come from many who shared cleanroom time with me: Arnab Choudhoury, Sean Coyer, Logan McLeod, Mark Meacham, Eileen Moss, and Swami Rajaraman. Kristin Michael has been a good friend from the start, and has spent much time discussing bioengineering and life with me as a colleague and roommate. Charlie Gersbach and Jennifer Phillips provided significant assistance and expertise with various cell models, and Nathan Gallant trained me for initial patterning techniques. Lindsay Bryant and Kellie Burns have made much needed last minute orders without fail and kept an impeccable lab. Dave Dumbauld and Tim Petrie have assisted with numerous explanations, discussions, and metallization of hundreds of samples.

Outside of work, many have assisted through friendship and support. My first friends in Atlanta: Robin Guillaud, Reetta Hasanen, Regis Worms, Doug Bakkum, Phillip Jones, and John Slanina have been welcome diversions from my work. Mike Schmittdiel has been a close friend and kindred spirit, and Abigail Wojtowicz a sensational salsa partner. Finally, my family has been a source of consistent support. My brother and sister have encouraged me, yet kept me grounded in reality. My parents have inspired me through their example of diligence and noble ambition, and encouraged me with their unwavering support.

TABLE OF CONTENTS

LIST OF TABLES

LIST OF FIGURES

NOMENCLATURE

AFM	Atomic Force Microscopy
EBL	Electron Beam Lithography
ECM	Extracellular Matrix
FN	Fibronectin
FBS	Fetal Bovine Serum
FIB	Focused Ion Beam
HDT	Hexadecanethiol
IF	Immunofluoresence
LBL	Layer-by-Layer
MIBL	Masked Ion Beam Lithography
NIL	Nanoimprint Lithography
PBS	Phosphate Buffered Saline
PC	Polycarbonate
PDMS	Polydimethylsiloxane
PEG	Polyethylene Glycol
PMMA	Polymethyl Methacrylate
SAM	Self-Assembled Monolayer
SEM	Scanning Electron Microscope
μCP	Micro-Contact Printing

SUMMARY

This dissertation aims to further the understanding of the complex communication that occurs as cells interact with topographical and chemical patterns on a biomaterial interface. The research accomplishes this through two aims – fabricating cell substrate surface topography and chemical patterns independently using non-cleanroom approaches, and analyzing higher order cellular response to surface features. The work will impact biomaterial surface modification and fabrication which will apply to biomedical implanted devices, tissue engineering scaffolds, and biological analysis devices.

The first aim seeks to apply non-traditional topographical and chemical patterning methods in order to create independent topographical and chemical patterns on cell culture substrates. Experiments use the resulting patterned substrates to quantify cellular alignment to surface topography and compare the relative influence of topographical and chemical patterns on cellular response. The combined patterning methods of imprint lithography and micro-contact printing result in a high-throughput technique applicable to a variety of materials and a range of feature sizes from nanoscale through microscale, thereby enabling future analysis of cell response to surface features.

The second aim evaluates the impact of topographical and chemical features on cellular differentiation. Experiments use patterned topography overlaid with a characterized chemical model layer to evaluate the effects of topography on myoblast differentiation and alignment. Chemical patterns that independently control available cell spreading area and modulate cell-cell contact are used to investigate the impact of cell-cell contact on differentiation.

CHAPTER 1

INTRODUCTION

Cells respond to external mechanical and chemical cues from their environment, either via interactions with extracellular matrix (ECM) and other cells in an *in vivo* environment, or with a biomaterial surface via mechanical and chemical features at the cell-biomaterial interface *in vitro*. In addition to providing a structural scaffold for living tissues, the ECM also actively serves as a complex communication channel to regulate cell shape, survival, migration, adhesion, development, and function. Similarly, biomaterial surfaces can influence cellular response via mechanical and chemical features at the cell-biomaterial interface. Many cellular components and biological structures possess length scales ranging from 1 nm -100 μm, so patterning biomaterial surfaces with features on similar length scales provides a path to eliciting specific cellular responses and studying the interactions of living cells and biomaterials.

1.1 Patterning Cell-surface Interfaces

The cell-surface interface is composed of both mechanical and chemical features [1]. The mechanical features of a cell-surface interface can be classified either as roughness or topography [2]. Surface *roughness* refers to 3-D features possessing random size, shape, and periodicity, whereas surface *topography* refers to 3-D patterns of deliberately designed size, shape, periodicity. C*hemical patterns* [3] are additionally defined by their prescribed size, shape, and periodicity as well as their chemical

composition. Figure 1.1 illustrates examples of defined biomaterial surfaces Top-down surface patterning methods, where features are fabricated according to a controlled design, allow nearly arbitrary configuration of mechanical and chemical features to be transferred to biomaterial surfaces. The resulting user-defined model interface allows presentation of controlled and consistent features to cells in order to study their response and corresponding mechanisms of interaction.

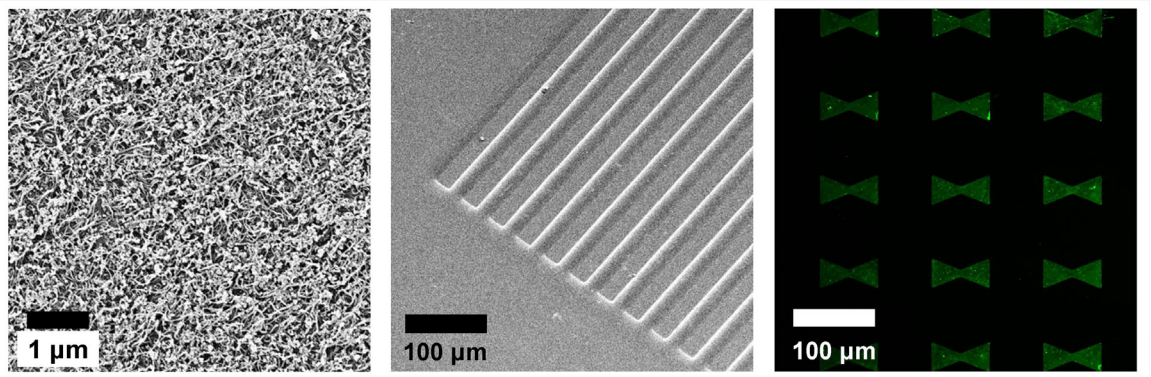

Figure 1.1 Examples of cell surface interface features. Carbon nanotubes on polymer exhibit characteristics of *roughness* (left) while embossed grooves in polymer represent *topography* (center). Fluorescently labeled protein 'bowties' result from a distinct *chemical pattern* of self-assembled monolayers.

1.2 Motivation for Topographical and Chemical Patterning of Cell Substrates

Interrelated mechanical and chemical biomaterial properties influence cell function [4] and impact the performance of biomaterials *in vivo* [5]. Since cell-surface interfaces control biological reactions [6], understanding cellular response to various configurations of surface features is a crucial component of biomaterial design. Patterning cell substrates with well-defined mechanical and chemical features creates model interfaces to characterize cellular interaction and function.

Topographic patterns possess user-defined dimensions more precisely controlled than general surface roughness. Although roughness impacts cellular response [7, 8],

patterning topography on cell substrates gives more precise and consistent surface features. The topographically patterned substrates allow quantitative characterization of cellular functions such as migration [9] and alignment [10] to well-controlled mechanical features. Additionally, topographical fabrication techniques provide consistent surface feature sizes with length scales down to the sub-micron level [11].

Although uniform surface chemistry can alter the activity of adsorbed protein [12] and influence cellular function [13], chemical patterns provide an additional level of cellular influence by regulating cell shape [14] and spreading area [15]. In addition, chemical patterning permits regulation of cell-cell contact of different cell phenotypes [16] and regulation cell adhesion strength [17].

Patterning of both topography and chemistry enables user-defined cell-material interfaces for the study of cellular response to biomaterials. Additionally, fabrication techniques for cell culture substrates with well-defined micro and nanoscale topography and chemical patterns can provide a development platform for the manufacturing of clinically relevant biomaterials in the future.

1.3 Previous Work and Future Direction

A limitation in the investigation of cell-biomaterial interface interactions is a lack of ideal methods to fabricate topography on cell substrates. Micro and nanofabrication techniques borrowed from micro-electromechanical systems (MEMS) pattern well-defined geometries of topography at sub-cellular length scales on cell substrate surfaces [2]. However, these techniques limit material selection and require cleanroom facilities, thereby increasing cost. In addition, current nanoscale topographic patterning requires

electron beam lithography, which severely restricts throughput due to serial patterning. Establishing a cell substrate topography fabrication technique that resolves these issues while maintaining the ability to create well-defined geometries of topographic features will accelerate further investigation into cell-topographic interactions.

Further functionalizing topographically patterned substrates through the addition of chemical patterns adds another level of control over cell-biomaterial interactions. However, previously reported cell substrates have either possessed chemical patterns dependent on the underlying topography [18-20] or independent chemical patterns requiring photolithographic patterning [21]. Chemical patterns independent of underlying topography will permit analysis of the relative influence of topographical and chemical patterning on cell response, while using non-cleanroom methods to fabricate them enhances material selection and reduces cost.

Cells respond significantly to surface features, with potential responses varying from lower-order responses such as changes in alignment and shape, to more complex, higher-order responses such as proliferation and differentiation. Cell alignment to topography is well established [22, 23], but the impact of topographic patterns on cell differentiation is not well characterized. Some evidence indicates altered phenotypic marker expression of cells cultured on topographically patterned substrates [24, 25]. In contrast, certain topographical patterns show no significant effect on cell differentiation [26]. Since surface chemistry has significant effects on cell differentiation [27, 28], and topographical patterning methods do not necessarily preserve uniform surface chemistry, reported effects of topographical patterning on cell behavior may stem from chemical rather than topographical cues. A model substrate with well-defined topography overlaid

with a uniform chemical model layer would potentially decouple the effects of chemistry and topography thereby providing a system for specifically studying the effects of topography on differentiation.

Finally, chemical patterning can provide not only a controlled cell-material interaction, but also a controlled cell-cell interaction [29]. Cell-material interaction impacts differentiation [27], as do chemical patterns controlling available cell spreading area [30]. Chemical patterns that maintain characterized cell-material interaction and restrict spreading area, while controlling cell-cell contact would provide a model to examine the particular effects of cell-cell interaction on differentiation..

1.4 Dissertation Overview

This dissertation furthers the understanding of the response of cells to micro- and nanoscale topographical and chemical patterns of a biomaterial-cell interface through two aims. The first aim applies non-traditional fabrication techniques to create independent topography and chemical patterns on substrates in order to study morphological response to the two pattern types. The second aim characterizes the higher-order response of cellular differentiation to both topography and chemical patterns.

Chapter 2 reviews previous methods of patterning biomaterial interfaces and responses of cells to surface patterns. Patterning methods include techniques resulting in both topographical and chemical surface patterns, and include traditional microfabrication techniques as well as recently developed techniques. Cellular responses include altered morphologies and alignment, as well as higher-order effects such as differentiation. Chapter 3 presents the application of hot-embossing to cell substrate

fabrication, enabling high-throughput fabrication of topography in a wide range of biomaterials. Resulting morphological and alignment response of cells and subcellular structures to the embossed topography are quantified.

Chapters 4 and 5 report the combination of hot-embossing and micro-contact printing to create topographical patterns overlaid with chemical patterns that are independent of the underlying topography. Chapter 4 quantifies cellular alignment to compare the relative influence of the microscale topographical and chemical patterns on cellular response. Chapter 5 reports cellular response to both continuous and discontinuous chemical patterns overlaid onto nanoscale grooves.

Chapter 6 describes the combination of a chemical model layer with an embossed topography. The influence of the topography on cellular alignment and differentiation is quantified for two cell models. Chapter 7 analyzes the ability of chemical surface patterns to control cell-cell contact and reports the influence of the patterns on differentiation.

1.5 References

[1] Jung DR, Kapur R, Adams T, Giuliano KA, Mrksich M, Craighead HG, et al. Topographical and physicochemical modification of material surface to enable patterning of living cells. Critical Reviews in Biotechnology. 2001;21(2):111-54.

[2] Flemming RG, Murphy CJ, Abrams GA, Goodman SL, Nealey PF. Effects of synthetic micro- and nano-structured surfaces on cell behavior. Biomaterials. 1999 Mar;20(6):573-88.

[3] Kane RS, Takayama S, Ostuni E, Ingber DE, Whitesides GM. Patterning proteins and cells using soft lithography. Biomaterials. 1999;20(23-24):2363-76.

[4] Schwartz Z, Boyan BD. Understanding Mechanisms at the Bone-Biomaterial Interface. JCell Biochem. 1994;56:340-7.

[5] Brodbeck W, Patel J, Voskerician G, Christenson E, Shive M, Nakayama Y, et al. Biomaterial adherent macrophage apoptosis is increased by hydrophilic and anionic substrates *in vivo*. Proceedings of the National Academy of Science. 2002;99(16):10287-92.

[6] Castner DG, Ratner BD. Biomedical surface science: Foundations to frontiers. Surface Science. 2002;500(1-3):28-60.

[7] Boyan BD, Sylvia VL, Liu Y, Sagun R, Cochran DL, Lohmann CH, et al. Surface roughness mediates its effects on osteoblasts via protein kinase A and phospholipase A2. Biomaterials. 1999;20(23-24):2305-10.

[8] Baharloo B, Textor M, Brunette DM. Substratum roughness alters the growth, area, and focal adhesions of epithelial cells, and their proximity to titanium surfaces. Journal of Biomedical Materials Research. 2005;74A:12-22.

[9] Clark P, Connolly P, Curtis AS, Dow JA, Wilkinson CD. Topographical control of cell behaviour. I. Simple step cues. Development. 1987 March 1, 1987;99(3):439-48.

[10] Clark P, Connolly P, Curtis ASG, Dow JAT, Wilkinson CDW. Topographical Control of Cell Behavior 2. Multiple Grooved Substrata. Development. 1990 Apr;108(4):635-44.

[11] Clark P, Connolly P, Curtis ASG, Dow JAT, Wilkinson CDW. Cell Guidance by Ultrafine Topography *In Vitro*. Journal of Cell Science. 1991 May;99:73-7.

[12] Keselowsky BG, Collard DM, Garcia AJ. Surface chemistry modulates fibronectin conformation and directs integrin binding and specificity to control cell adhesion. Journal of Biomedical Materials Research Part A. 2003 Aug 1;66A(2):247-59.

[13] Hubbell JA. Bioactive biomaterials. 1999;10(2):123-9.

[14] Gallant ND, Capadona JR, Frazier AB, Collard DM, Garcia AJ. Micropatterned surfaces for analyzing cell adhesion strengthening Langmuir. 2002 2002;18:5579-84.

[15] Chen CS, Mrksich M, Huang S, Whitesides GM, Ingber DE. Micropatterned surfaces for control of cell shape, position, and function. Biotechnology Progress. 1998 May-Jun;14(3):356-63.

[16] Bhatia SN, Yarmush ML, Toner M. Controlling cell interactions by micropatterning in co-cultures: hepatocytes and 3T3 fibroblasts. Journal of Biomedical Materials Research. 1997 1997/02//;34(2):189-99.

[17] Gallant ND, Michael KE, Garcia AJ. Cell Adhesion Strengthening: Contributions of Adhesive Area, Integrin Binding, and Focal Adhesion Assembly. Mol Biol Cell. 2005 September 1, 2005;16(9):4329-40.

[18] Mrksich M, Chen CS, Xia Y, Dike LE, Ingber DE, Whitesides GM. Controlling cell attachment on contoured surfaces with self-assembled monolayers of alkanethiolates on gold. ProcNatlAcadSciUSA. 1996;93(20):10775-8.

[19] Revzin A, Tompkins RG, Toner M. Surface Engineering with Poly(ethlyne glycol) Photolithography to Create High-Density Cell Arrays on Glass. Langmuir. 2003;19:9855-62.

[20] Miller C, Jeftinija S, Mallapragada S. Synergistic effects of physical and chemical guidance cues on neurite alignment and outgrowth on biodegradable polymer substrates. Tissue Engineering. 2002 Jun;8(3):367-78.

[21] Britland S, Morgan H, Wojiak-Stodart B, Riehle M, Curtis A, Wilkinson C. Synergistic and Hierarchical Adhesive and Topographic Guidance of BHK Cells. Experimental Cell Research. 1996;228:313-25.

[22] Curtis A, Wilkinson C. Topographical Control of Cells. Biomaterials. 1997 Dec;18(24):1573-83.

[23] Oakley C, Brunette DM. The Sequence of Alignment of Microtubules, Focal Contacts and Actin-Filaments in Fibroblasts Spreading on Smooth and Grooved Titanium Substrata. Journal of Cell Science. 1993 Sep;106:343-54.

[24] Zinger O, Zhao G, Schwartz Z, Simpson J, Wieland M, Landolt D, et al. Differential regulation of osteoblasts by substrate microstructural features. Biomaterials. 2005;26:1837-47.

[25] Perizzolo D, Lacefield WR, Brunette DM. Interaction between topography and coating in the formation of bone nodules in culture for hydroxyapatite- and titanium-coated micromachined surfaces. Journal of Biomedical Materials Research. 2001 Sep 15;56(4):494-503.

[26] Matsuzaka K, Yoshinari M, Shimono M, Inoue T. Effects of multigrooved surfaces on osteoblast-like cells *in vitro*: Scanning electron microscopic observation and mRNA expression of osteopontin and osteocalcin. Journal of Biomedical Materials Research Part A. 2004;68A(2):227-34.

[27] Keselowsky BG, Collard DM, Garcia AJ. Integrin binding specificity regulates biomaterial surface chemistry effects on cell differentiation. Proceedings of the National Academy of Science. 2005 April 26, 2005;102(17):5953-7.

[28] Lan MA, Gersbach CA, Michael KE, Keselowsky BG, Garcia AJ. Myoblast proliferation and differentiation on fibronectin-coated self assembled monolayers presenting different surface chemistries. Biomaterials. 2005 Aug;26(22):4523-31.

[29] Nelson CM, Pirone DM, Tan JL, Chen CS. Vascular Endothelial-Cadherin Regulates Cytoskeletal Tension, Cell Spreading, and Focal Adhesions by Stimulating RhoA. Mol Biol Cell. 2004 June 1, 2004;15(6):2943-53.

[30] McBeath R, Pirone DM, Nelson CM, Bhadriraju K, Chen CS. Cell Shape, Cytoskeletal Tension, and RhoA Regulate Stem Cell Lineage Commitment. Developmental Cell. 2004;6(4):483-95.

CHAPTER 2

REVIEW OF MICRO AND NANOPATTERNING BIOMATERIAL INTERFACES

Patterning biomaterial surfaces with synthetic topographical and chemical features provides a means of engineering cell-biomaterial interfaces, thereby enabling the study of cellular response to specific external cues. Cleanroom-based fabrication techniques have created precise and consistent topographical and chemical patterns on cell substrates at the micro- and nano-scale, allowing characterization of cellular response to well-defined surface features. Techniques such as imprint lithography and micro-contact printing have advanced substrate fabrication by expanding material selection and increasing throughput. Independent combination of topographical and chemical patterns has provided sophisticated interfaces suitable for comparing the relative influence of and interplay between topographical and chemical patterns. Deliberately patterned topographical and chemical features have influenced cellular responses ranging from morphology and alignment through adhesion and differentiation. Enhanced patterning techniques will continue to lead cell substrate fabrication towards sophisticated, user-defined configurations of topographic and chemical patterns, providing a platform to establish mechanisms of cellular response to cell-material interfaces.

2.1 Introduction

Patterning biomaterial surfaces with synthetic topographical and chemical features provides a means of engineering cell-biomaterial interfaces. A precisely engineered biomaterial interface can provide controlled interaction with biological analytes in biosensors, cues for cellular growth in tissue engineering scaffolds, and largely determines the biological response to implanted devices.

Cells respond to external mechanical and chemical cues either within an *in vivo* environment via interactions with extracellular matrix (ECM) or with a biomaterial surface via mechanical and chemical features at the cell-biomaterial interface. Surface mechanical features can be classified either as *roughness* or *topography*. Surface *roughness* is comprised of 3-D features possessing randomness in size, shape, and periodicity, whereas surface *topography* possesses well-defined 3-D features of deliberately designed size, shape, and organization with a regular periodicity. Surface *chemical patterns* are defined by their chemical composition, as well as their feature size, shape, and periodicity. Various patterning techniques can produce surface topography on cell substrates with a wide variety of feature shapes and sizes [1, 2] and a variety of chemical patterns that influence cellular function [3]. Although roughness, topography, and chemistry all affect cellular response [4, 5], topography and chemical patterns applied to cell substrate surfaces provide user-defined and well-characterized substrates for the investigation of specific cell responses to surfaces.

This chapter reviews both cell substrate surface patterning techniques and cellular responses to substrate surface patterns. The review focuses on top-down patterning methods for cell culture substrates, as they provide methodologies for deliberate and

user-configurable feature geometries in well-controlled models for cellular study. The techniques section discusses traditional cleanroom microfabrication methods, such as photolithography and electron beam lithography, for patterning both topography and chemistry. Additional topographical patterning techniques include molding methods such as injection molding, casting, and imprint lithography. Discussion of non-cleanroom chemical patterning techniques includes various methods with an emphasis on micro-contact printing. Methods of independently patterning chemistry and topography are also discussed.

Additionally this review discusses the response of cells to synthetic surface patterns. For response of cells to topography, the review focuses on 'contact guidance' of cells to surface features and includes effects of topography on higher-order responses such as proliferation and differentiation. For response of cells to chemical patterns, the review discusses restriction of location and shape, and consequent influence on adhesion and cell-cell contact, as well as modulation of apoptosis, proliferation, and differentiation. Evaluation of relative influence of and interplay between topographical and chemical patterns is also discussed.

2.2 Techniques for Surface Patterning Cell Substrates

The evaluation of cellular response to surface patterns requires substrate fabrication techniques that provide feature consistency, high-resolution patterning, and high-throughput production of substrates. Feature consistency leads to substrates inducing repeatable cellular response, enabling robust, and quantitative analysis. High-resolution patterning results in features that appropriately mimic the sub-micron and

nanoscale feature sizes present in cellular components and ECM. High throughput fabrication processes provide sufficient numbers of samples to provide statistically, and potentially clinically, relevant sample sizes for biological assays. Patterning techniques for both topography and chemical patterns fall into two main sub-categories: 1) cleanroom methods based on traditional microfabrication or 2) non-traditional techniques that do not depend on cleanroom methods.

2.2.1 Topographical Patterning Methods

2.2.1.1 Traditional Cleanroom Techniques

Cleanroom techniques provided initial approaches to pattern micro and nano-scale resolution topographies on cell substrates of materials such as silicon and glass with good consistency [1]. Although silicon and glass are not necessarily ideal biomaterials, cleanroom techniques provided a means to attain consistent micron and sub-micron resolution features to demonstrate cellular response to the material interface. Cleanroom manufacturing techniques of cell substrates generally pattern features using masked ion beam lithography, photolithography, or electron beam lithography, then transfer the topography from the resist to the base substrate with an etching step.

Masked Ion Beam Lithography

Although not a common technique, masked ion beam lithography (MIBL) has created topography in non-standard microfabrication materials such as polymethylmethacrylate (PMMA) [6] allowing additional material selection over silicon-based manufacturing techniques. A nickel mesh placed onto the PMMA film served as a mask while an ion beam rastered over the entire sample. Shown in Figure 2.1, the

resulting substrate possessed topography about 400 nm deep, with horizontal dimensions similar to the nickel screen pattern. The consequential implantation of ions into the material resulted in a chemical modification where the ion beam etched the material.

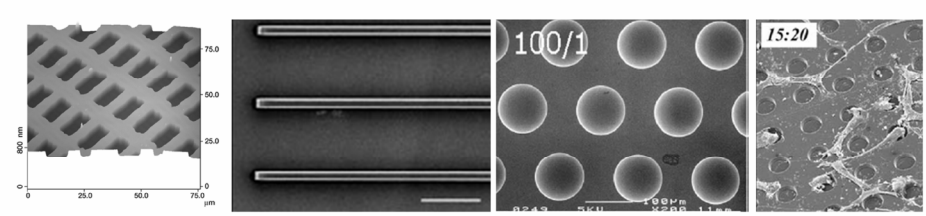

Figure 2.1 Masked cleanroom-based methods of topographic patterns resulted in cell substrates of various materials. Masked ion beam etching of PMMA [6], direct photopatterning of polyimide on glass [7], photolithography and subsequent chemical etching of titanium [8], and photolithography and subsequent reactive ion etching of quartz [9], are various approaches. Images from [6] reprinted with kind permission of Springer Science and Business Media. Images from [7, 9] reprinted from Biomaterials with permission from Elsevier.

Photolithography

Photolithography creates microscale patterns on a substrate by selectively exposing areas of a photo-active polymer resist coating. The exposed material is then removed chemically or thermally to produce the pattern. Typically, the photopatterning is followed by a subsequent etching step to transfer the polymer pattern into the substrate material, resulting in surface topographic features on the substrate.

Photolithography has patterned cell substrates possessing features of square grooves, V-grooves, and pits ranging in size from .5 μm through several hundred μm [1]. Early photopatterned cell substrates possessed microscale grooves ranging from 70 - 165 μm etched into silicon with epithelial cells cultured on the microgrooves aligning to them [10, 11]. Figure 2.1 shows examples where more recent photolithography has directly patterned polyimide channels [7], and patterned circular pits for subsequent chemical etching of titanium [8] and reactive ion etching of quartz [9].

The resolution of photolithography has been extended to create features as small as 130 nm by substituting X-ray radiation for ultraviolet light and exposing the resist through a holographically produced mask [12]. As some cellular features possess length scales below 100 nm, it is critical to explore cellular response to features with nanoscale dimensions, requiring a technique with better resolution than photolithography. Photolithography is also limited by expensive cleanroom facilities and a subsequent etching step thereby slowing throughput and predominantly limiting material selection to silicon, glass, or quartz which are not readily applied to biomaterial applications.

Electron Beam Lithography

EBL is similar to photolithography, but exposes the resist through a finely-focused and precisely controlled beam of electrons. EBL patterning has regularly obtained feature sizes of 10 nm [13]. Figure 2.2 shows early cell culture substrates patterned through EBL which possessed 1, 2 and 4 μm wide grooves [14], and more recent substrates that possessed features ranging from 70 – 4000 nm [15, 16]. The serial processing nature of EBL limits the total patterned area of the substrate as well as the maximum feature size, resulting in low-throughput and substantial cost if patterns covering large areas are required. In addition, EBL is somewhat limited in material selection as it requires materials suitable for subsequent cleanroom etching techniques.

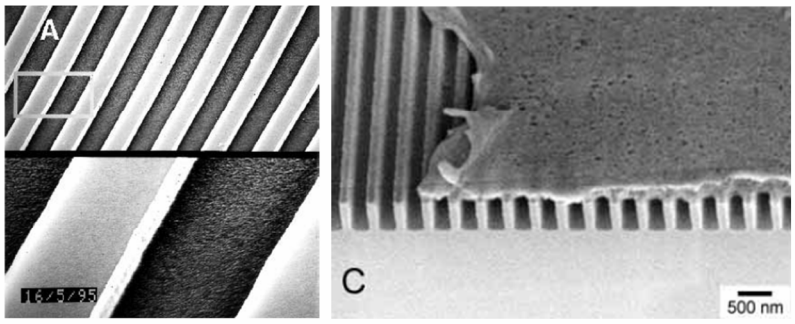

Figure 2.2 Electron beam lithographically patterned topographical substrates consisting of 2 μm wide grooves in quartz [14] and 400 nm pitch grooves in silicon [16]. Reproduced with permission of the Company of Biologists.

2.2.1.2 Molding Techniques

Molding techniques take advantage of the high resolution features created through traditional cleanroom techniques by replicating them in inexpensive polymer-based materials in a low-cost, high-throughput process. Molding techniques such as injection molding require thermoplastic materials, while casting techniques require a material that can be dissolved in a solvent or cured. Polymers provide an advantage in molding techniques as they have exhibited high resolution with the potential to replicate features of sub-nanometer size [17].

Injection Molding

Injection molding forces a polymer in melt form into a rigid mold to create 3-D structures of nearly arbitrary shape. The method has demonstrated the ability to replicate biomimetic features down to 4 nm [18]. A nickel mold, fabricated by electroplating a fibrillar collagen sample, served as tooling for an injection molding machine. Resulting substrates possessed replicas of the 3-4 nm collagen features, with replication fidelity dependent on polymer type and limited by the fidelity of the tooling rather than the injection molding process. Although injection molding shows great potential for mass

production, its complex tooling and machinery carries high cost and inhibits substrate redesign, thereby limiting its application to research.

Casting: Solvent Casting and Cured Polymer Casting

Casting approaches replicate simple 2-D molds using a polymer in solution or a pre-polymer that is later cured. As no significant heat or pressure is used, casting approaches do not require complex machinery, making them conducive to production on an experimental scale for cell culture studies as well as on a mass-production scale.

In solvent casting, polymers are dissolved in a solvent and cast onto a mold prior to solvent evaporation. Solvent cast topographical cell substrates typically are polystyrene since it is a standard cell culture material. Solvent cast polystyrene substrates have possessed features as small as .5 μm wide grooves using a photolithographically patterned mold [19]. Figure 2.3 shows solvent cast polystyrene replicas of an etched silicon mold. The 2 μm wide grooves showed consistent replication of the mold, including nanoscale roughness inherent to the mold [20, 21]. One consequence of the solvent casting process was presence of residual solvent in the substrate after evaporation. Although cell growth was not significantly impacted by the residual solvent [20], solvent residue could potentially have unknown toxic effects.

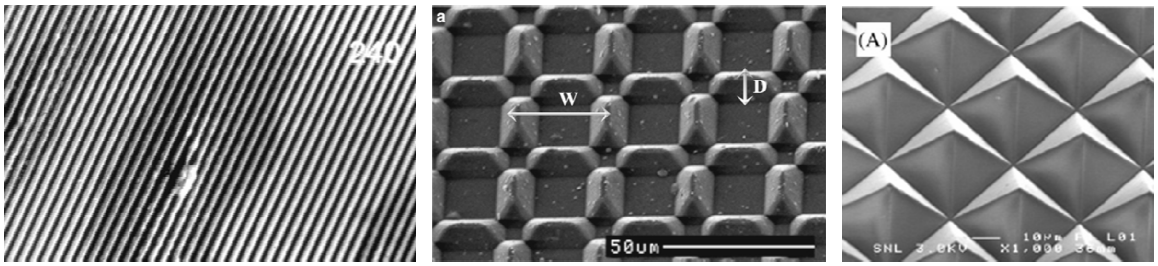

Figure 2.3 Molding techniques replicated molds in a low-cost, high-throughput fashion. Techniques employed various materials such as solvent casting 2 μm wide grooves in polystyrene [21], epoxy casting of 34 μm wide squares with discontinuous edges [22], and casting 33 μm wide pyramids in PDMS [23] Image from [22] reprinted with kind permission of Springer Science and Business Media. Image from [23] reprinted with permission from Elsevier.

In cured polymer casting, a cureable polymer or pre-polymer is loaded onto the mold, cured, and released to create a relief replica of the mold topography. An early example of a cured polymer topographical cell substrate possessed V-grooves cast in epoxy using an etched silicon mold [24]. Recent epoxy cast cell substrates have possessed complex patterns of discontinuous edges [25] as shown in Figure 2.3. Polydimethylsiloxane (PDMS), a cureable inorganic polymer, has been used extensively since its initial use for topographic cell substrates [26], due to its non-toxicity and inertness for most biological studies. In addition, the mechanical modulus of PDMS has been adjusted to investigate aspects of contractility in cells [27] adding further functionality to a cell culture substrate. Topographically patterned features on PDMS cell substrates have included 33 μm wide pyramids [23], as shown in Figure 2.3, and 350 nm wide grooves [28]. Although both solvent casting and cured polymer casting are high-throughput techniques with excellent resolution, they inherently limit material selection to those that can be solvent cast or cured.

2.2.2 Chemical Patterning Methods

Chemical surface patterning results in geometrically confined features composed of biologically interactive chemistries. Chemical patterning may consist of direct patterning of the biologically interactive chemical or indirect patterning of the chemical through a patterned intermediate layer that selectively promotes or suppresses the adhesion of the biologically interactive chemical. Intermediate self-assembled monolayers (SAMs) have promoted or suppressed adsorption of protein and consequent adhesion of cells dependent on user-specified terminal groups of the SAMs [29]. Once the SAM was patterned, immersion of the substrate in the protein or cell solution resulted

in geometric patterns due to the selective adsorption or adhesion. As reviewed here, chemical patterning serves to geometrically control cell attachment to substrates, resulting in influence of cells through spatial control.

2.2.2.1 Traditional Cleanroom Techniques

Photolithography

Chemical patterning through photolithography has produced substrates through both direct and indirect patterning approaches. Photopatterning of a protein has resulted in a substrate capable of a limited-interaction co-culture of cells [30]. Post-photopatterning liftoff resulted in lanes of collagen, surrounded by non-functionalized borosilicate. Cell adhesion was then modulated by seeding without serum, restricting strong cell adhesion to the collagen lanes, then seeding a second cell type with serum to allow adhesion to the non-functionalized areas. In this way, cell types were confined to specific areas thereby controlling heterotypic cell-cell interactions. Indirect photopatterning by liftoff of a polyethylene glycol (PEG) silane SAM from a glass substrate resulted in bare glass adhesive areas surrounded by PEG [31] as shown in Figure 2.4. Since PEG typically suppresses attachment of cells, seeding of cells on the substrate resulted in restriction of cells to the bare glass. Simple patterns have been created through photopatterning and liftoff of metals, with circular patterns of aluminum on a niobium background [32] as illustrated in Figure 2.4.

Beyond patterns that either suppress or promote cell adhesion, photopatterning of a specifically designed photo-active biotin resulted in precise geometric shapes of biotin-presenting SAMs that enabled further specific interaction [33]. After binding of avidin to the biotin layer, further biotin-conjugated antibodies were bound to the avidin layer

resulting in geometric patterns with highly-specific preferential adhesion characteristics. The result, shown in Figure 2.4, was the ability to restrict specific, fluorescently-labeled antibodies to lanes. To further the functionality of chemically patterned substrates, subsequent modification of photopatterned chemistry using layer-by-layer (LBL) assembly and multiple photolithography steps has resulted in multiple patterned chemistries on one substrate [34]. The LBL assembly enabled control of the thickness of the chemical features, as well as tuning of the physical-chemical properties. Although photolithography allows patterning of a variety of specific chemistries, resolution of the method is fundamentally limited.

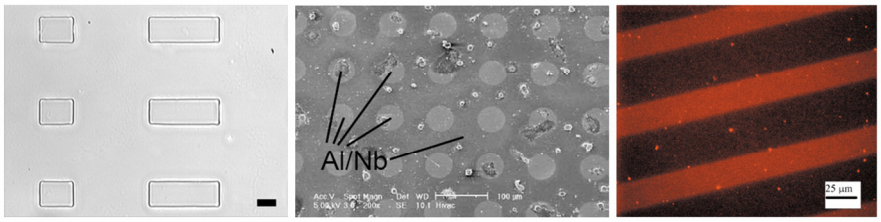

Figure 2.4 Photolithography patterned chemistry through different subsequent steps for different chemistries such as liftoff of PEG SAMs yielding 25 µm wide rectangles of exposed glass [31], liftoff of metal to produce aluminum dots on a niobium background [32], and directly photolinkable biotin to create biospecifically adhesive lanes [33]. Image from [31, 33] reprinted with kind permission of Springer Science and Business Media. Image from [32] reprinted with permission from Elsevier.

Electron Beam Lithography

EBL has patterned resists to control SAM placement or ablated patterns directly into SAMs with reliable feature sizes in the range of 10 nm [13]. EBL has patterned gas-phase deposited SAMs with a minimum line width of 27 nm [35]. Utilizing this SAM patterning method has resulted in collagen patterned in 30-100 nm wide tracks [36] as shown through AFM in Figure 2.5. Direct ablation of patterns into an existing SAM has resulted in patterning of biologically-active molecules with 250 nm linewidths [37]. Recent work has used EBL-ablated patterns with feature sizes as small as 40 nm in a

protein resistant SAM [38]. The ablated patterns allowed selective backfilling of protein-coated spheres resulting in protein patterns of sub-100 nm dimensions, shown through an AFM image in Figure 2.5. Although resolution of EBL chemical patterning is excellent, low-throughput and expense remain as limitations.

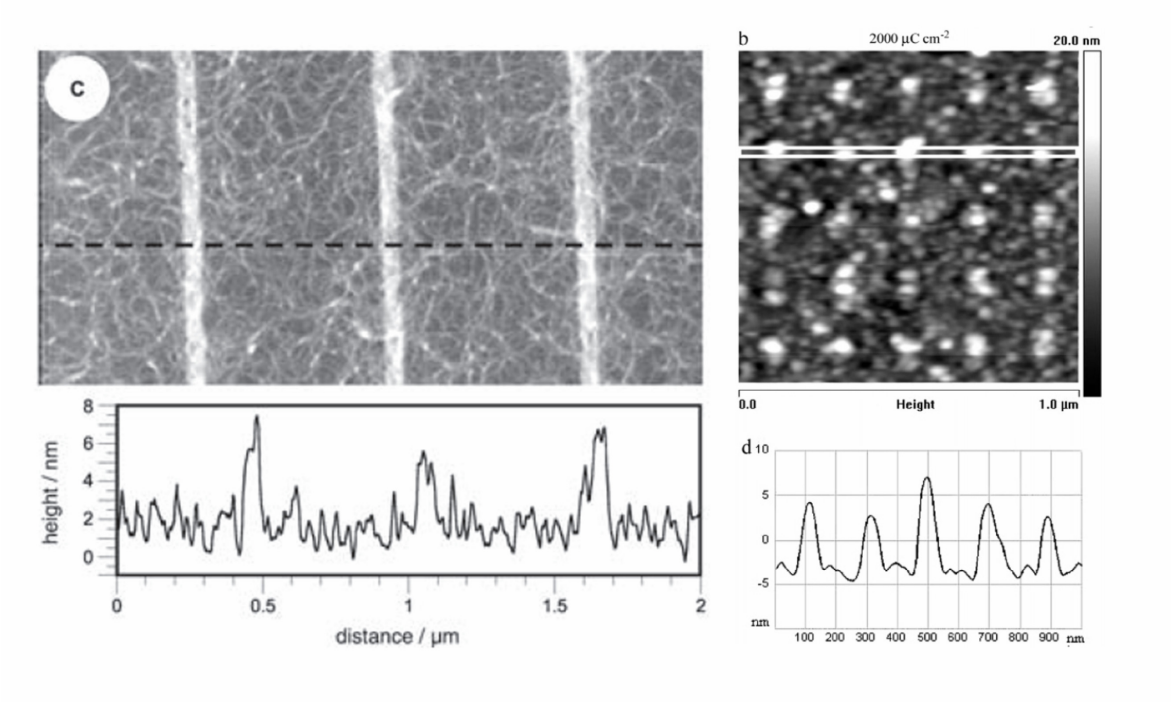

Figure 2.5 EBL produced sub-micron chemical features. Collagen adsorbed to methyl-terminated SAMs patterned through EBL exposed resist [36], and protein-coated spheres adsorbed to areas where PEG SAMs were ablated by EBL [38]. Rightmost images reprinted from [38], copyright 2006 American Chemical Society.

2.2.2.2 Non-traditional Techniques

Chemical patterning through non-cleanroom methods has been accomplished through a wide variety of methods, each with particular advantages and drawbacks. Several techniques have emerged that have specific advantages. Mechanical scraping of collagen has produced 50 µm wide lanes in a very inexpensive and simple manner [39]. Implantation of biologically relevant ions has been demonstrated for microscale patterns [6]. Stencil peeling has selectively removed cells or proteins from a substrate resulting in

defined patterns of microscale dimensions [40]. The stencil, patterned through photolithography and subsequent etching, consisted of a thin layer of parylene adhered to a substrate before cell seeding or protein adsorption. Biologically-active lipid bilayers as small as 1.3 μm have been patterned through stencil peeling [41]. Since the patterning of the stencil occurred before cell seeding, this technique provided a method to pattern live cells directly. Focused ion beams (FIB) have been used to induce localized topographical changes in gallium arsenide substrates that permit selective adsorption of protein into dot formations of approximately 100 nm diameter [42]. Similarly, microscale patterns of cell adhesive areas have been patterned using FIB ion implantation on polyhydroxymethylsiloxane [43]. Both processes required only one patterning step with the potential for nanoscale feature dimensions, however the resulting patterns were substrate material dependent and limited material selection. Dip-pen nanolithography (DPN), has created 100 nm patterns of mercaptohexadecanoic acid (MHA), with surrounding areas passivated by a PEG-terminated monolayer [44]. Specifically, 200 nm patterns of MHA coated in a fibronectin fragment served as patterning for cellular focal adhesions. While DPN produces nanoscale chemical patterns and is relatively substrate independent, the serial nature of the process limits its throughput.

Micro-contact Printing

Micro-contact printing (μCP) represents the most often used method to create chemical patterns for cell substrates. Direct μCP prints an 'ink' of a biologically active compound, such as a protein, onto a substrate through contact transfer of the compound from an elastomeric stamp to the substrate. In a similar fashion, indirect μCP uses a SAM as an ink which is transferred from the stamp for initial chemical functionalization [45],

with subsequent backfilling of a second background SAM creating a distinct difference in adhesive properties between the pattern and background. Protein adsorption or cell adhesion is restricted by the difference in adhesive properties. Cell substrates patterned through μCP exhibited the ability to distinctly restrict cell spreading and consequently control cell shape [46].

Direct μCP of Biologically Active Chemicals

Direct printing of proteins and biological macromolecules results in geometric patterns without the use of underlying SAMs. Directly printed protein patterns have survived long incubation times, as laminin lanes printed on a layer of bovine serum albumin (BSA) on polystyrene tissue culture dishes have remained stable in media or buffer for 4 weeks [47]. The 5-50 μm wide lanes permitted myoblast adhesion while the background BSA suppressed myoblast adhesion. Direct printing functions well for various proteins or biological macromolecule mixtures. For example, direct printing of an ECM-gel containing poly-D-lysine created grids of 4-6 μm wide lanes connecting circular nodes of 12-14 μm in diameter [48]. The printed areas served as adhesive sites for control of neuron placement. Direct printing has been expanded to include μCP of patterns onto biological tissues such as printing of 10 μm wide polyvinyl alcohol (PVA) lanes onto a human lens capsule [49]. Figure 2.6 shows a further enhancement of direct printing which used a flat PDMS stamp patterned with antigens through microwells [50]. The microwells localized delivery of multiple antigens, each to distinct locations on the stamp, enabling the spatially specific binding of antibodies from an antibody solution. The stamp could then print multiple antibodies in one step on a glass substrate.

Resolution of μCP has been improved so that precise control of stamp aspect ratio

and shape has resulted in μCP of features less than 100 nm using antibodies as an ink [51]. Pattern degradation of direct-μCP protein features surrounded by a PEG SAM showed minimal outgrowth of cells from the patterns after a 13 day culture and minimal degradation of patterns after 13 days in serum containing medium [52]. Direct μCP provides a non-cleanroom approach to chemical patterning that is high-throughput, stable for cell culture times, and patterns a variety of chemistries.

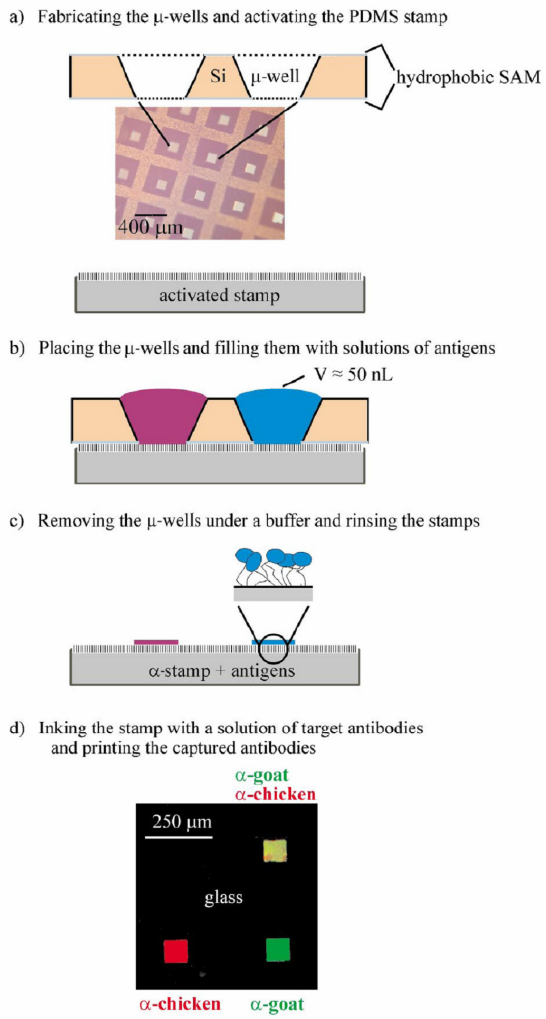

Figure 2.6 Local delivery of antigens enabled μCP of multiple chemistries with one stamping step. After antigen patterning, the stamp was inked from a mixed solution of antibodies, and could then print the antibodies onto a substrate. [50]

Indirect μCP of SAMs

Indirect μCP creates patterned SAMs that in turn selectively suppress or promote protein adsorption or cell adhesion, thereby geometrically restricting cell location, size, and shape. Since SAMs have been characterized for specific protein adsorption and activity [53, 54], indirect μCP can provide a well-controlled chemical model layer in addition to geometrical patterning. Indirect μCP has demonstrated pattern sizes as small as .3 μm squares by printing methyl-terminated SAMs [55]. Printing of an adhesive SAM, followed by backfilling with PEG-terminated SAM, resulted in control of adhesive island sizes. The adhesive island sizes in turn precisely controlled cell spread area to several designated increments in order to quantitatively study effects of cell spreading area on cell function [56]. Precise control of cell size and shape through indirect μCP of adhesive islands has resulted in providing consistency to adhesion studies [57] and modulating adhesion strength through controlling available cell spreading area [58]. Indirect μCP has also produced stable patterns, as μCP MHA surrounded by PEG areas showed good pattern fidelity over an 89 hour cell culture [59]. Like direct μCP, indirect μCP is a non-cleanroom, high-throughput, and stable chemical patterning method with the added feature of a possessing a well-defined underlying chemical model layer.

2.2.3 Combined Topographical and Chemical Patterning

Since cells *in vivo* respond to both topographical and chemical cues simultaneously, patterning both topography and chemistry leads to biomaterial interfaces with the potential to better mimic complex *in vivo* scenarios. In addition, studying the relative influence of and interplay between topographical and chemical cues necessitates the independent combination of both types of patterns. Although some chemical patterns

have displayed shallow topographic features inherent to them [34, 60], and some topographic features have been composed of a functional chemistry [61], deliberate chemical patterning has the potential to add functionality to cell substrates possessing patterned topography. Specifically, chemical functionalization of spaces in between etched microwells has been demonstrated [62], as well as on plateaus between grooves [63]. However, the chemical patterns relied on and were spatially concurrent with the underlying topography, thus rendering the two patterning methods dependent on one another. Independent patterning of chemistry on topography has increased the sophistication of substrate interfaces and enabled new investigations into cellular response. Using photolithography, cell adhesive chemical lanes were patterned on a substrate possessing topographical grooves etched into fused silica [64, 65]. Since the chemical lanes were patterned independently of the topography, they could be user-specified to be oriented parallel or perpendicular to the grooves. The independent nature of the patterns enabled investigation of the relative influence of chemical and topographical patterns on cell response, however it required cleanroom fabrication to do so. Independent patterning of chemistry on topography without cleanroom techniques would permit rapid substrate fabrication and increase material selection.

2.3 Cellular Response to Surface Patterns

2.3.1 Cellular Response to Topography

2.3.1.1 Morphological Response

Alignment, Orientation, Elongation

Cells respond morphologically to topography by alignment to and elongation along topographic features, termed 'contact guidance' [66]. More consistent microfabricated topography has advanced quantification of the extent of morphological changes, including alignment angles of cells and focal adhesions to microscale grooves [67]. Spatial distribution of proteins and other functional cellular components have been altered along with gross morphological changes of the cell. Human bone marrow stromal cells (HBMSCs) have shown not only alignment of the actin cytoskeleton, cell body, and focal adhesions to topography, but also concentration of tubulin protein to grooves [68]. Focal adhesions of osteoblasts have preferentially concentrated on raised topographical features, with consequent localization of focal adhesion kinase to the raised features [22].

Response of Cells to Discontinuities

The response of cells to topography may depend on the presence of surface discontinuities. A single step discontinuity in a cell substrate impeded cell migration across it according to step height, regardless of whether the cell was ascending or descending the step [69]. Gaps in discontinuous topography influenced alignment of fibroblasts in a similar fashion as contact guidance [25]. The alignment, or gap guidance,

occurred for cells located between topographic features necessitating alignment of the cell body to accommodate the presence of the raised topography.

Cytoskeletal Involvement in Alignment to Topography

Examination of the sequence of alignment events has provided some insight into the involvement of cytoskeletal components in cellular alignment to topography. For fibroblasts on microscale grooves, myotubules aligned to the features first, followed by focal adhesions, actin filaments, then the overall cell body [70]. Further study using cytoskeletal inhibiting drugs has shown that cells with disrupted microtubules aligned to grooves wider than 1 μm wide, but did not align to smaller grooves whereas inhibition of actin filaments did not disrupt alignment on any groove sizes [71]. Disruption of actin filaments, microtubules, or both, did not significantly inhibit neurite alignment to grooves of 1, 2 and 4 μm widths [14]. Conversely, cellular alignment due to gap guidance has been inhibited by disruption of cytoskeletal components, as indicated by a reduction in the percentage of aligned cells due to the presence of either actin filament or microtubule inhibiting drugs [25]. Although cytoskeletal components have played some role in alignment of cells to topography, it is unclear exactly how large of an impact they have.

Parameters of Topography That Influence Cell Morphology

Topographical parameters, specifically dimensions of the topographic features, have impacted the extent of cellular alignment and elongation. Typically, depth of grooves has had more effect on cellular alignment than width or pitch of grooves. For example, the fraction of aligned cells to microscale grooves increased more with an increase in depth of 1.7 μm than a change in pitch of 20 μm [72]. Similarly, varying

groove width from 1-10 μm did not significantly impact the extent of cellular alignment [67] whereas for a constant width and pitch, the fraction of aligned cells increased as groove depth increased from 200 nm to 1 μm [73]. Elongation of cells, as measured by ratio of cell major axis to minor axis, also increased with groove depth. Figure 2.7 shows data for epithelial cells which have aligned to grooves as narrow as 330 nm, with the fraction of aligned cells similar for grooves with pitches ranging from 400-2000 nm and a depth of 600 nm [16]. However, when the groove depth was decreased to 150 nm, the fraction of aligned cells remained similar for pitches ranging from 400-4000 nm indicating that sensitivity to depth and pitch may be interrelated. Using a similar substrate with 600 nm deep grooves, keratocytes aligned similarly for groove pitches ranging from 800-4000 nm, with significantly lower alignment levels on 400 nm pitch grooves, indicating the significance of feature dimensions may also depend on cell type [74]. Although cells display varying levels of sensitivity dependent upon topographic feature parameters, cells have responded to some extent on groove widths as small as 100 nm [75]. Cellular alignment or response to groove widths less than 100 nm has yet to be established.

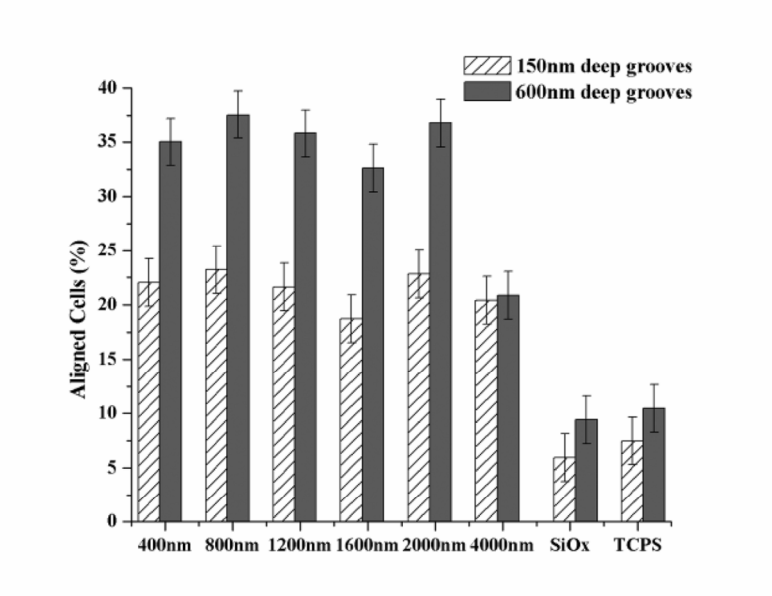

Figure 2.7 Percentage of cells aligned within 10° of grooves. Cell alignment was constant for all pitches on 150 nm deep grooves, while cell alignment was constant only for groove pitches 200-2000 nm for 600 nm deep grooves [16]. Reproduced with permission of the Company of Biologists.

2.3.1.2 Higher-order Cellular Response to Topography

In addition to simple morphological changes, cells have exhibited some potential to modulate higher-order cell function in response to surface feature changes. Surface *roughness* has impacted differentiation in cell models such as bone marrow cells [76] and MG63 osteoblasts [77, 78], indicating that substrate mechanical features can impact higher-order cell function. Cells cultured on well-defined surface *topography* have also exhibited altered levels of bone-markers. Cells produced higher levels of alkaline-phosphatase (ALP) on topographically patterned pyramids than on smooth substrates [23]. Cells cultured on topographically patterned composite materials exhibited higher levels of ALP as compared to cells cultured on smooth composites [79]. However, the topographic patterning may have exposed varying amounts of the composite materials inducing a surface chemistry change concurrent with the topography. Bone markers have not only been altered by the presence of topography but modulated by surface

topographical parameters such as circular pit size and spacing [8] as well as groove depth [80] with effects of topography extending to *in vivo* conditions [81].

Topographical influence of differentiation has not been limited to bone cell models. Neuritogenesis in PC12 neural cells has been modulated by varying substrate groove widths [82]. Neuron markers were upregulated in cells cultured on grooves as compared to cells cultured on smooth substrates, while glial markers were similar on both substrate types [83]. Conversely, several studies have shown a lack of influence of topography on differentiation [84] and proliferation [85] of osteoblasts, indicating topographical influence of higher-order effects may require specific cell-topography interactions. Although some effects have been documented, the overall effect of topography on differentiation remains uncharacterized. In particular, attempts to decouple the differentiation effects of chemistry from topography have been limited, as previous studies have not used a characterized chemistry overlaid on the topography of interest.

2.3.2 Cellular Response to Chemical Patterns

2.3.2.1 Influence of Chemical Patterns on Location and Shape

Chemical patterns have influenced cell function through restriction of cell location and spreading with consequential control of cell shape. Patterns with dimensions similar to cells have controlled the shape of cells to rectangles [46], with precise control of cell shape restricted to teardrop shaped patterns [86] as well as squares, triangles, and other shapes [87]. Patterning adhesive islands of sub-cellular dimension has also influenced cell spreading, location, and shape. Although cells spanned several

adhesive islands of sub-cellular dimension, the preferential adhesion to islands has controlled overall cell location [44], concentration of cell receptors [88] and even cell shape [55]. Cell location has been controlled by providing chemical patterns conducive to cell adhesion such as laminin lanes [89], irradiated areas of polymer with enhanced adhesive properties [43], and multiple chemistries with varying propensities for cell adhesion [34]. Selective removal of cells has also patterned cell location by using lift off techniques [30] and temperature responsive materials [90] to remove cells after seeding. Patterning of hexagonal adhesive islands onto a lens capsule demonstrated control of cell location on non-synthetic substrates of human tissue [91].

2.3.2.2 Influence of Chemical Patterns on Cell Extension, Adhesion, and Cell-cell contact

Chemical patterning has influenced the extension of various cellular processes. Cells on square-shaped adhesive islands, observed through time-lapse techniques, preferentially extended filopodia, lamellopodia, and microspikes at corners of square adhesive islands [92]. Cytoskeletons and focal adhesions were oriented such that traction forces would be concentrated at the corners, with concentrations of fibronectin secreted at the corners [87]. Preferential cellular extension location and orientation of stress fibers may lead to directional migration of cells. Cells cultured on a teardrop shape exhibited preferential extension of lamellopodia at the blunt end, with actin filaments predominantly parallel to the long axis of the tear drop. When released from the pattern, the cell migrated in the direction of the blunt end along the long axis of the tear drop.

Chemical patterning has played a significant role in cell adhesion. Control of cell shape through the μCP of circular adhesive islands resulted in accurate quantification of

cell adhesive strength by a spinning disk assay [57]. Both cellular adhesive shear strength and quantity of bound integrin α5 subunit increased with adhesive island size [58].

Chemical patterns have served to regulate cell-cell contact. Regulation of heterotypic cell-cell contact has been accomplished through patterning adhesive areas and plating hepatocytes, then rinsing non-adherent hepatocytes and plating fibroblasts [30]. The resulting co-culture possessed lanes of hepatocytes surrounded by spaces of fibroblasts, enabling limitation of the amount of contact between the two phenotype populations through modulation of lane width. The amount of cell-cell contact has also been regulated on an individual scale through chemical patterning. Non-adhesive agarose gel patterned on glass limited cell location to 'bowtie' shaped areas of bare glass, with either one cell on each half of a bowtie, or a single cell occupying one side of the bowtie [93]. The bowtie patterns provided a controlled cell spreading area and level of cell-cell contact between the two cells. Figure 2.8 shows images and quantitative data that indicate more focal adhesions were observed on cells with cell-cell contact, as compared to single cells, with the effect abrogated by blocking VE-cadherin. Cell-cell contact in neurons has been achieved through μCP of ECM in a neural network formation [94]. Neurons preferentially adhered at patterned nodes, with axons and dendrites extended along patterned lanes, allowing connection of cells at adjacent nodes. The result was a prescribed network of interconnected neurons, controlled through the chemical patterns.

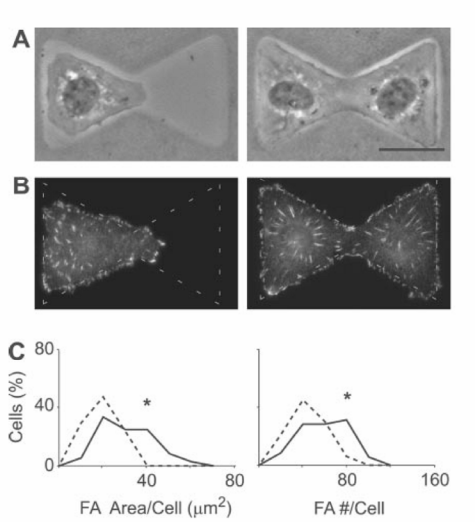

Figure 2.8 Endothelial cells restricted to bowtie-shaped glass areas surrounded by agarose gel. Single and pairs of cells shown through phase-contrast (A), and vinculin staining (B). Overall focal adhesion area and focal adhesions per cell were significantly higher for paired cells than single cells (C). [93] Reprinted from Developmental Cell, 6, McBeath R, Pirone DM, Nelson CM, Bhadriraju K, Chen CS, Cell Shape, Cytoskeletal Tension, and RhoA Regulate Stem Cell Lineage Commitment, 483-495, Copyright (2004), with permission from Elsevier.

2.3.2.3 Chemical Pattern Influence of Apoptosis, Proliferation, Differentiation

Effects of chemical patterns on apoptosis, proliferation, and differentiation have largely been due to restriction of cell spreading area. Epithelial cells cultured on adhesive islands ranging in size from 25-1600 μm^2 exhibited more apoptotic markers on smaller islands and higher DNA synthesis on larger islands [95, 96]. Bone cells cultured on cell adhesive islands with areas varying from 75-10000 μm^2 synthesized DNA in proportion to projected cell area [97]. In addition, nuclear shape index varied with available cell spreading area, and collagen synthesis was highest for intermediate nuclear shape index. Restriction of cells to lanes has resulted in modulation from proliferative or apoptotic states to differentiative states. Epithelial cells restricted to lanes of 30 μm width aligned, spread and proliferated while cells restricted to lanes of 10 μm width down-regulated proliferation and expressed a differentiated epithelial morphology of tube-like structures. Cardiac myoblasts cultured on chemically patterned lanes have also

exhibited differentiation. As compared to unpatterned areas, cardiac myocytes on laminin lanes developed morphology similar to native heart tissue and began beating, with beating frequency synchronization dependent on lane spacing [47].

Precise control of spread cell area has resulted in modulation between different phenotype fates. A larger percentage of human mesenchymal stem cells cultured on adhesive islands underwent adipogenesis on small islands of 1024 μm^2 and osteogenesis on large islands of 10000 μm^2 [98]. Cells exhibited progression towards both lineages on intermediate islands of 2025 μm^2. Figure 2.9 provides data illustrating the effect of pattern size on cell lineage. Chemical pattern size and shape clearly influenced multiple cell functions, specifically differentiation. Precisely controlling cell-cell contact through chemical patterns may also have effects on differentiation, although this aspect has not been characterized.

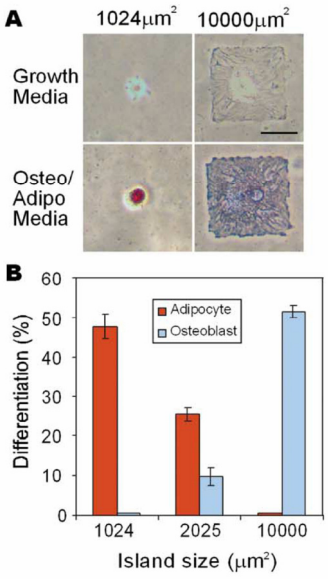

Figure 2.9 Human mesenchymal stem cells exhibited lineage commitment dependent on adhesive island size. Brightfield images of cells on islands with lipids stained red and alkaline phosphatase stained blue (A). Percentage differentiation of cells according to island size (B). [98]

2.3.3 Cellular Response to Combined Chemistry and Topography

2.3.3.1 Chemical Patterning to Restrict Cells to Topographic Features

Combining chemical and topographical patterns in some cases has biased cell location to user-specified topographic features. For example, patterning ridges with a cell adhesive domain resulted in restriction of cells to ridges, while patterning the ridges with an adhesion suppressing domain resulted in cells restricted to grooves [63]. In a similar fashion, patterning the plateau area in between microwells with a cell adhesion resistant SAM encouraged cell localization to the microwells [61, 62]. Appropriate sizing of microwells resulted in restriction of single cells to the microwells. Chemical patterning concurrent with the topography provided selective cell adhesion to specific topographic features.

2.3.3.2 Chemical Patterning to Investigate Relative Influence of Patterns

Both chemical and topographical patterns have exhibited the ability to influence alignment of cells, however the relative influence of the two pattern types is not well understood. Independently patterning chemistry and topography has allowed investigation into the competitive and possibly synergistic effects of combined patterns. Photolithographic patterning of grooves in fused silica and adhesive lanes enabled independent placement of chemical lanes either parallel or orthogonal to the grooves. With lanes patterned parallel to grooves, fibroblast alignment increased beyond levels experienced with either type of pattern alone [64]. For lanes placed orthogonally the grooves of matched pitch, a larger fraction of fibroblasts aligned to the lanes rather than the grooves for all groove depths and widths. Neurite alignment of dorsal root ganglia behave similarly, with enhanced alignment for lanes and grooves parallel [65]. However,

for lanes orthogonal to grooves, lanes dominated neurite alignment except for grooves with depths greater than or equal to 1 μm. Using a cleanroom approach produced substrates with independent chemical and topographical patterns, which enabled examination of relative pattern influence and interplay between the two pattern types.

As both topography and chemical patterns have significant influence on cells, independent control of both patterns results in substrates applicable to further investigations of the complex cell-material interface. Patterning substrates through non-traditional fabrication methods would allow independent control of topography and chemistry, while providing opportunities for high-throughput fabrication and substrate material selection.

2.4 Summary and Conclusions

Micro and nanopatterned substrates have enabled quantitative analysis of the response of cells to well-defined biomaterial interfaces, furthering understanding of the complex communication between cell and material. Cleanroom microfabrication tools advanced the field to create patterns reliably with feature sizes on sub-cellular length scales. Non-cleanroom techniques, such as casting and micro-contact printing, have emerged to meet demands for processes with the ability to fabricate numerous samples in a high-throughput fashion for robust biological assays. Current non-cleanroom methods show potential to achieve substrate surface features deep into the nanoscale. Application of additional non-cleanroom methods to cell substrate fabrication will enhance cell-material interface research by enabling feature sizes in the nanoscale regime, widening material selection, and providing large sample sizes without costly equipment. In

addition, future work combining non-cleanroom chemical and topographical patterning methods to create independent chemical and topographical patterns can further the specificity and sophistication of cell-material interfaces while improving ease of fabrication.

Morphological response of cells to material surfaces has been characterized for various parameters of surface topography and chemical patterns. However, the mechanism for morphological response, in particular contact guidance, remains largely unknown. Although cytoskeletal involvement has been implicated for some cases, involvement of specific biological molecules has not been established. While higher-order cellular response to chemical patterns has been characterized for some cases, topographic influence on proliferation and differentiation remains predominantly uncharacterized with much potential for future investigation. Although basic guidelines have been established through the use of independent chemical and topographical patterning, the relative influence of and complex interplay between topographic and chemical patterns remain as areas for further exploration. Enhanced patterning techniques will continue to lead cell substrate fabrication towards sophisticated, user-defined configurations of topographic and chemical patterns, providing a platform to establish mechanisms of cellular response to cell-material interfaces.

2.5 References

[1] Flemming RG, Murphy CJ, Abrams GA, Goodman SL, Nealey PF. Effects of synthetic micro- and nano-structured surfaces on cell behavior. Biomaterials. 1999 Mar;20(6):573-88.

[2] Curtis A, Wilkinson C. Topographical control of cells. Biomaterials. 1997 Dec;18(24):1573-83.

[3] Falconnet D, Csucs G, Grandin HM, Textor M. Surface engineering approaches to micropattern surfaces for cell-based assays. Biomaterials. 2006 Jun;27(16):3044-63.

[4] Schwartz Z, Boyan BD. Understanding Mechanisms at the Bone-Biomaterial Interface. JCell Biochem. 1994;56:340-7.

[5] Allen LT, Fox EJP, Blute I, Kelly ZD, Rochev Y, Keenan AK, et al. Interaction of soft condensed materials with living cells: Phenotype/transcriptome correlations for the hydrophobic effect. PNAS. 2003 May 27, 2003;100(11):6331-6.

[6] He W, Gonsalves KE, Batina N, Poker DB, Alexander E, Hudson M. Micro/nanomachining of polymer surface for promoting Osteoblast cell adhesion. Biomedical Microdevices. 2003 Jun;5(2):101-8.

[7] Mahoney MJ, Chen RR, Tan J, Saltzman WM. The influence of microchannels on neurite growth and architecture. Biomaterials. 2005;26:771-8.

[8] Zinger O, Zhao G, Schwartz Z, Simpson J, Wieland M, Landolt D, et al. Differential regulation of osteoblasts by substrate microstructural features. Biomaterials. 2005;26:1837-47.

[9] Berry CC, Campbell G, Spadiccino A, Robertson M, Curtis ASG. The influence of microscale topography on fibroblast attachment and motility. Biomaterials. 2004;25:5781-8.

[10] Brunette DM, Kenner GS, Gould TRL. Grooved Titanium Surfaces Orient Growth and Migration of Cells from Human Gingival Explants. Journal of Dental Research. 1983;62(10):1045-8.

[11] Brunette DM. Fibroblasts on Micromachined Substrata Orient Hierarchically to Grooves of Different Dimensions. Experimental Cell Research. 1986 May;164(1):11-26.

[12] Clark P, Connolly P, Curtis ASG, Dow JAT, Wilkinson CDW. Cell Guidance by Ultrafine Topography Invitro. Journal of Cell Science. 1991 May;99:73-7.

[13] Broers AN, Hoole ACF, Ryan JM. Electron beam lithography - Resolution limits. Microelectronic Engineering. 1996;32(1-4):131.

[14] Rajnicek AM, Britland S, McCaig CD. Contact guidance of CNS neurites on grooved quartz: influence of groove dimensions, neuronal age and cell type. Journal Of Cell Science. 1997 Dec;110:2905-13.

[15] Diehl KA, Foley JD, Nealey PF, Murphy CJ. Nanoscale topography modulates corneal epithelial cell migration. Journal of Biomedical Materials Research A. 2005 December 1, 2005;75(3):603-11.

[16] Teixeira AI, Abrams GA, Bertics PJ, Murphy CJ, Nealey PF. Epithelial contact guidance on well-defined micro- and nanostructured substrates. Journal of Cell Science. 2003 May 15;116(10):1881-92.

[17] Xu Q, Mayers BT, Lahav M, Vezenov DV, Whitesides GM. Approaching Zero: Using Fractured Crystals in Metrology for Replica Molding. J Am Chem Soc. 2005 January 26, 2005;127(3):854-5.

[18] Gadegaard N, Mosler S, Larsen NB. Biomimetic Polymer Nanostructures by Injection Molding. Macromolecular and Materials Engineering. 2005;288:76-83.

[19] Chesmel KD, Black J. Cellular-Responses To Chemical And Morphologic Aspects Of Biomaterial Surfaces .1. A Novel In-Vitro Model System. Journal Of Biomedical Materials Research. 1995 Sep;29(9):1089-99.

[20] Walboomers XF, Croes HJE, Ginsel LA, Jansen JA. Growth behavior of fibroblasts on microgrooved polystyrene. Biomaterials. 1998 Oct;19(20):1861-8.

[21] Walboomers XF, Ginsel LA, Jansen JA. Early spreading events of fibroblasts on microgrooved substrates. Journal of Biomedical Materials Research. 2000 Sep 5;51(3):529-34.

[22] Hamilton D, Wong K, Brunette D. Microfabricated Discontinuous-Edge Surface Topographies Influence Osteoblast Adhesion, Migration, Cytoskeletal Organization, and Proliferation and Enhance Matrix and Mineral Deposition In Vitro. CalcifTissue Int. 2006;78(5):314.

[23] Liao H, Andersson A-S, Sutherland D, Petronis S, Kasemo B, Thomsen P. Response of rat osteoblast-like cells to microstructured model surfaces in vitro. Biomaterials. 2003;24(4):649.

[24] Brunette DM. Spreading and Orientation of Epithelial-Cells on Grooved Substrata. Experimental Cell Research. 1986 Nov;167(1):203-17.

[25] Hamilton DW, Brunette DM. "Gap guidance" of fibroblasts and epithelial cells by discontinuous edged surfaces. Experimental Cell Research. 2005;309(2):429-37.

[26] Schmidt JA, von Recum AF. Texturing of polymer surfaces at the cellular level. Biomaterials. 1991;12(4):385.

[27] Chrzanowska-Wodnicka M, Burridge K. Rho-stimulated contractility drives the formation of stress fibers and focal adhesions. 1996 1996/06//;133(6):1403-15.

[28] Yim KF, Reano RM, Pang SW, Yee AF, Chen CS, Leong KW. Nanopattern-induced changes in morphology and motility of smooth muscle cells. Biomaterials. 2005;26:5405-13.

[29] Prime KL, Whitesides GM. Self-assembled organic monolayers: model systems for studying adsorption of proteins at surfaces. Science. 1991 1991/05/24/;252(5010):1164-7.

[30] Bhatia SN, Yarmush ML, Toner M. Controlling cell interactions by micropatterning in co-cultures: hepatocytes and 3T3 fibroblasts. Journal of Biomedical Materials Research. 1997 1997/02//;34(2):189-99.

[31] Irimia D, Karlsson JOM. Development of a cell patterning technique using poly(ethylene glycol) disilane. Biomedical Microdevices. 2003 Sep;5(3):185-94.

[32] Scotchford CA, Ball M, Winkelmann M, Voros J, Csucs C, Brunette DM, et al. Chemically patterned, metal-oxide-based surfaces produced by photolithographic techniques for studying protein- and cell-interactions. II: Protein adsorption and early cell interactions. Biomaterials. 2003 Mar;24(7):1147-58.

[33] Orth RN, Clark TG, Craighead HG. Avidin-Biotin Micropatterning Methods for Biosensor Applications. Biomedical Microdevices. 2003;5(1):29-34.

[34] Mohammed JS, DeCoster MA, McShane MJ. Fabrication of interdigitated micropatterns of self-assembled polymer nanofilms containing cell-adhesive materials. Langmuir. 2006 Mar 14;22(6):2738-46.

[35] Pallandre A, Glinel K, Jonas AM, Nysten B. Binary nanopatterned surfaces prepared from silane monolayers. Nano Letters. 2004 Feb;4(2):365-71.

[36] Denis FA, Pallandre A, Nysten B, Jonas AM, Dupont-Gillain CC. Alignment and assembly of adsorbed collagen molecules induced by anisotropic chemical nanopatterns. Small. 2005 Sep;1(10):984-91.

[37] Harnett CK, Satyalakshmi KM, Craighead HG. Bioactive templates fabricated by low-energy electron beam lithography of self-assembled monolayers. Langmuir. 2001 Jan 9;17(1):178-82.

[38] Rundqvist J, Hoh JH, Haviland DB. Directed immobilization of protein-coated nanospheres to nanometer-scale patterns fabricated by electron beam lithography of poly(ethylene glycol) self-assembled monolayers. Langmuir. 2006 May 23;22(11):5100-7.

[39] Ra HJ, Picart C, Feng HS, Sweeney HL, Discher DE. Muscle cell peeling from micropatterned collagen: direct probing of focal and molecular properties of matrix adhesion. Journal of Cell Science. 1999 May;112(10):1425-36.

[40] Ilic B, Craighead H. Topographical patterning of chemically sensitive biological materials using a polymer-based dry lift off. Biomedical Microdevices. 2000;2(4):317-22.

[41] Orth RN, Kameoka J, Zipfel WR, Ilic B, Webb WW, Clark TG, et al. Creating biological membranes on the micron scale: Forming patterned lipid bilayers using a polymer lift-off technique. Biophysical Journal. 2003 Nov 1;85(5):3066-73.

[42] Bergman AA, Buijs J, Herbig J, Mathes DT, Demarest JJ, Wilson CD, et al. Nanometer-Scale Arrangement of Human Serum Albumin by Adsorption on Defect Arrays Created with a Finely Focused Ion Beam. Langmuir. 1998;14:6785-8.

[43] Satriano C, Carnazza S, Licciardello A, Guglielmino S, Marletta G. Cell adhesion and spreading on polymer surfaces micropatterned by ion beams. Journal of Vacuum Science & Technology A. 2003;21(4):1145-51.

[44] Lee K-B, Park S-J, Mirkin CA, Smith JC, Mrksich M. Protein Nanoarrays Generated By Dip-Pen Nanolithography. Science. 2002;295:1702.

[45] Kumar A, Whitesides GM. Features of gold having micrometer to centimeter dimensions can be formed through a combination of stamping with an elastomeric stamp and an alkanethiol "ink" followed by chemical etching. Applied Physics Letters. 1993;63(14):2002-4.

[46] Singhvi R, Kumar A, Lopez GP, Stephanopoulos GN, Wang DIC, Whitesides GM, et al. Engineering Cell-Shape and Function. Science. 1994 Apr 29;264(5159):696-8.

[47] McDevitt TC, Angello JC, Whitney ML, Reineck H, Hauschka SD, Murry PS, et al. *In vitro* generation of differentiated cardiac myofibers on micropatterned laminin surfaces. Journal of Biomedical Materials Research. 2002;60(3):472-9.

[48] Vogt AK, Stefani FD, Best A, Nelles G, Yasuda A, Knoll W, et al. Impact of micropatterned surfaces on neuronal polarity. Journal of Neuroscience Methods. 2004 Apr 30;134(2):191-8.

[49] Lee CJ, Huie P, Leng T, Peterman MC, Marmor MF, Blumenkranz MS, et al. Microcontact printing on human tissue for retinal cell transplantation. Archives of Ophthalmology. 2002 Dec;120(12):1714-8.

[50] Renault J, Bernard A, Juncker D, Michel B, Bosshard H, Delamarche E. Fabricating Microarrays of Functional Proteins Using Affinity Contact Printing. Angewandte Chemie International Edition. 2002;41(13):2320-3.

[51] Renault J, Bernard A, Bietsch A, Michel B, Bosshard H, Kreiter M, et al. Fabricating Arrays of Single Protein Molecules on Glass Using Microcontact Printing. Journal of Physical Chemistry. 2003;B23(107):703-11.

[52] Lussi JW, Falconnet D, Hubbell JA, Textor M, Csucs G. Pattern stability under cell culture conditions--A comparative study of patterning methods based on PLL-g-PEG background passivation. Biomaterials. 2006;27(12):2534.

[53] Keselowsky BG, Collard DM, Garcia AJ. Surface chemistry modulates fibronectin conformation and directs integrin binding and specificity to control cell adhesion. Journal Of Biomedical Materials Research Part A. 2003 Aug 1;66A(2):247-59.

[54] Keselowsky BG, Collard DM, Garcia AJ. Integrin binding specificity regulates biomaterial surface chemistry effects on cell differentiation. PNAS. 2005 April 26, 2005;102(17):5953-7.

[55] Lehnert D, Wehrle-Haller B, David C, Weiland U, Ballestrem C, Imhof BA, et al. Cell behaviour on micropatterned substrata: limits of extracellular matrix geometry for spreading and adhesion. 2004 2004/01/01/;117(Pt 1):41-52.

[56] Chen CS, Mrksich M, Huang S, Whitesides GM, Ingber DE. Micropatterned surfaces for control of cell shape, position, and function. Biotechnology Progress. 1998 May-Jun;14(3):356-63.

[57] Gallant ND, Capadona JR, Frazier AB, Collard DM, Garc¡a AJ. Micropatterned surfaces for analyzing cell adhesion strengthening Langmuir. 2002 2002///;18:5579-84.

[58] Gallant ND, Michael KE, Garcia AJ. Cell Adhesion Strengthening: Contributions of Adhesive Area, Integrin Binding, and Focal Adhesion Assembly. Mol Biol Cell. 2005 September 1, 2005;16(9):4329-40.

[59] Endler EE, Nealey PF, Yin J. Fidelity of micropatterned cell cultures. Journal Of Biomedical Materials Research Part A. 2005 Jul 1;74A(1):92-103.

[60] Thissen H, Johnson G, Hartley PG, Kingshott P, Griesser HJ. Two-dimensional patterning of thin coatings for the control of tissue outgrowth. Biomaterials. 2006;27(1):35.

[61] Revzin A, Tompkins RG, Toner M. Surface Engineering with Poly(ethlyne glycol) Photolithography to Create High-Density Cell Arrays on Glass. Langmuir. 2003;19:9855-62.

[62] Dusseiller MR, Schlaepfer D, Koch MK, Kroschewski R, Textor M. An inverted microcontact printing method on topographically structured polystyrene chips for arrayed micro-3-D culturing of single cells. Biomaterials. 2005;26:5917-25.

[63] Mrksich M, Chen CS, Xia Y, Dike LE, Ingber DE, Whitesides GM. Controlling cell attachment on contoured surfaces with self-assembled monolayers of alkanethiolates on gold. ProcNatlAcadSciUSA. 1996;93(20):10775-8.

[64] Britland S, Morgan H, Wojiak-Stodart B, Riehle M, Curtis A, Wilkinson C. Synergistic and Hierarchical Adhesive and Topographic Guidance of BHK Cells. Experimental Cell Research. 1996;228:313-25.

[65] Britland S, Perridge C, Denyer M, Morgan H, Curtis A, Wilkinson C. Morphogenetic guidance cues can interact synergistically and hierarchically in steering nerve cell growth. Experimental Biology Online. 1996;1(2).

[66] Weiss P. Experinments on cell and Axon Orientation in Vitro. Journal of Experimental Zoology. 1945;100(3):353-86.

[67] Walboomers XF, Croes HJE, Ginsel LA, Jansen JA. Growth behavior of fibroblasts on microgrooved polystyrene. Biomaterials. 1998;19(20):1861.

[68] Dalby MJ, McCloy D, Robertson M, Wilkinson CDW, Oreffo ROC. Osteoprogenitor response to defined topographies with nanoscale depths. Biomaterials. 2006;27(8):1306.

[69] Clark P, Connolly P, Curtis AS, Dow JA, Wilkinson CD. Topographical control of cell behaviour. I. Simple step cues. Development. 1987 March 1, 1987;99(3):439-48.

[70] Oakley C, Brunette DM. The Sequence of Alignment of Microtubules, Focal Contacts and Actin-Filaments in Fibroblasts Spreading on Smooth and Grooved Titanium Substrata. Journal of Cell Science. 1993 Sep;106:343-54.

[71] Oakley C, Jaeger NAF, Brunette DM. Sensitivity of fibroblasts and their cytoskeletons to substratum topographies: Topographic guidance and topographic compensation by micromachined grooves of different dimensions. Experimental Cell Research. 1997 Aug 1;234(2):413-24.

[72] Clark P, Connolly P, Curtis ASG, Dow JAT, Wilkinson CDW. Topographical Control of Cell Behavior .2. Multiple Grooved Substrata. Development. 1990 Apr;108(4):635-44.

[73] Uttayarat P, Toworfe GK, Dietrich F, Lelkes PI, Composto RJ. Topographic guidance of endothelial cells on silicone surfaces with micro- to nanogrooves: Orientation of actin filaments and focal adhesions. Journal of Biomedical Materials Research Part A. 2005;75A(3):668-80.

[74] Teixeira AI, Nealey PF, Murphy CJ. Responses of human keratocytes to micro- and nanostructured substrates. Journal of Biomedical Materials Research. 2004 6 October 2004;71A:369-76.

[75] Hu W, Yim EKF, Reano RM, Leong KW, Pang SW. Effects of nanoimprinted patterns in tissue-culture polystyrene on cell behavior. 2005: AVS; 2005. p. 2984.

[76] Rosa AL, Beloti MM, van Noort R. Osteoblastic differentiation of cultured rat bone marrow cells on hydroxyapatite with different surface topography. Dental Materials. 2003;19(8):768.

[77] Lee SJ, Choi JS, Park KS, Khang G, Lee YM, Lee HBHB. Response of MG63 osteoblast-like cells onto polycarbonate membrane surfaces with different micropore sizes. Biomaterials. 2004;25(19):4699.

[78] Lossdorfer S, Schwartz Z, Wang L, Lohmann CH, turner JD, Wieland M, et al. Microrough implant surface topographies increase osteogenesis by reducing osteoclast formation and activity. Journal of Biomedical Materials Research. 2004;70A:361-9.

[79] Rea SM, Brooks RA, Best SM, Kokubo T, Bonfield W. Proliferation and differentiation of osteoblast-like cells on apatite-wollastonite/polyethylene composites. Biomaterials. 2004;25:4503-12.

[80] Perizzolo D, Lacefield WR, Brunette DM. Interaction between topography and coating in the formation of bone nodules in culture for hydroxyapatite- and titanium-coated micromachined surfaces. Journal of Biomedical Materials Research. 2001 Sep 15;56(4):494-503.

[81] Chehroudi B, McDonnell D, Brunette DM. The effects of micromachined surfaces on formation of bonelike tissue on subcutaneous implants as assessed by radiography and computer image processing. Journal of Biomedical Materials Research. 1997 Mar 5;34(3):279-90.

[82] Foley JD, Grunwald EW, Nealey PF, Murphy CJ. Cooperative modulation of neuritogenesis by PC12 cells by topography and nerve growth factor. Biomaterials. 2005;26(17):3639.

[83] Recknor JB, Sakaguchi DS, Mallapragada SK. Directed growth and selective differentiation of neural progenitor cells on micropatterned polymer substrates. Biomaterials. 2006;27(22):4098.

[84] Matsuzaka K, Yoshinari M, Shimono M, Inoue T. Effects of multigrooved surfaces on osteoblast-like cells *in vitro*: Scanning electron microscopic observation and mRNA expression of osteopontin and osteocalcin. Journal of Biomedical Materials Research Part A. 2004;68A(2):227-34.

[85] Wang JHC, Grood ES, Florer J, Wenstrup R. Alignment and proliferation of MC3T3-E1 osteoblasts in microgrooved silicone substrata subjected to cyclic stretching. Journal of Biomechanics. 2000;33:729-35.

[86] Jiang X, Bruzewicz DA, Wong AP, Piel M, Whitesides GM. Directing cell migration with asymmetric micropatterns. PNAS. 2005 January 25, 2005;102(4):975-8.

[87] Brock A, Chang E, Ho CC, LeDuc P, Jiang X, Whitesides GM, et al. Geometric Determinants of Directional Cell Motility Revealed Using Microcontact Printing. Langmuir. 2003 March 4, 2003;19(5):1611-7.

[88] Orth RN, Wu M, Holowka DA, Craighead HG, Baird BA. Mast cell activation on patterned lipid bilayers of subcellular dimensions. Langmuir. 2003 Mar 4;19(5):1599-605.

[89] Schmalenberg KE, Uhrich KE. Micropatterned polymer substrates control slignment of proliferating Schwann cells to direct neuronal regeneration. Biomaterials. 2005;26:1423-30.

[90] Yamato M, Konno C, Utsumi M, Kikuchi A, Okano T. Thermally responsive polymer-grafted surfaces facilitate patterned cell seeding and co-culture. Biomaterials. 2002 Jan;23(2):561-7.

[91] Lee CJ, Blumenkranz MS, Fishman HA, Bent SF. Controlling Cell Adhesion on Human Tissue by Soft Lithography. Langmuir. 2004;20:4155-61.

[92] Parker KK, Brock AL, Brangwynne C, Mannix RJ, Wang N, Ostuni E, et al. Directional control of lamellipodia extension by constraining cell shape and orienting cell tractional forces. FASEB J. 2002 August 1, 2002;16(10):1195-204.

[93] Nelson CM, Pirone DM, Tan JL, Chen CS. Vascular Endothelial-Cadherin Regulates Cytoskeletal Tension, Cell Spreading, and Focal Adhesions by Stimulating RhoA. Mol Biol Cell. 2004 June 1, 2004;15(6):2943-53.

[94] Vogt AK, Wrobel G, Meyer W, Knoll W, Offenhausser A. Synaptic plasticity in micropatterned neuronal networks. Biomaterials. 2005;26(15):2549.

[95] Chen CS, Mrksich M, Huang S, Whitesides G, Ingber DE. Geometric control of cell life and death. 1997 1997///;276:1425-8.

[96] Dike LE, Chen CS, Mrksich M, Tien J, Whitesides GM, Ingber DE. Geormetric Control of Switching Between Growth, Apoptosis, and Differentiation during Angiogenesis using Micropatterned Substrates. In Vitro Cell Developmental Biology - Animal. 1999;35:441-8.

[97] Thomas CH, Collier JH, Sfeir CS, Healy KE. Engineering gene expression and protein synthesis by modulation of nuclear shape. 2002 2002/02/19/;99(4):1972-7.

[98] McBeath R, Pirone DM, Nelson CM, Bhadriraju K, Chen CS. Cell Shape, Cytoskeletal Tension, and RhoA Regulate Stem Cell Lineage Commitment. Developmental Cell. 2004;6(4):483-95.

CHAPTER 3

HOT EMBOSSING FOR MICRO PATTERNED CELL SUBSTRATES

This chapter reports the development of a technique for preparing microtextured polymer substrates for cell growth and studies the response of osteoblast cells grown on these surfaces. The surfaces were manufactured with hot embossing, where a silicon micromachined printing master was pressed into a thermoplastic polymer substrate at elevated temperature, forming a regular microgroove pattern in the polymer. The grooves were approximately 5 μm deep, 4 μm wide, and had a periodicity of 34 μm. The polymer substrate was polyimide, which can be spin cast and printed in its uncured form, and is mechanically rigid and chemically non-reactive after full cure. Osteoblast cells were grown on the textured polymer substrate and their responses to grooved and smooth surfaces were observed with fluorescence microscopy. Alignment and aspect ratio were analyzed for the cell body, cell nucleus, and focal adhesions. Cell membrane body, cell nucleus, and focal adhesions all strongly aligned with the microgrooves, while only the cell body shape changed on the microgrooved surface. This novel substrate preparation technique offers the opportunity for low-cost and rapid manufacture of microtextured surfaces that can be used to control cell shape and alignment.

3.1 Introduction

Hot embossing imprint lithography [1] offers the opportunity to manufacture features in thermoplastic materials with dimensions as small as 10 nm [2] over areas of

several square centimeters [3]. In hot embossing imprint lithography, a silicon micromachined stamp is pressed into a thermoplastic material at elevated temperature, forming a relief of its features in the plastic. This manufacturing technique has been previously used to manufacture nanometer-scale transistors [4], pattern magnetic islands for high-density data storage [5], and form microfluid channels in plastic for lab-on-a-chip applications [6]. The major advantages of hot embossing imprint lithography include its very low cost compared to silicon micromachining technology since only one master must be made to produce many printed samples, the ability to print into organic materials that are inconvenient or impossible to process with silicon micromachining or chemical etching approaches, and the ability to form three-dimensional features that are difficult to produce in silicon. Furthermore, unlike other surface micropatterning techniques the hot embossing technique is highly scalable and is well-suited for large-scale manufacturing of cell substrates. The present chapter uses hot embossing to prepare microtextured polymer surfaces and examines the alignment of osteoblast cells attached to the microtextured surface.

The size and shape of mechanical features on a surface influences the placement, orientation, morphology, and function of cells that grow on that surface [7-10]. Motivated by early studies that show cell response to microscale mechanical features [7, 11], several groups have modified surfaces to control the behavior of cells. Methods for modifying or controlling surface texture can be grouped into approaches for engineering either roughness or topography. Surface roughness indicates a random pattern of features usually much smaller than the cell, while surface topography describes patterns of features placed deliberately on the surface. The surface roughness of a sample for

cellular growth can be modified via sandblasting, plasma spraying, and mechanical polishing of the surface [12-15]. Observations relating cellular response to surface topography date back to the early 1900s when Harrison first observed the elongation of cells in the direction of surface features [16], now referred to as contact guidance. A review [17] is available of the key works examining cell response to rough and topographically structured surfaces.

Recently, micromachining techniques have been developed to create specifically sized and deliberately shaped features [11, 18-34] in surfaces to control cell response. The substrates are made of a variety of materials including silicon [11, 18-34], glass [32], and polymer [20, 22, 23, 25, 27] and have been shown to influence both cellular alignment and focal adhesion structures. It is extremely desirable to prepare polymer substrates for cell growth rather than glass or silicon substrates, because of the low cost and chemical functionality available in polymers. Furthermore, it is extremely difficult to manufacture complex three dimensional shapes with traditional silicon microfabrication techniques, while nearly any topography could be replicated in polymer. Previous research studying the growth of living cells on microtextured polymer surfaces [11, 19-30, 35] has almost entirely been limited to casting based manufacturing [11, 20-30], an approach which strictly limits the polymers available to those that are cast able, or photo-patterning [19, 35], which restricts the polymer choice to photocurable polymers and requires chemical processing to develop the polymers. In a casting process, a polymer liquid is poured onto a micromachined silicon surface and cured in place, thus replicating the silicon features in the polymer [11, 20-30]. Other cast polymers such as hydrogels and bio-degradable poly(lactic-glycolic acid) (PLGA) have been used to create

microtopography for cellular growth with similar results of contact guidance [26]. To our knowledge, no one has published data of cellular response to embossed micropatterns on a polymer substrate.

This chapter describes a method for preparing microgrooves in surfaces with hot embossing imprint lithography for the purpose of modifying cell growth on these surfaces. Samples of polyimide were manufactured with grooves 4 μm in width with a periodicity of 34 μm. MC3T3-E1 osteoblast-like cells were examined through fluorescence microscopy after a 24 h incubation period. The cell bodies, nuclei and focal adhesions showed alignment to the microgrooves whether they attach to the top of a mesa or the bottom of a groove. Grooves influenced the cell body shape factor while they did not influence the nucleus shape factor or the focal adhesion shape factor.

3.2 Experimental Method

In hot embossing imprint lithography, a silicon micromachined master is pressed into a thermoplastic material at elevated temperature, thus forming relief structures in the polymer. Figure 3.1 illustrates the hot embossing process. Both the master and the substrate must be carefully prepared and analyzed for repeatable fabrication of microgrooved cell substrates.

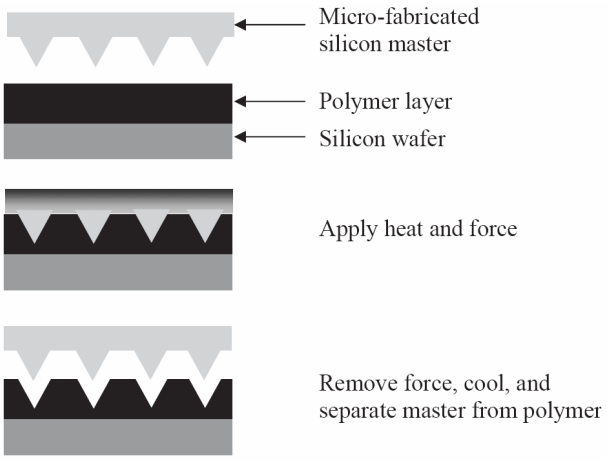

Figure 3.1 Schematic of the hot-embossing process

A silicon master was fabricated using standard micromachining techniques and used to emboss micropatterns into a polymer substrate. Preparation of the silicon master starts with a standard four inch 525 µm thick silicon wafer (Nova Electronic Materials). A 1.5 µm thick layer of Shipley 1813 photoresist spun at 2000 rpm for 30 s was soft-baked at 120° C for 3 min. Exposure of the photoresist was done at 450 nm, 25 mJ/cm^2, for 11 s. The mask for the exposure had dark features that were 2µm long by 4 µm wide bars on a 34 µm pitch in a parallel line format. The photoresist was developed with MF319 for 1 min 30 s, and then rinsed with deionized water. The features were etched using a deep reactive ion etch (Bosch Process) for 22 cycles, etching roughly 0.3 µm/cycle. Any residual photoresist was removed through an oxygen plasma etch for 5 min. Scanning electron microscopy (SEM) was used to characterize the features etched into the silicon master.

The microstructured polymer–metal surfaces were prepared in the following manner. A 4 inch silicon wafer was treated with an adhesion enhancer then spin coated with a polyimide layer. The adhesion enhancer (HD Microsystems VM651) was mixed

in a 1:200 ratio with deionized water, poured over the entire surface of the wafer, and allowed to react for 20 s. After spin-drying the wafer on a spin-coating system for 30 s at 3000 rpm, polyimide (HD Microsystems PI2525) was applied to the wafer and spun for 30 s at 3000 rpm resulting in an approximately 8.5 μm thick layer. The wafer was then soft-baked on a hot plate at 120° C for 30 s followed by 150° C for 30 s. Hot embossing of the polyimide was performed using a custom-built heated press, which allows uniform temperature control of the cell substrate, and measurement of the embossing load force. The sample was loaded polymer side up onto the heated stage with the silicon master on top of it, feature side down. Light load (0-5 N) was applied while the temperature was ramped to 150° C. At this point, the load was increased to 3.5 kN and maintained for 90 s while the temperature remained constant. The sample was removed, allowed to cool, and then separated from the master. Full curing and solvent evaporation of the polymer was achieved by heating it on a hot plate at 200° C for 2 h, then 350° C for 1 h. Atomic force microscopy (AFM), SEM, and standard nanoindentation measurements were used to characterize the printed polymer film.

MC3T3-E1 osteoblasts were cultured in α-minimal essential medium containing 10% serum and 1% penicillin–streptomycin. The cells were passaged every 2 days using standard culture techniques. Patterned polymer surfaces were washed with 95% ethanol and rinsed in PBS. Surfaces were then coated with fibronectin (20 μg/ml) for 30 min, followed by a 1-h incubation in 1% heat denatured bovine serum albumin (BSA). The cells were seeded at a density of 400 cells/mm^2 and cultured for 24 h in humidified atmosphere at 37° C and 5% CO_2.

Focal adhesion structures were immunostained as described in [36, 37]. Cells were treated with cold 0.5% Triton X-100 cytoskeleton buffer (50 mm NaCl, 150 mM sucrose, 3 mM $MgCl_2$, 20 μg/ml aprotinin, 1 μg/ml leupeptin, 1 mM phenylmethylsulfonyl fluoride, and 50 mM tris-(hydroxymethyl)aminomethane, pH 6.8) for 5 min to remove cell membranes and soluble cytoskeletal components. The remaining cellular components were fixed in 3.7% formaldehyde in PBS for 2 min, and then blocked in 5% FBS for 1 h. Samples were incubated in anti-vinculin primary antibody (Upstate Biotechnologies) for 1 h, rinsed twice with PBS, incubated for 10 min in 5% FBS in PBS, and rinsed twice with PBS. Samples were subsequently incubated in secondary anti-IgG antibody, rhodamine–phalloidin, and Hoechst or CM-DiI lipophilic stain (Molecular Probes) for 1 h, rinsed as before, and mounted.

Microscope images were processed using standard image processing software. For each image, the color channels were extracted individually and converted to grayscale. The appropriate features were captured by evaluating intensity threshold at the border of the feature, then converting the grayscale image to a binary image. The result is each feature being represented in white, with a black background. In the case of examining cell bodies, the outline of the cell body was unable to be discerned by the software alone. To correct this problem, the outline of the cell was manually traced after the contrast was optimized. To evaluate elongation of an object, the area was digitally captured and fitted with an ellipse. The major axis of the ellipse was divided by the minor axis to get the aspect ratio. To evaluate alignment, the angle of the major axis with respect to the microgrooves was taken.

3.3 Results and Discussion

In order to qualify the hot embossing technique for fabricating microgrooved cell substrates, analysis was performed on the microgrooved polymer substrate fabrication process and the cell response to the substrate, and these were compared to previous studies on microfabricated substrates for cell contact guidance.

Figure 3.2 shows the fabricated master, with printing features approximately 7 μm tall, as well as SEM (top) and AFM (bottom) images of the printed polymer substrate. The AFM data show a uniform surface roughness on top of the mesas of less than 10 nm. The depth of the grooves was determined to be approximately 5 μm through SEM examination. Nano indentation measurements made on the polyimide show a modulus of 5.5 GPa both before and after cure, and a hardness of 0.2 GPa before cure and 0.5 GPa after cure. Thus, the cured polymer is compliant at small strains but extremely resistant to large strains. In order to provide a surface with a well-understood surface chemistry for cellular growth, the polyimide was coated with a 15 nm layer of titanium followed by a 100 nm layer of gold, using an electron beam evaporator. By coating our embossed samples with metal, the cell substrate could be further chemically treated relatively independently of its base material, as in [37]. The polymer also has the potential to be impregnated with biochemicals to control cell function, while its normal form is non-toxic.

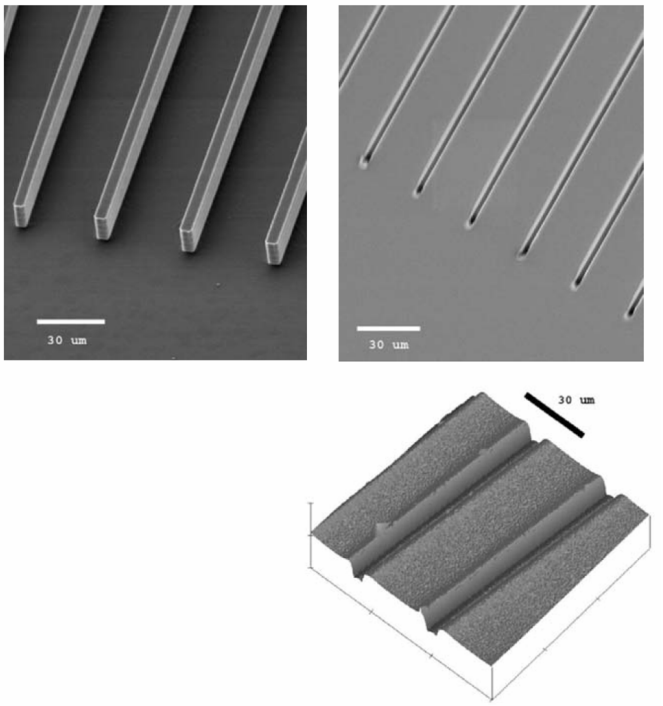

Figure 3.2 Left: Scanning electron microscope image of the microfabricated silicon master. The mesas are 7 μm tall, 4 μm wide, and have a pitch of 34 μm. Right top: SEM image of the printed polymer surface, prior to cell growth and right bottom: AFM image. The trenches are approximately 5 μm deep and 4 μm wide, which is close to the size of the mesa features on the master.

A rigorous scientific assessment of the impact of substrate topography on cell growth and attachment requires quantification of the alignment and shape of the cell body, the cell nucleus, and focal adhesions. Many groups have presented quantitative data on cell body shape [20, 21, 27, 31-33] and cell body alignment [25, 27, 31-33], and one has presented quantitative data on focal adhesion alignment [21]. Several groups have made contributions to this research area without reporting quantitative information about the above figures of merit, but rather reported only the fabrication process [11, 19-35], qualitative observations [11, 19-35], and chemical analysis [20, 22, 29]. The present chapter reports quantitative experimental results on both alignment and morphology of cell body, nucleus, and focal adhesion. To the best of our knowledge, this chapter is the first to report quantitative results on all six of these figures of merit.

To quantify the alignment and shape change of the cell body induced by the micropattern, fluorescence microscopy images were taken of the cells stained with a lipophilic membrane stain. Figure 3.3a shows an image of the cell membrane for cells grown on smooth and grooved surfaces. The lipophilic stain only stains the cell body and not any extracellular proteins, resulting in an outline of the cell shape. Qualitatively, osteoblasts on a smooth surface exhibited a random orientation and varying aspect ratios. Osteoblasts on the micropatterned surface showed a preferential alignment to the microgrooves and an elongated shape, or higher aspect ratio. Most cells were located on the mesas, rather than in the grooves although they still showed alignment along the grooves. Figure 3.3b shows quantitative data of cell body alignment and aspect ratio. For cells grown on a smooth surface, the alignment of the cell body major axis with respect to an arbitrary axis at 0° the data was uniformly distributed with a mean of 45.0° (as expected for a uniform distribution of values between 0° and 90°) as seen on the upper left chart. For cells grown on a textured surface, cell body angle with respect to the microgrooves at angle 0° showed a clear pattern in the upper right chart. There is an approximately normal distribution around the microgroove orientation direction with a mean of 9.1°. The means of the two samples are statistically different (two population t-test, significance level=0.01). The standard deviation of the angle is much lower for the microgrooved surface (stdev=8.6) than for the smooth surface (stdev=27.9) showing the tighter grouping of the micropatterned data. Cell body elongation can be described as an increase in aspect ratio. The two population means of aspect ratios are significantly different (two population t-test, significance level=0.01), indicating a 53% increase in

aspect ratio due to the microgrooves. The data shows a more normal grouping around the average for the micropatterned substrates when compared to the smooth substrates.

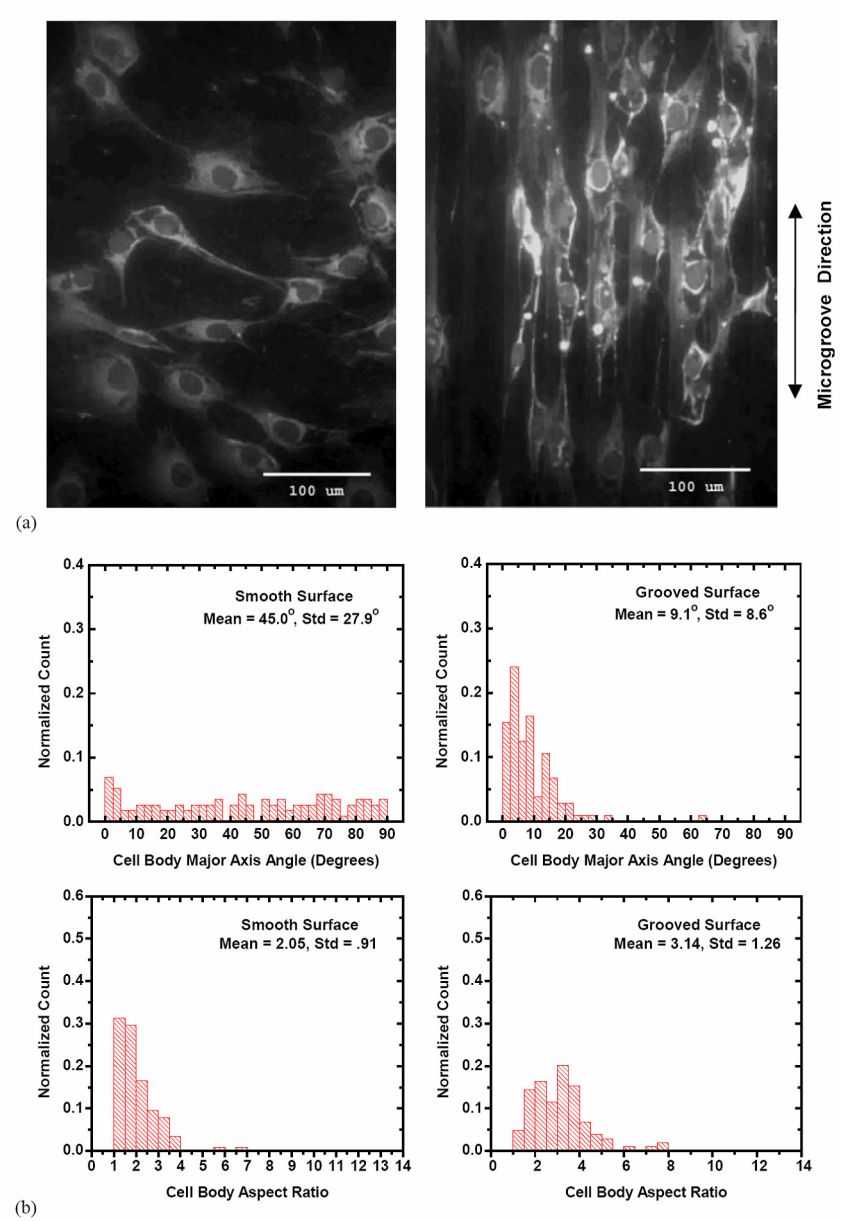

Figure 3.3 (a) Fluorescence microscopy images of cell membranes for cells grown on a smooth surface (left) and on a microprinted surface (right). The image clearly shows the cell membrane (cell body) alignment on the microprinted surface. (b) Histograms of cell body features from membrane stain image analysis. Cell body alignment on a smooth surface (top left) and micropatterned surface (top right). Cell body aspect ratio on smooth surface (bottom left) and micropatterned surface (bottom right).

To quantify the alignment and shape change of the cell nuclei, fluorescence spectroscopy photos were taken of the osteoblasts on smooth and micropatterned substrates. Figure 3.4a shows a fluorescence microscopy image of the osteoblasts stained for DNA (nucleus) on a smooth substrate (left) and on a micropatterned substrate (right). The nuclei of cells on a smooth substrate exhibited a slightly elongated shape, with no apparent alignment, while the nuclei of cells on micropatterned substrates also displayed an elongated shape, but were strongly aligned to the microgrooves. Figure 3.4b shows quantitative data of nucleus alignment and aspect ratio. The nucleus demonstrated strong alignment to the microgrooves, as can be seen by comparing the approximately normal distribution about 0° for the micropatterned surface to the uniform distribution of the smooth surface. Although the standard deviations of alignment angles of smooth (27.0°) and grooved (21.7°) are similar, the grooved standard deviation is still slightly lower and the means are significantly different (two population t-test, significance level = 0.01) with the grooved mean being lower. Although alignment of nuclei was significantly impacted by microgrooves, the shape of the nucleus was not. The lower two plots of Figure 3.4b are histograms of aspect ratio for nuclei on a smooth surface (left) and a micropatterned surface (right). There was not a significant change in aspect ratio of the nucleus from smooth to micropatterned substrates. A two-population t-test confirms that the means were not significantly different. The standard deviations were similar for grooved and smooth (0.44 and 0.37, respectively).

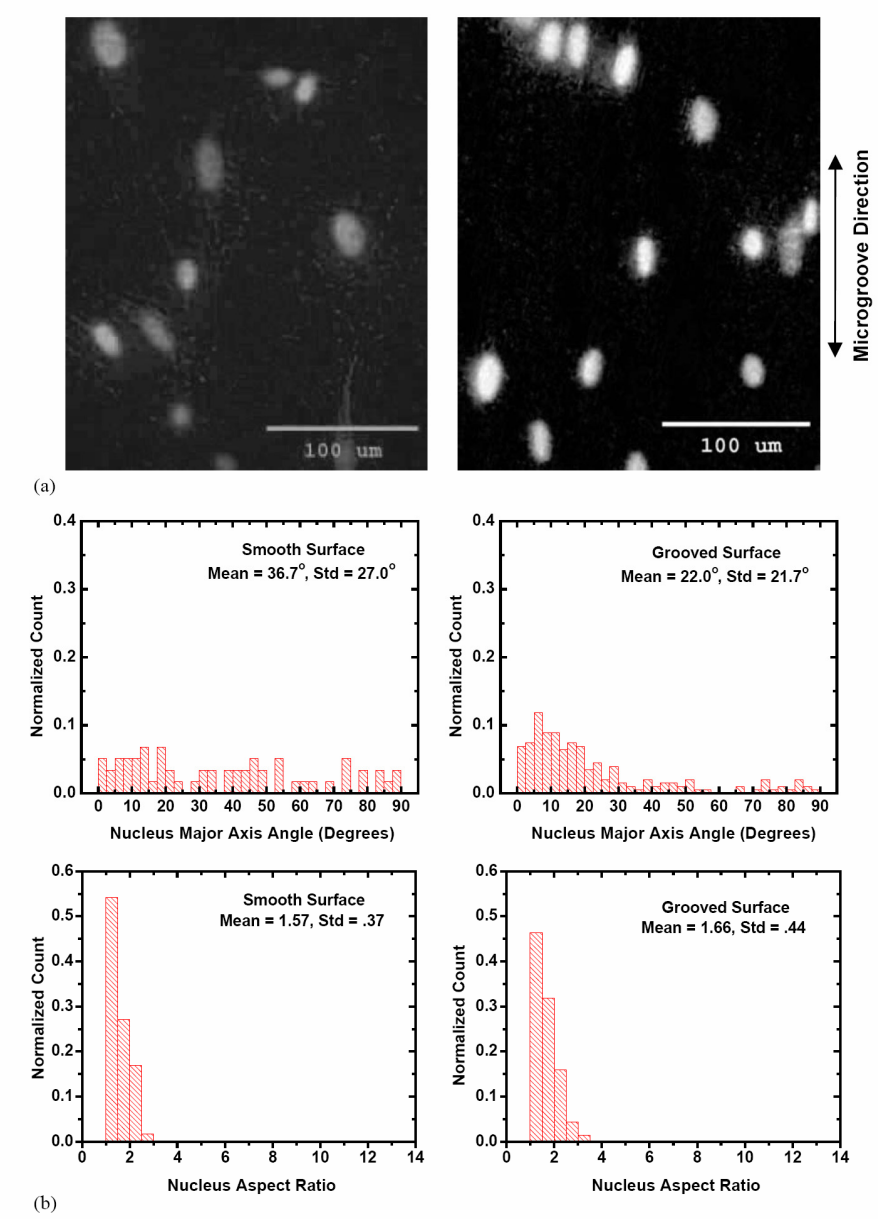

Figure 3.4 (a) Fluorescence microscope images cell nuclei on smooth surface (left) and microprinted surface (right). (b) Histograms of cell nuclei. Nuclear alignment on a smooth surface (top left) and micropatterned surface (top right). Nucleus aspect ratio on a smooth surface (bottom left) and micropatterned surface (bottom right).

To quantify the alignment and shape change of focal adhesions, fluorescence images of cells stained for vinculin were taken at higher magnification (100X objective). On a smooth surface, the focal adhesions appear to fan out from the center of the cell in

all directions. On a grooved surface, the focal adhesions of the cell on the microgrooves are predominantly aligned with the grooves. Figure 3.5 shows the angle that the focal adhesions make with respect to the microgrooves. The smooth substrate produced cells with focal adhesions that have random orientations as illustrated by the uniformly distributed data in the histogram. The focal adhesion angles of cells on micropatterned substrates produced a normal distribution centered on 0° indicating a strong alignment. The standard deviations demonstrated a somewhat tighter grouping to the data with microgrooves (26.6 for smooth, 22.6 for grooved). In this case the means are significantly different (two population t-test, significance level=0.01) with the grooved substrate having the lower mean (25.1° compared to 50.1° for smooth). Aspect ratios of the focal adhesions do not change significantly due to the microgrooves and their standard deviations are similar (1.36 for smooth, 1.28 for microgrooved).

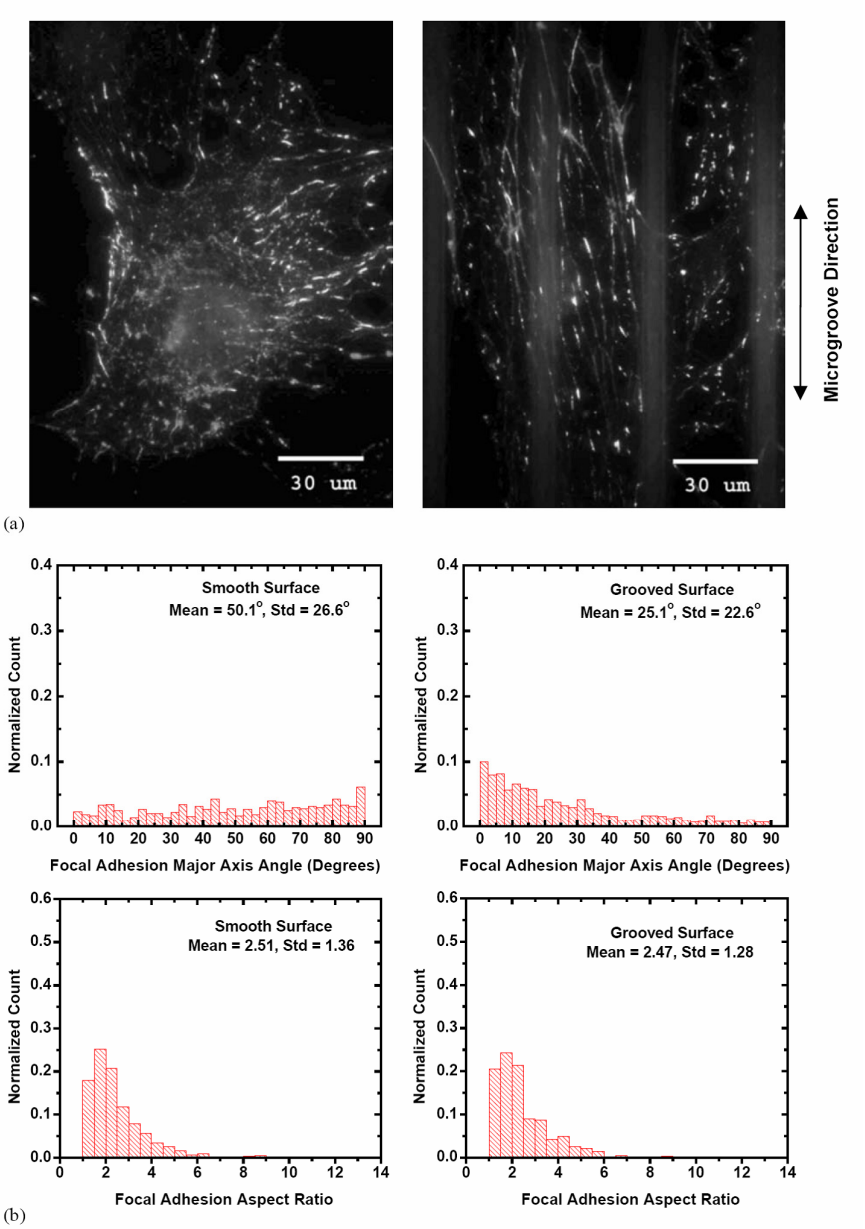

Figure 3.5 (a) Fluorescence microscope images of the osteoblast focal adhesions for cells grown on a smooth surface (left) and on a microprinted surface (right). (b) Histograms of focal adhesion features from vinculin-stained images. Focal adhesion alignment on a smooth surface (top left) and micropatterned surface (top right). Focal adhesion aspect ratio on a smooth surface (bottom left) and micropatterned surface (bottom right).

The results of the cell culture on the hot embossed micropatterned surfaces show contact guidance of the cells on the ridges and grooves of the substrate as described by a change in aspect ratio of the cell bodies, as well as an alignment of the cell bodies, focal

adhesions and nuclei. These are expected results as similar results are seen previously for other types of microtextured surfaces [11, 19-35] indicating that the present substrate hot embossing technique still results in topographical control of the cells. Specifically, the results of several key studies match the results presented here. In one study, titanium-coated, micromachined silicon samples with microscale V-shaped grooves were used as substrates to grow fibroblasts [34]. The resulting cells exhibited contact guidance with an elongated shape and the axis of elongation oriented along the axis of the microgrooves on the silicon. Subsequently, the same group [31] used a cast polymer replica of the silicon substrate. Quantitative analysis of the cells showed that the average angle of the cells major axis with respect to the microgrooves was 6.5°. The work in this chapter matches nicely with these results qualitatively as well as quantitatively since we found average alignment angles to be of comparable size (no more than 10°). A more recent work by a different group investigated the dependence of endothelial cell alignment and shape on the width of microchannels in silicon [33]. The extensive quantitative analysis of cell alignment and shape in this work showed that cell alignment is quite strong for channel widths on the order of 50 μm and cell elongation increases over 50% when comparing a 25 μm channel to a smooth surface. Our results show a similarly strong cellular alignment and 53% increase in elongation for a 30 μm mesa when compared to a smooth surface. The major result of the present study is that hot embossed microgrooves in thermoplastic cell substrates induce cell contact guidance in the same manner as reported for other microtextured cell substrates. While previous research on polymer substrates for cell contact guidance was strictly limited to castable or photodefinable polymers, the manufacturing technique of this chapter opens opportunities to perform substrate contact

guidance of cells in theoretically any thermoplastic polymer. Furthermore, compared with previously published polymer micropatterning techniques, the manufacturing process is highly scalable and substantially less expensive. While the patterns of the current study were grooves, in principle any structure could be replicated in polymer, including indents, posts, and more complex three-dimensional structures. We envision roll-to-roll printing manufacturing of large quantities of biologically active thermoplastic polymers.

3.4 Conclusions

This chapter reports a hot embossing technique for creating micropatterned polymer substrates for cell culture. The cell bodies aligned to the microgrooves and significantly elongated when compared to cells on a smooth surface. The cell nuclei strongly aligned to the microgrooves but did not significantly elongate due the microgrooves. The focal adhesions of cells on micropatterned substrates showed a significant alignment, but not significant change in shape. These results agree with previously published work on cell contact guidance, while using the new process of hot embossing. While previous research on polymer substrates for cell contact guidance was strictly limited to castable or photodefinable polymers, the manufacturing technique of this chapter opens opportunities to perform substrate contact guidance of cells in thermoplastic polymers. Compared

to other available techniques that have been shown to fabricate microtextured polymer surfaces as cell substrates, the hot embossing manufacturing technique of the present work is less expensive, faster, and more highly scalable to high-volume manufacturing.

3.5 Acknowledgements

The authors thank T.L. Wright and H.D. Rowland for their cooperative work on microfabrication, B.A. Nelson for his assistance with AFM metrology, and G.L.W. Cross of Trinity College Dublin for the Nanoindentation measurement.

3.6 References

[1] Chou SY, Krauss PR, Renstrom PJ. Imprint lithography with 25-nanometer resolution. Science. 1996 Apr 5;272(5258):85-7.

[2] Chou SY, Krauss PR, Zhang W, Guo L, Zhuang L. Sub-10 nm imprint lithograpy and applications. Journal of Vacuum Science & Technology B. 1997;15(6):2897-904.

[3] Lebib A, Chen Y, Bourneix J, Carcenac F, Cambril E, Couraud L, et al. Nanoimprint lithography for a large area pattern replication. Microelectronic Engineering. 1999;46:319-22.

[4] Guo LJ, Krauss PR, Chou SY. Nanoscale silicon field effect transistors fabricated using imprint lithography. Applied Physics Letters. 1997 Sep;71(13):1881-3.

[5] McClelland GM, Hart MW, Rettner CT, Best ME, Carter KR, Terris BD. Nanoscale patterning of magnetic islands by imprint lithography using a flexible mold. Applied Physics Letters. 2002 Aug;81(8):1483-5.

[6] Lee GB, Chen SH, Huang GR, Sung WC, Lin YH. Microfabricated plastic chips by hot embossing methods and their applications for DNA separation and detection. Sensors and Actuators B-Chemical. 2001 Apr;75(1-2):142-8.

[7] Weiss P. Experinments on cell and Axon Orientation in Vitro. Journal of Experimental Zoology. 1945;100(3):353-86.

[8] von Recum AF, van Kooten TG. The Influence of Micro-Topography on Cellular Response and the Implications for Silicone Implants. Journal of Biomaterials Science-Polymer Edition. 1995;7:181-98.

[9] Curtis A, Wilkinson C. Topographical Control of Cells. Biomaterials. 1997 Dec;18(24):1573-83.

[10] Schwartz Z, Boyan BD. Understanding Mechanisms at the Bone-Biomaterial Interface. JCell Biochem. 1994;56:340-7.

[11] Rovensky Y, Slavnaja I, Vasiliev J. Behavior of fibroblast-like cells on grooved surfaces. Experimental Cell Research. 1971;65:193-201.

[12] Martin JY, Schwartz Z, Hyummert TW, Schraub DM, Simpson J, Lankford JJ, et al. Journal of Biomedical Materials Research. 1995;29:389-401.

[13] Lauer G, Wiedmann-Al-Ahmad M, Otten JE, Huebner U, Schmelzeisen R, Shchilli W. The Titanium Surface Texture Effects Adherence and Growth of Human

Gingival Keratinocytes and Human Maxillar Osteoblast-Like Cells in Vitro. Biomaterials. 2001;22:2799-809.

[14] Kononen M, Hormia M, Kivilahti J, Hautaniemi J, Thesleff I. Effect of Surface Processing on the Attachment, Orientation, And Proliferation of Human Gingival Fibroblasts on Titanium. Journal of Biomedical Materials Research. 1992 Oct;26(10):1325-41.

[15] Cooper LF, Masuda T, Whitson SW, Yliheikkila P, Felton DA. Formation of mineralizing osteoblast cultures on machined, titanium oxide grit-blasted, and plasma-sprayed titanium surfaces. International Journal of Oral & Maxillofacial Implants. 1999 Jan-Feb;14(1):37-47.

[16] Harrison RG. Anat Rect. 1912;6:181.

[17] Flemming RG, Murphy CJ, Abrams GA, Goodman SL, Nealey PF. Effects of synthetic micro- and nano-structured surfaces on cell behavior. Biomaterials. 1999 Mar;20(6):573-88.

[18] Clark P, Connolly P, Curtis ASG, Dow JAT, Wilkinson CDW. Topographical Control of Cell Behavior 2. Multiple Grooved Substrata. Development. 1990 Apr;108(4):635-44.

[19] Clark P, Connolly P, Curtis AS, Dow JA, Wilkinson CD. Topographical control of cell behaviour. I. Simple step cues. Development. 1987 March 1, 1987;99(3):439-48.

[20] Schmidt J, von Recum AF. Microphage response to microtextured silicone. Biomaterials. 1992;13:1059-69.

[21] Oakley C, Brunette DM. The Sequence of Alignment of Microtubules, Focal Contacts and Actin-Filaments in Fibroblasts Spreading on Smooth and Grooved Titanium Substrata. Journal of Cell Science. 1993 Sep;106:343-54.

[22] van Kooten TG, Whitesides JF, von Recum AF. Influence of silicone (PDMS) surface texture on human skin fibroblast proliferation as determined by cell cycle analysis. Journal of Biomedical Materials Research. 1998 Spr;43(1):1-14.

[23] Wang JHC, Grood ES, Florer J, Wenstrup R. Alignment and proliferation of MC3T3-E1 osteoblasts in microgrooved silicone substrata subjected to cyclic stretching. Journal of Biomechanics. 2000;33:729-35.

[24] van Kooten TG, von Recum AF. Cell adhesion to textured silicone surfaces: The influence of time of adhesion and texture on focal contact and fibronectin fibril formation. Tissue Engineering. 1999 Jun;5(3):223-40.

[25] Walboomers XF, Croes HJE, Ginsel LA, Jansen JA. Contact guidance of rat fibroblasts on various implant materials. Journal of Biomedical Materials Research. 1999 Nov;47(2):204-12.

[26] Motlagh D, Senyo S, Desai TA, Russell B. Micro-groove dimensions affect orientation and cell-cell contact. Journal of Molecular and Cellular Cardiology. 2002 Jul;34(7):A32-A.

[27] Mata A, Boehm C, Fleischman A, Muschler G, Roy S. Analysis of connective tissue progenitor cell behavior on polydimethylsiloxane smooth and channel micro-textures. Biomedical Microdevices. 2002;4:267-75.

[28] Parker J, Walboomers XF, Von den Hoff JW, Maltha JC, Jansen JA. Soft tissue response to microtextured silicone and poly-L-lactic acid implants: fibronectin pre-coating vs. radio-frequency glow discharge treatment. Biomaterials. 2002 Sep;23(17):3545-53.

[29] Motlagh D, Senyo SE, Desai TA, Russell B. Microtextured substrata alter gene expression, protein localization and the shape of cardiac myocytes. Biomaterials. 2003 Jun;24(14):2463-76.

[30] Matsuzaka K, Walboomers XF, Yoshinari M, Inoue T, Jansen JA. The attachment and growth behavior of osteoblast-like cells on microtextured surfaces. Biomaterials. 2003 Jul;24(16):2711-9.

[31] Brunette DM. Fibroblasts on Micromachined Substrata Orient Hierarchically to Grooves of Different Dimensions. Experimental Cell Research. 1986 May;164(1):11-26.

[32] Li S, Bhatia SN, Hu Y-L, Li Y-S, Usami S, Chien S. Effect of Morphological Patterning on Endothelial Cell Migration. Biorheology. 2001;28:101-8.

[33] Gray BL, Lieu DK, Collins SD, Smith RL, Barakat AI. Microchannel Platform for the Study of Endothelial Cell Shape and Function. Biomedical Microdevices. 2002;4:9-16.

[34] Brunette DM, Kenner GS, Gould TRL. Grooved Titanium Surfaces Orient Growth and Migration of Cells from Human Gingival Explants. Journal of Dental Research. 1983;62(10):1045-8.

[35] Clark P, Connolly P, Curtis ASG, Dow JAT, Wilkinson CDW. Topographical Control of Cell Behavior .2. Multiple Grooved Substrata. Development. 1990 Apr;108(4):635-44.

[36] Garc¡a AJ, Boettiger D. Integrin-fibronectin interactions at the cell-material interface: initial integrin binding and signaling. Biomaterials. 1999 1999/12//;20(23-24):2427-33.

[37] Gallant ND, Capadona JR, Frazier AB, Collard DM, Garcia AJ. Micropatterned surfaces for analyzing cell adhesion strengthening Langmuir. 2002 2002;18:5579-84.

[38] Abbott N, Folkers J, Whitesides G. Manipulation of the wettability of surfaces on the 0.1-to 1-micrometer scale through micromachining and molecular self-assembly. Science. 1992;257:1380-2.

CHAPTER 4

COMBINED MICROSCALE MECHANICAL TOPOGRAPHY AND CHEMICAL PATTERNS ON POLYMER CELL CULTURE SUBSTRATES

This chapter presents a technique to independently form mechanical topography and surface chemical patterns on polymer cell substrates, and studies the response of osteoblast cells to these surface patterns. The patterns were formed in two separate steps: hot embossing imprint lithography formed the mechanical topography and micro-contact printing created the chemical pattern. All substrates were composed of polyimide and coated in a titanium/gold bilayer to enable the micro-contact printing of hexadecanethiol groups. The resulting substrate had surface features consisting of embossed grooves 4 μm deep and 8 μm wide spaced by 16 μm wide mesas and micro-contact printed adhesive lanes 10 μm wide with spacings that ranged from 10 μm to 100 μm. The spacing areas were coated in an ethylene glycol terminated alkanethiol to suppress protein and cell adhesion. When presented with either mechanical topography or chemical patterns alone, the cells significantly aligned to the pattern presented. When presented with mechanical topography overlaid with an orthogonal chemical pattern, the cells aligned to the mechanical topography. As the chemical pattern spacing was increased, osteoblasts remained aligned to the mechanical topography. Unlike traditional microfabrication approaches based on photolithography and wet chemistry, the patterning

technique presented is compatible with a large number of biomaterials, can form patterns with features much smaller than 1 μm, and is highly scalable to large substrates.

4.1 Introduction

The interactions between an implant material surface and host cells play central roles in the integration, biological performance, and clinical success of implanted biomedical devices, including orthopedic joint replacements, biosensors, and drug delivery devices [1-4]. The mechanical topography and chemistry of a material surface can modulate diverse cellular responses, including survival, adhesion, spreading, migration, proliferation, and expression of differentiated phenotypes [5, 6]. Nevertheless, the relative contributions of mechanical topography and chemical properties of a material when presented in combination on cellular responses are not well understood. This understanding could lead to the development of new classes of materials with precisely designed interfaces for improved biological performance and integration.

Cellular responses to mechanical and chemical features on surfaces generally depend upon whether the features are patterned or random, and can further depend upon the specific pattern(s) presented. *Mechanical topography* is a pattern of mechanical structures with regular and specifically designed size, shape, and periodicity. This surface property fundamentally differs from *mechanical roughness*, which is a group of mechanical features that exhibits randomness and polydispersity in terms of size, shape, and periodicity. Many groups have examined the effect of mechanical topography on cellular activities using various substrate materials [7-10]. Mechanical topography of the underlying substrates has been shown to influence cell morphology [11-15], migration [16, 17], initial focal adhesion

density and size [18], spreading [19], contact guidance [20], and differentiation [21]. A *chemical pattern* can be defined as a group of features of specific chemistry different from the chemistry of their surroundings that have regular and specifically designed size, shape, and periodicity. Several groups have used patterns of surface chemistry to influence cellular responses such as adhesion [22], shape and function [23], and attachment location [24] as well as to produce co-cultures of cells [25]. In both cases, mechanical topography and surface chemistry patterning must be well-controlled in order to accurately assess and manipulate surface-cell interactions.

While previous work has thoroughly examined cell interactions, in particular cellular alignment and contact guidance, with either microscale mechanical topography [16, 19, 26-30] or chemical patterns [31, 32], studies of cell interactions with substrates possessing combined mechanical topography and chemical patterns are limited, resulting in a poor understanding of the relative impact and interplay of the two surface properties in regulating cellular activities. Previous analyses have demonstrated differential cellular responses to mechanical topography for different surface chemistries [33-36], but the chemical patterns were defined by the mechanical topography, and hence not independent. Notably, Britland and co-workers combined microscale topography with independently micropatterned chemical domains on glass substrates to modulate cellular alignment of fibroblasts [37]. However, these investigators used patterns generated by standard photolithography approaches, which are not well suited to the processing of biomedically relevant biomaterials.

In the present work, we describe a technique for the fabrication of cell culture substrates having a mechanical topography overlaid with chemical patterns by combining

hot-embossing imprint lithography (HIL) with micro-contact printing (μCP). HIL is a high-temperature surface-forming process in which a micromachined master is pressed into a thermoplastic polymer at elevated temperature [38]. HIL can replicate features as small as 10 nm [39], is scaleable to large surface areas and works for most thermoplastic polymers, expanding the choice of substrate material to include standard thermoplastics, conductive polymers, and biodegradable polymers such as those used in tissue engineering scaffolds. This advancement in cell culture substrate fabrication allows chemical pattern geometry to be decoupled from the mechanical topography such that the mechanical topography neither determines nor limits the configuration of the chemical pattern. The fabrication technique is scalable to very large areas in the 100 cm^2 range, and could pattern features smaller than 100 nm in lateral size. These combined topographical-chemical substrates allow investigation of the relative impact of the two patterns on cell contact guidance and greatly expands the choice of materials and surface chemistries to those not previously accessible for cell substrates.

4.2 Materials and Methods

4.2.1 Hot-embossing imprint lithography

To generate mechanical topography, a uniformly-heated temperature-controlled press was used to emboss a microstructured silicon master into a film of uncured polyimide shown in Figure 4.1. The silicon masters were made using standard photolithography and deep reactive ion etching to a depth of 4 μm. The master vertical sidewalls were smoothed by thermally growing silicon dioxide that was then stripped.

The microstructured polymer surfaces were prepared starting with a 8.5 μm thick layer of PI2525 polyimide (HD Microsystems), spin-coated onto a silicon wafer, and soft-baked to purge the solvent. For embossing, a preload of <5 N was applied while the temperature was ramped to 150˚C. The load was then increased to 1.8 kN and maintained for 10 minutes. The samples were allowed to cool prior to separation. The process resulted in a complete relief replication of the master in the polyimide with 8 μm wide grooves 4 μm deep separated by 16 μm wide mesas, uniformly covering the 8 mm square substrate. The substrates were baked until fully cured according to the manufacturer's specifications. Using an electron beam evaporator, a 10 nm thick layer of titanium and then a 20 nm thick layer of gold were coated onto the substrate. Smooth substrates were prepared identically except that a polished wafer was used as a master for the embossing, to ensure smoothness and that control substrates were exposed to the same chemical and temperature history as the test substrates. Through SEM observation, smooth substrates did not have feature sizes larger than 5 nm.

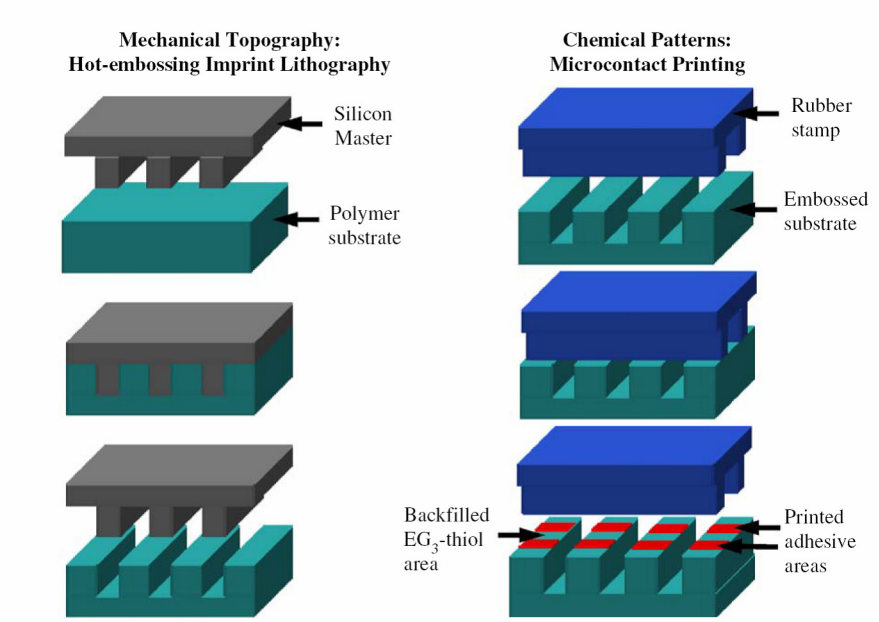

Figure 4.1 Hot embossing imprint lithography and micro-contact printing combine to manufacture the cell substrates. HIL forms microgrooves by pressing a silicon master into a thermoplastic at elevated temperature. μCP forms chemical patterns by depositing alkanethiol ink where the stamp contacts the substrate. The two patterns are formed in independent steps, and thus the chemical pattern is independent from the mechanical topography.

4.2.2 Micro-contact printing

Substrates were prepared with mechanical topography only, fibronectin-coated chemical patterns only, or a combination of mechanical topography overlaid with various chemical patterns. Table 4.1 lists all configurations of substrates. The spacing of the grooves, 16 μm, was chosen to be less than the typical diameter of a spread cell (30-50 μm). The fibronectin lane width at 10 μm was chosen to be smaller than a cell diameter in order to elicit cell confinement to the lane. A mechanically patterned topographical substrate with uniform fibronectin coating was the mechanical topography baseline, a smooth substrate with fibronectin lanes separated by EG3-functionalized regions was the chemical pattern baseline, and a smooth HDT substrate with uniform fibronectin coating

was included as an unpatterned control. It was expected that for the combined samples, the orthogonal arrangement of mechanical topography and chemical patterns would induce a type of "tug-of-war" where cells aligned to the dominant pattern, thus illustrating the relative impact of each pattern on cellular alignment. Fibronectin lane spacings were chosen to be (i) less than the embossed groove spacing at 10 μm, (ii) similar to the groove spacing at 20 μm, (iii) larger than the groove spacing at 50 μm, and (iv) a distance which cells would not normally span at 100 μm. Each configuration was analyzed in three separate replicate experiments.

Sample	Mechanical Topography	Surface Chemistry	Average Alignment Angle	Percentage Cells Aligned (within 10°)
Unpatterned Control	**Smooth** no mechanical patterns	**Uniform Fibronectin** coating on CH_3 terminated SAMs	48.3° *Alignment to arbitrary reference	8.5% *Alignment to arbitrary reference
Mechanical Topography Baseline	**Embossed** 8 μm grooves separated by 16 μm mesas	**Uniform Fibronectin** coating on CH_3 terminated SAMs	9.6°	73.2%
Chemical Pattern Baseline	**Smooth** no mechanical patterns	**Fibronectin Lanes** 10 μm wide spaced by 20 μm wide lanes of PEG terminated SAMs	81.9° *Alignment to fibronectin lanes	80.6% *Alignment to fibronectin lanes
Combined 10	**Embossed** 8 μm grooves separated by 16 μm mesas	**Fibronectin Lanes** 10 μm wide spaced by 10 μm wide lanes of PEG terminated SAMs	12.4°	65.9%
Combined 20	**Embossed** 8 μm grooves separated by 16 μm mesas	**Fibronectin Lanes** 10 μm wide spaced by 20 μm wide lanes of PEG terminated SAMs	11.9°	67.1%
Combined 50	**Embossed** 8 μm grooves separated by 16 μm mesas	**Fibronectin Lanes** 10 μm wide spaced by 50 μm wide lanes of PEG terminated SAMs	13.7°	54.0%
Combined 100	**Embossed** 8 μm grooves separated by 16 μm mesas	**Fibronectin Lanes** 10 μm wide spaced by 100 μm wide lanes of PEG terminated SAMs	12.2°	62.4%

Alignment is taken with respect to mechanical lines except where indicated.

Table 4.1 Description of sample configurations and resulting alignments. Substrates had either topography, chemistry, or a combination of the two. The combination substrates had the same topography, with chemical patterns whose spacings vary from below that of the topography to larger than a spread cell. Cells aligned strongly to either mechanical topography or chemical patterns when presented separately. On all combined substrates, cells aligned to the mechanical topography rather than the chemical patterns.

4.2.3 Cell alignment

MC3T3-E1 osteoblast-like cells were cultured on the patterned substrates and cell alignment was analyzed via fluorescence microscopy and image analysis. Cells were seeded at 450 cells/mm^2 on the substrates and cultured for 24 hours in α-minimal

essential medium supplemented with 10% fetal bovine serum and 1% penicillin-streptomycin. For immunostaining, cells were permeabilized in 0.1% Triton X-100 and fixed in 3.7% formaldehyde. Samples were incubated in anti-fibronectin rabbit antibody for 1 hour followed by AlexaFluor 488-conjugated anti-rabbit IgG antibody and Hoescht DNA stain for 1 hour. A Nikon E600 epifluorescence microscope equipped with a Spot RT low light camera and ImagePro was used to collect and analyze all cell images. Each cell nucleus was fit with an ellipse, and the angle of the major axis of the elliptical cell nucleus was determined. Previous studies indicated that nuclear alignment angle gave a reliable and robust indication of overall cellular alignment as determined by actin cytoskeleton and nuclear staining.[15] The measurements of the magnitude of the nuclear alignment angle resulted in non-normal histograms with data ranging 0° - 90°. For each substrate configuration, over 100 data points taken from 3 replications of the experiment were analyzed using a Wilcoxon Rank Sum test with $p < 0.05$ considered statistically significant. Cell orientation was quantified by (i) the fraction of cells aligned to within 10° of the major substrate features, and (ii) the average alignment angle of cells on a given substrate type. Cells were considered strongly aligned when their nuclear orientation is close to the orientation of the substrate features. For each substrate configuration, average alignment angles of each replication did not differ significantly.

4.3 Results

4.3.1 Hot-embossed and micro-contact printed substrates

The substrate surface morphology and topographic features were examined with SEM. The HIL process produced relief replicas of the master while maintaining feature fidelity. Resulting grooves were 4 μm deep, 8 μm wide, spaced by 16 μm wide mesas. Feature dimensions both before and after the metal coating process were the same, indicating no damage to the samples during metal coating. After μCP and etching, substrates were once again examined with SEM. The HDT chemical lanes served as an etch mask, and thus the resultant substrate had HDT-functionalized gold lanes spaced by titanium areas that were not HDT protected as shown in Figure 4.2. The etched substrates served as clear illustrations of the combined mechanical topography and chemical patterning technique as well as subjects to dimensionally characterize the printing process.

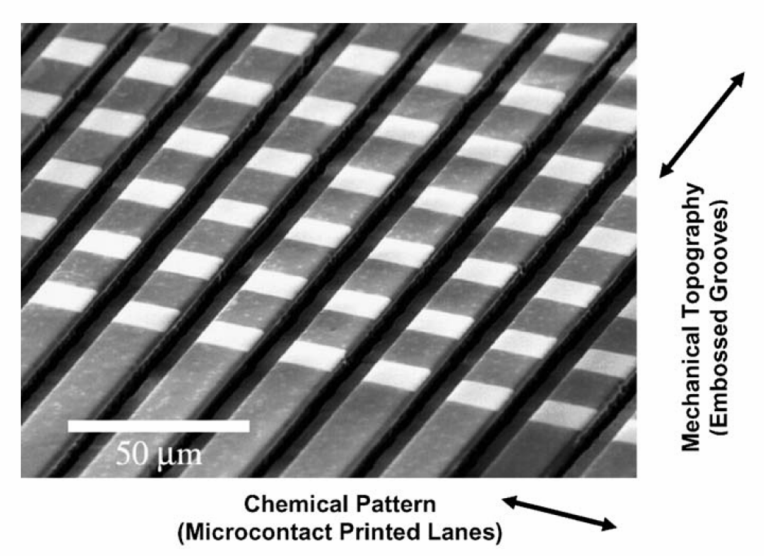

Figure 4.2 A test substrate with mechanical topography combined with chemical patterns. During etching, the micro-contact-printed HDTs protected gold areas that appear white in the image. Unprotected areas that have been etched to the titanium layer are grey.

Cell culture substrates, after μCP, EG_3-thiol backfilling, and fibronectin solution incubation, were immunostained and examined via microscopy. This approach resulted in a substrate with a chemical pattern of fibronectin-coated HDT lanes spaced by non-fouling EG_3-thiol domains that ran orthogonal to the mechanical topography of the embossed grooves as shown in Figure 4.3. Breaks in the fibronectin lanes corresponded to intersections with the 8 μm wide grooves.

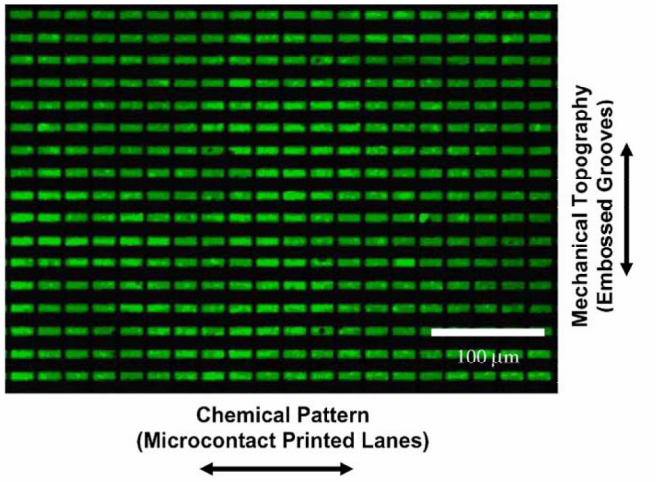

Figure 4.3 A cell culture substrate with mechanical topography and fibronectin patterns. The μCP HDT lanes allow adsorption of fibronectin, while the EG_3-thiol backfilled domains remain bare.

4.4 Alignment of osteoblasts to surface patterns

The relative impact of mechanical topography vs. chemical patterning on cell alignment was evaluated by comparing average alignment angles for substrates with each patterning type. First the extent of cellular alignment on the two patterns was evaluated separately to create baseline data on samples having either mechanical topography only or chemical patterns only. The baseline data was then compared to cellular alignment on

substrates with consistent mechanical topography overlaid with various chemical patterns in order to observe the relative impact of the two on cellular alignment. For a given field of osteoblasts on a substrate, the nuclei and actin cytoskeleton were observed separately using IF techniques. The alignment of the overall cytoskeleton and the alignment of the nucleus were in agreement for >95% cells Figure 4.4.

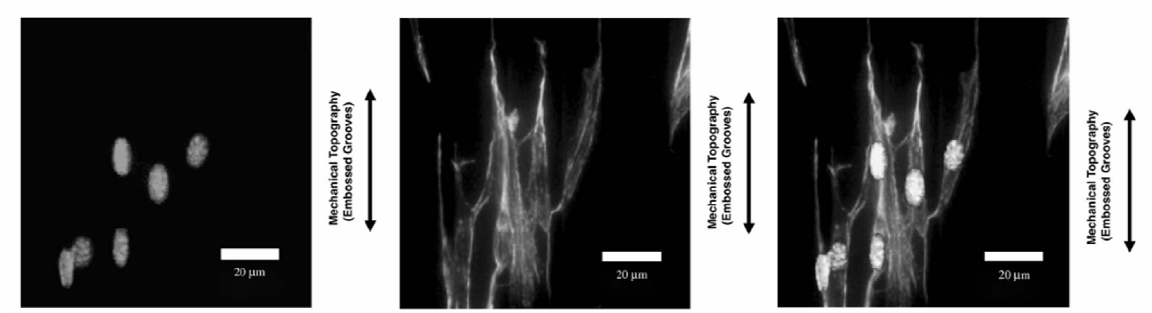

Figure 4.4 Immunofluoresence images of one location of osteoblasts on a grooved substrate. The nuclei (left) and the cytoskeletons (middle) align in the direction of the microgrooves. When viewed together (right) it is clear that nuclear alignment is an accurate indicator of overall cellular alignment.

All samples were compared qualitatively by IF images and quantitatively with histograms of average nuclear alignment angles Figure 4.5. Average alignment angle and percentage of aligned cells are summarized in Table 4.1. On the mechanical topography baseline, which had mechanical topography grooves and uniform surface chemistry, cells strongly aligned to the grooves. Over 73% of the cells aligned to within 10˚ of the mechanical topography and the average alignment angle was 9.6˚, close to the mechanical topography oriented at 0˚. On the chemical pattern baseline, which was smooth but printed with fibronectin lanes, more than 80% of the cells aligned to the chemical pattern and the average alignment angle was 81.9˚, close to the chemical pattern orientation of 90˚. The chemical pattern baseline result was in agreement with previous

reports where chemical patterns confined cells and induced alignment [23, 33, 40-50]. When presented alone, both the mechanical topography and the chemical pattern significantly influenced cell alignment.

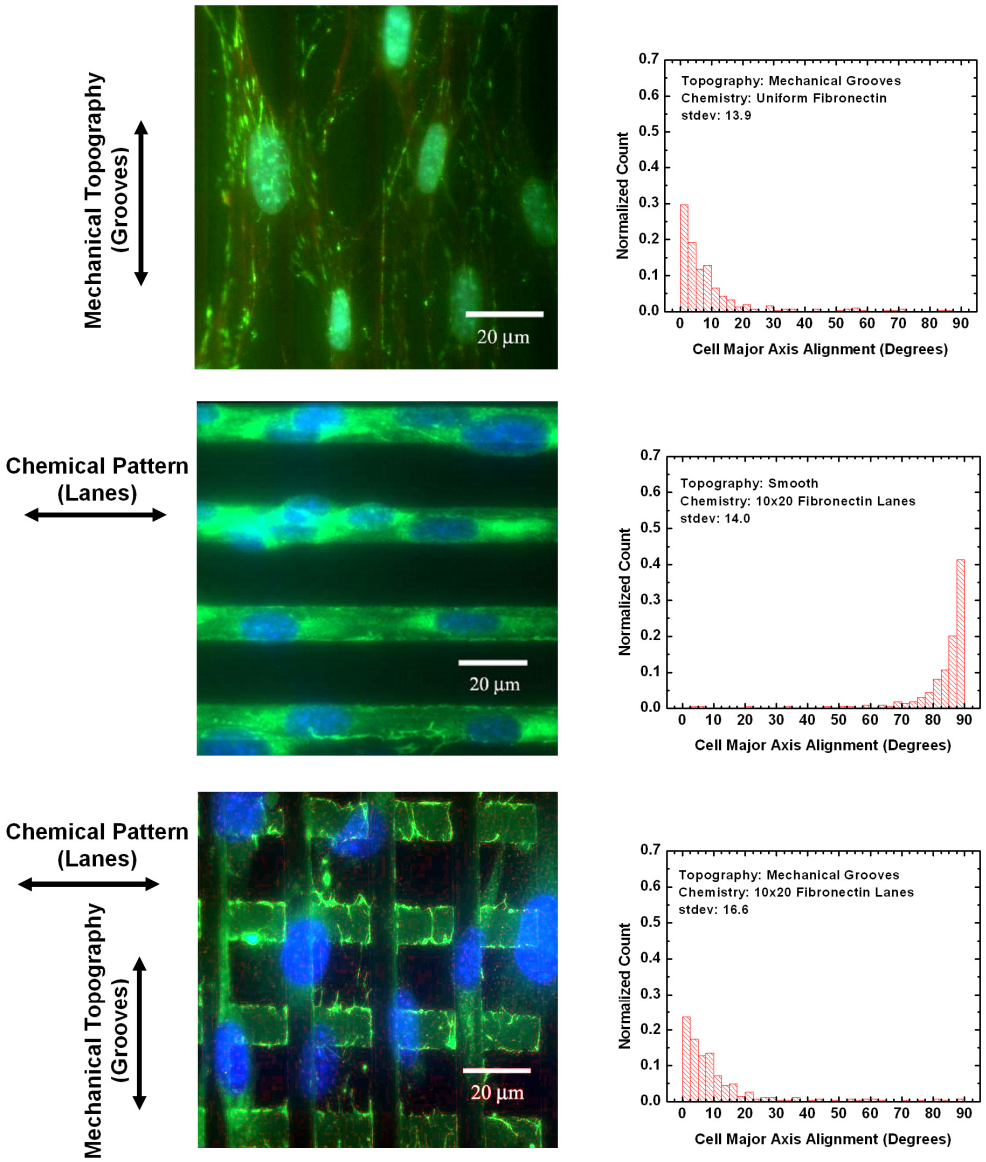

Figure 4.5 Immunofluoresence images of cells on patterned substrates with corresponding histograms of cell alignment angle. Grooves are vertical (0˚) and lanes are horizontal (90˚). Cells showed strong alignment to mechanical grooves (top) and stronger alignment to protein lanes (middle) when presented separately. When presented combined mechanical grooves and orthogonal protein lanes on one substrate, the cells align to the mechanical grooves (bottom).

Cells were cultured on substrates having combined mechanical topography and chemical patterns in order to determine the relative impact of the two patterning methods on cell alignment. The substrates had fibronectin lanes overlaid orthogonally to the mechanical grooves, with the same groove width and chemical lane width as the baseline samples. The cell alignment data was distributed such that alignment to the mechanical grooves occurred at 0˚ and alignment to the fibronectin lanes occurred at 90˚. Remarkably, over 65% of cells aligned to the mechanical grooves rather than the fibronectin lanes. The average alignment angle was almost 12˚, close to the mechanical baseline. The cell alignment angle was more broadly distributed than either baseline sample. Although the mechanical topography dominated the alignment over the chemical pattern, the presence of chemical patterns on the combined substrate influenced the fraction of cells aligned and average alignment angle. To determine impact of chemical lane spacing on alignment, cells were cultured on substrates with the same topographical pattern as above but each with different fibronectin lane spacing. Table 4.1 shows a description of all substrate types and data for cell alignment and average angle. As spacing of the fibronectin lanes increased from 10 μm to 100 μm on grooved substrates, cells remained aligned to the grooves and average alignment angles for all combined substrates were similar. In all cases, regardless of chemical pattern spacing, the cells preferentially aligned to the mechanical grooves bridging up to 50 μm of non-adhesive EG_3-functionalized domains.

4.5 Discussion

This study showed the mechanical topography dominating the alignment mechanism over the chemical patterns for the pattern feature sizes examined. Although nuclear alignment was used as a quantitative measure of alignment, actin cytoskeletons and overall cell bodies aligned in a consistent fashion. Cells were located on mesas and in grooves, although more cells were located on mesas for samples with chemical and mechanical patterns due to the adhesive areas being located only on the mesas. Cells were located not only on the fibronectin patterns but also on the non-adhesive areas as well. IF staining for fibronectin indicated that focal adhesion clusters were present on adhesive areas.

Pattern continuity had significant impact on the results of this experiment. In the configurations presented, the printed fibronectin lanes did not reach the bottom of the grooves, resulting in a *discontinuous* chemical pattern with cells aligning to the mechanical topography. In contrast, Britland et al. used *continuous* chemical lanes which dominated the alignment of cells over the effects of the underlying mechanical topography [37]. Since it has been observed on chemically patterned substrates that cells tend to migrate along the patterns eventually aligning to them [28], the alignment mechanism may depend on directed migration. In this study, migration distance along the lanes was quite limited since the grooves bounded the chemical lanes. This may indicate that the extent of cellular alignment due to chemical patterns depends on continuous, well-defined features that allow significant directed migration of the cells.

Limited adhesive interactions with the substrate did not impair contact guidance due to mechanical topography. Cells were often found in or bridging the non-adhesive areas and

that adhesive areas were limited to the top of the mesas. Therefore, cellular contact with the mechanical topography on adhesive domains was very limited. This limited interaction becomes more severe as the chemical lane spacing increases and a smaller fraction of the substrate is patterned with adhesive chemistry. However, cells interacted with the topography and aligned to it to the same extent regardless of the increasing lane spacing and the consequently decreasing fraction of adhesive interaction. It has been proposed by several groups that focal contacts and actin nucleation are the initial response to topography and are critical in cellular response to topography including alignment [37, 51, 52]. In this study, focal contacts were not predominantly aligned to features and were somewhat limited in quantity due to the lack of adhesive area. In this case, cellular response to topography may be predominantly guided by more of a tactile mechanism such as filopod or cell protrusion guidance as proposed by Teixeira et al. [30] and guided to a more limited extent by adhesive interaction and focal contact alignment.

In this study, although chemical patterns induced stronger alignment than mechanical topography when presented separately, mechanical topography dominated alignment for all chemical patterns when combined. Instead of significantly inducing alignment, the chemical patterns in this study served as preferred attachment sites for the cells, often resulting in consistent spacing between cells. As noted by Clark et al., cells at the edges of cell colonies responded differently to topographical cues than cells that were separate from the colonies [53]. The technique presented here ensured that cells were more consistently spaced so the effects of cell colonies on mechanical topography guidance were minimized.

Since it was observed that chemical patterning alone had a stronger impact on cellular alignment than mechanical topography alone, the chemical lane spacing was varied in this

experiment rather than the mechanical topography spacing. However, previous work has shown that both mechanical topography spacing and depth can influence the extent of cell alignment [29, 53]. The results presented here apply to the specific pattern sizes and surface chemistry examined, and the dominance of mechanical or chemical patterns may change as feature sizes are altered or substrate chemistry is changed. Therefore, by varying mechanical topography dimensions or surface chemistry, it may be possible to create substrates with minimal alignment due to mechanical topography thereby allowing chemical patterns to dominate cellular alignment. Future experiments must investigate the effects of size, shape, spacing, and pattern continuity for both mechanical and chemical features in order to gage relative impact of the patterns on cellular adhesion, motility, and contact guidance.

4.6 Conclusion

This chapter presents a method to manufacture substrates for cell culture with independently fabricated mechanical topography and chemical patterns. The manufacturing technique is highly scalable, is amenable to features from 10 nm to above 1 mm, and greatly expands the number of substrates and chemistries that could be used to study cell responses. When presented with either the mechanical topography or the chemical lanes alone, the cells significantly aligned to the pattern presented. When presented with a combination of the features, the cells responded to and aligned preferentially with the mechanical features in every sample type considered. A wide range of polymer substrate materials could be employed and the technique is scalable to large surface areas suitable for culturing large cell populations. In addition, this method

of substrate manufacturing requires no cleanroom facilities. A key feature of the technique is its ability to independently control mechanical and chemical features on a surface, allowing progress towards answering questions regarding the relative impact of surface topography and chemical patterns on cell-substrate interaction.

4.7 References

[1] Anderson JM. Biological responses to materials. Annu Rev Mater Res. 2001;31:81-110.

[2] Hench LL, Polak JM. Third-generation biomedical materials. Science. 2002 Feb;295(5557):1014-+.

[3] Vreeland WN, Barron AE. Functional materials for microscale genomic and proteomic analyses. Current Opinion in Biotechnology. 2002 Apr;13(2):87-94.

[4] Hubbell JA. Materials as morphogenetic guides in tissue engineering. 2003;14(5):551-8.

[5] Curtis ASG, Wilkinson CD. Reactions of cells to topography. Journal of Biomaterials Science-Polymer Edition. 1998;9(12):1313-29.

[6] Castner DG, Ratner BD. Biomedical surface science: Foundations to frontiers. Surface Science. 2002;500(1-3):28-60.

[7] Curtis A, Wilkinson C. Topographical Control of Cells. Biomaterials. 1997 Dec;18(24):1573-83.

[8] Jung DR, Kapur R, Adams T, Giuliano KA, Mrksich M, Craighead HG, et al. Topographical and physicochemical modification of material surface to enable patterning of living cells. Critical Reviews in Biotechnology. 2001;21(2):111-54.

[9] Flemming RG, Murphy CJ, Abrams GA, Goodman SL, Nealey PF. Effects of synthetic micro- and nano-structured surfaces on cell behavior. Biomaterials. 1999 Mar;20(6):573-88.

[10] Weiss P. Experinments on cell and Axon Orientation in Vitro. Journal of Experimental Zoology. 1945;100(3):353-86.

[11] Baac HW, Lee JH, Seo JM, Park TH, Chung H, Lee SD, et al. Submicron-scale topographical control of cell growth using holographic surface relief grating. Materials Science & Engineering C-Biomimetic and Supramolecular Systems. 2004 Jan;24(1-2):209-12.

[12] Motlagh D, Senyo SE, Desai TA, Russell B. Microtextured substrata alter gene expression, protein localization and the shape of cardiac myocytes. Biomaterials. 2003 Jun;24(14):2463-76.

[13] Wang JHC, Grood ES, Florer J, Wenstrup R. Alignment and proliferation of MC3T3-E1 osteoblasts in microgrooved silicone substrata subjected to cyclic stretching. Journal of Biomechanics. 2000;33:729-35.

[14] Schmidt J, von Recum AF. Macrophage response to microtextured silicone. Biomaterials. 1992;13:1059-69.

[15] Charest JL, Bryant LE, Garcia AJ, King WP. Hot embossing for micropatterned cell substrates. Biomaterials. 2004;25(19):4767-75.

[16] Mata A, Boehm C, Fleischman A, Muschler G, Roy S. Analysis of connective tissue progenitor cell behavior on polydimethylsiloxane smooth and channel micro-textures. Biomedical Microdevices. 2002;4:267-75.

[17] Yim KF, Reano RM, Pang SW, Yee AF, Chen CS, Leong KW. Nanopattern-induced changes in morphology and motility of smooth muscle cells. Biomaterials. 2005;26:5405-13.

[18] van Kooten TG, von Recum AF. Cell adhesion to textured silicone surfaces: The influence of time of adhesion and texture on focal contact and fibronectin fibril formation. Tissue Engineering. 1999 Jun;5(3):223-40.

[19] Dalby MJ, Giannaras D, Riehle MO, Gadegaard N, Affrossman S, Curtis ASG. Rapid fibroblast adhesion to 27 nm high polymer demixed nano-topography. Biomaterials. 2004 Jan;25(1):77-83.

[20] Walboomers XF, Croes HJE, Ginsel LA, Jansen JA. Contact guidance of rat fibroblasts on various implant materials. Journal of Biomedical Materials Research. 1999 Nov;47(2):204-12.

[21] Zinger O, Zhao G, Schwartz Z, Simpson J, Wieland M, Landolt D, et al. Differential regulation of osteoblasts by substrate microstructural features. Biomaterials. 2005;26:1837-47.

[22] Gallant ND, Capadona JR, Frazier AB, Collard DM, Garcia AJ. Micropatterned surfaces for analyzing cell adhesion strengthening Langmuir. 2002 2002;18:5579-84.

[23] Mrksich M, Dike LE, Tien J, Ingber DE, Whitesides GM. Using Microcontact Printing to Pattern the Attachment of Mammalian Cells to Self-Assembled Monolayers of Alkanethiolates on Transparent Films of Gold and Silver. Experimental Cell Research. 1997;235:305-13.

[24] Mrksich M, Dike LE, Tien J, Ingber DE, Whitesides GM. Using microcontact printing to pattern the attachment of mammalian cells to self-assembled monolayers of alkanethiolates on transparent films of gold and silver. Experimental Cell Research. 1997 1997/09/15/;235(2):305-13.

[25] Bhatia SN, Yarmush ML, Toner M. Controlling cell interactions by micropatterning in co-cultures: hepatocytes and 3T3 fibroblasts. Journal of Biomedical Materials Research. 1997 1997/02//;34(2):189-99.

[26] Vozzi G, Flaim C, Ahluwalia A, Bhatia S. Fabrication of PLGA scaffolds using soft lithography and microsyringe deposition. Biomaterials. 2003 2003/06//;24(14):2533-40.

[27] Brunette DM. Fibroblasts on Micromachined Substrata Orient Hierarchically to Grooves of Different Dimensions. Experimental Cell Research. 1986 May;164(1):11-26.

[28] Li S, Bhatia SN, Hu Y-L, Li Y-S, Usami S, Chien S. Effect of Morphological Patterning on Endothelial Cell Migration. Biorheology. 2001;28:101-8.

[29] Gray BL, Lieu DK, Collins SD, Smith RL, Barakat AI. Microchannel Platform for the Study of Endothelial Cell Shape and Function. Biomedical Microdevices. 2002;4:9-16.

[30] Teixeira AI, Abrams GA, Bertics PJ, Murphy CJ, Nealey PF. Epithelial contact guidance on well-defined micro- and nanostructured substrates. Journal of Cell Science. 2003 May 15;116(10):1881-92.

[31] Svitkina T, Rovensky Y, Bershadsky A, Vasiliev J. Transverse pattern of microfilament bundles induced in epitheliocytes by cylindrical substrata. Journal of Cell Science. 1995;108:735-45.

[32] Tai HC, Buettner HM. Neurite outgrowth and growth cone morphology on micropatterned surfaces. Biotechnology Progress. 1998 May-Jun;14(3):364-70.

[33] Mrksich M, Chen CS, Xia Y, Dike LE, Ingber DE, Whitesides GM. Controlling cell attachment on contoured surfaces with self-assembled monolayers of alkanethiolates on gold. ProcNatlAcadSciUSA. 1996;93(20):10775-8.

[34] Revzin A, Tompkins RG, Toner M. Surface Engineering with Poly(ethlyne glycol) Photolithography to Create High-Density Cell Arrays on Glass. Langmuir. 2003;19:9855-62.

[35] Miller C, Jeftinija S, Mallapragada S. Synergistic effects of physical and chemical guidance cues on neurite alignment and outgrowth on biodegradable polymer substrates. Tissue Engineering. 2002 Jun;8(3):367-78.

[36] Dusseiller MR, Schlaepfer D, Koch MK, Kroschewski R, Textor M. An inverted microcontact printing method on topographically structured polystyrene chips for arrayed micro-3-D culturing of single cells. Biomaterials. 2005;26:5917-25.

[37] Britland S, Morgan H, Wojiak-Stodart B, Riehle M, Curtis A, Wilkinson C. Synergistic and Hierarchical Adhesive and Topographic Guidance of BHK Cells. Experimental Cell Research. 1996;228:313-25.

[38] Chou SY, Krauss PR, Renstrom PJ. Imprint lithography with 25-nanometer resolution. Science. 1996 Apr 5;272(5258):85-7.

[39] Chou SY, Krauss PR, Zhang W, Guo L, Zhuang L. Sub-10 nm imprint lithograpy and applications. Journal of Vacuum Science & Technology B. 1997;15(6):2897-904.

[40] Ilic B, Craighead H. Topographical patterning of chemically sensitive biological materials using a polymer-based dry lift off. Biomedical Microdevices. 2000;2(4):317-22.

[41] James CD, Davis R, Meyer M, Turner A, Turner S, Withers G, et al. Aligned microcontact printing of micrometer-scale poly-L-lysine structures for controlled growth of cultured neurons on planar microelectrode arrays. Ieee Transactions on Biomedical Engineering. 2000 Jan;47(1):17-21.

[42] Pan YV, McDevitt TC, Kim TK, Leach-Scampavia D, Stayton PS, Denton DD, et al. Micro-scale cell patterning on nonfouling plasma polymerized tetraglyme coatings by protein microcontact printing. Plasmas and Polymers. 2002 Jun;7(2):171-83.

[43] Morra M, Cassinelli C. Cell adhesion micropatterning by plasma treatment of alginate coated surfaces. Plasmas and Polymers. 2002 Jun;7(2):89-101.

[44] Yousaf MN, Houseman BT, Mrksich M. Using electroactive substrates to pattern the attachment of two different cell populations. Proceedings of the National Academy of Sciences of the United States of America. 2001 May 22;98(11):5992-6.

[45] Kang IK, Kim GJ, Kwon OH, Ito Y. Co-culture of hepatocytes and fibroblasts by micropatterned immobilization of beta-galactose derivatives. Biomaterials. 2004 Aug;25(18):4225-32.

[46] Irimia D, Karlsson JOM. Development of a cell patterning technique using poly(ethylene glycol) disilane. Biomedical Microdevices. 2003 Sep;5(3):185-94.

[47] Kaji H, Kanada M, Oyamatsu D, Matsue T, Nishizawa M. Microelectrochemical approach to induce local cell adhesion and growth on substrates. Langmuir. 2004 Jan 6;20(1):16-9.

[48] Dike LE, Chen CS, Mrksich M, Tien J, Whitesides GM, Ingber DE. Geometric Control of Switching Between Growth, Apoptosis, and Differentiation during Angiogenesis using Micropatterned Substrates. In Vitro Cell Developmental Biology - Animal. 1999;35:441-8.

[49] Magnani A, Priamo A, Pasqui D, Barbucci R. Cell behaviour on chemically microstructured surfaces. Materials Science & Engineering C-Biomimetic and Supramolecular Systems. 2003 Mar 3;23(3):315-28.

[50] Veiseh M, Wickes BT, Castner DG, Zhang M. Guided Cell Patterning on Gold-Silicon Dioxide Substrates by Surface Molecular Engineering. Biomaterials. 2004;25:3315-24.

[51] Matsuzaka K, Walboomers F, de Ruijter A, Jansen JA. Effect of microgrooved poly-l-lactic (PLA) surfaces on proliferation, cytoskeletal organization, and mineralized matrix formation of rat bone marrow cells. Clinical Oral Implants Research. 2000 Aug;11(4):325-33.

[52] Walboomers XF, Croes HJE, Ginsel LA, Jansen JA. Growth behavior of fibroblasts on microgrooved polystyrene. Biomaterials. 1998 Oct;19(20):1861-8.

[53] Clark P, Connolly P, Curtis ASG, Dow JAT, Wilkinson CDW. Topographical Control of Cell Behavior 2. Multiple Grooved Substrata. Development. 1990 Apr;108(4):635-44.

CHAPTER 5

POLYMER CELL CULTURE SUBSTRATES WITH COMBINED NANOTOPOGRAPHICAL PATTERNS AND MICROPATTERNED CHEMICAL DOMAINS

A combination of nanoimprint lithography and micro-contact printing was used to create cell substrates with well-defined nanotopographic patterns of grooves overlaid with independently controlled micropatterned chemical domains. Qualitative analysis of osteoblast-like cells cultured on the substrates showed alignment of cells and cell features to the nanotopographic grooves when surface chemistry was either uniform or a pattern of dots. When surface chemistry on the substrate was a pattern of lanes, cells aligned to the lanes. On all substrates, small cellular extensions, or filopodia, displayed no particular alignment to either nanotopographic grooves or chemical patterns. Large cell extensions were observed only parallel to either nanotopographic grooves or chemical lanes. The techniques used provide an easily-scaleable approach to creating cell substrates that will aid in studying the relative impact and interplay of chemical patterns and mechanical topography on cellular responses.

5.1 Introduction

The success of biomedical implants depends on the interaction of host cells with the biomaterial surface. Micro- and nano-scale patterns of both mechanical topography

and chemistry elicit cellular responses, although the relative impact and interplay of the topography vs. chemical patterns is not well understood. This chapter reports a method to fabricate cell culture substrates that combines nanoscale topography with independently controlled microscale chemical patterns. The chapter further reports qualitative responses of osteoblast-like cells grown on these surfaces.

Several groups have examined the effect of either mechanical topography or chemical patterns on cellular activities using various substrate materials [1-4]. Mechanical topography, defined here as deliberately constructed features with vertical dimensions and regular patterns, can influence cell morphology [5-9], migration [10-12], focal adhesion density and size [13], spreading [14], contact guidance [15], and differentiation [16]. Surface chemical patterns can influence cellular responses such as adhesion [17], shape and function [18], attachment location [19], and can produce co-cultures of cells [20]. Since mechanical topography and chemistry can impact cellular activities, each must be well controlled in order to fully understand biomaterial-cell interactions.

While it is well established that mechanical topography and chemical patterns influence cell-substrate interactions, the interplay of these two properties in regulating cellular activities remains poorly understood. Some studies report cell responses to mechanical topography for various surface chemistries [21-23], although the chemical patterns in these studies were concurrent with the mechanical topography. Photolithography has produced independent chemical patterns on mechanical topography to manipulate cellular responses [24], but requires cleanroom equipment not readily applicable to biological applications or nanoscale topographic features.

This chapter combines Nanoimprint Lithography (NIL) [25] to emboss well-defined nanoscale topographic features on polymer cell substrates with micro-contact printing (μCP) [26] to overlay independent chemical patterns onto the topography. Neither technique requires cleanroom equipment or toxic chemicals. Both processes are highly scaleable and applicable to implantable biomaterials. Cellular response to the resulting combined mechanical topography and chemical patterns is analyzed through scanning electron microscopy (SEM) and Immunofluoresence (IF) microscopy. Cells predominantly align to and extend along the nanogrooves on a substrate with a uniform chemistry. On a substrate with a non-continuous chemical pattern, the cells align to and extend along the nanogrooves rather than remaining constrained by the chemical pattern. However, on a substrate with a continuous chemical pattern, such as lanes, the cells align to and extend along the chemical pattern rather than the orthogonal nanogrooves.

5.2 Experimental Approach

NIL is a forming process in which a master with nanoscale features is pressed into a thermoplastic polymer resulting in a relief replica of the master on the substrate [25]. Figure 5.1 shows the NIL thermal embossing process. To fabricate the cell substrates, a nickel stamp with a 100 nm grating pattern was used as a master. The nickel stamp was fabricated by using NIL and an electroforming process. Using a Nanonex2000 NIL tool, silicon wafers coated in resist were imprinted with the 100 nm grating pattern. After gold coating, the wafers were placed into a Digital Matrix SA/3m 3 station electroforming machine containing a standard nickel sulfamate bath. Electro deposition produced a 1 mm thick nickel layer, which was then released from the wafer as the nickel stamp.

Figure 5.2 shows an SEM of the nickel stamp master. The resulting master lost no feature fidelity through dozens of embossing cycles and released easily from the substrates after embossing with no release layer present.

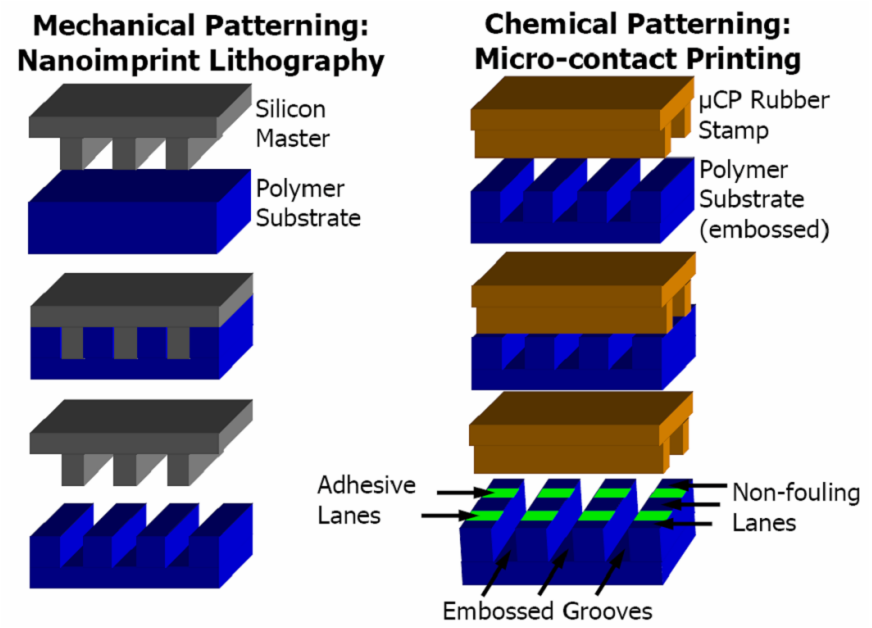

Figure 5.1 Nanoimprint Lithography creates nanoscale surface topography on a cell substrate by pressing a nickel master into a thermoplastic at elevated temperature. Micro-contact printing creates chemical patterns that are independent of the surface topography by depositing alkanethiol ink where the stamp contacts the substrate.

A polycarbonate sheet (Goodfellow CT303050) was loaded into a temperature-controlled press with the nickel stamp on top of it. The temperature was increased under light load, held steady as the load was increased, held constant with constant load for the prescribed embossing time, then reduced to room temperature under constant load. A relief replication of the master in the polycarbonate was produced with a pattern of grooves 100 nm wide by 100 nm deep on a 200 nm pitch uniformly covering the 79 cm^2 substrate. The substrate was then cut into 1 cm square substrates that were evaporative coated with a 10 nm thick titanium layer and a subsequent 20 nm thick gold layer to accommodate the subsequent μCP. Substrates were examined via SEM before and after

the coating process to ensure that feature sizes were not significantly altered due to polymer melt. Figure 5.2 shows the polycarbonate substrate after the metal coating process.

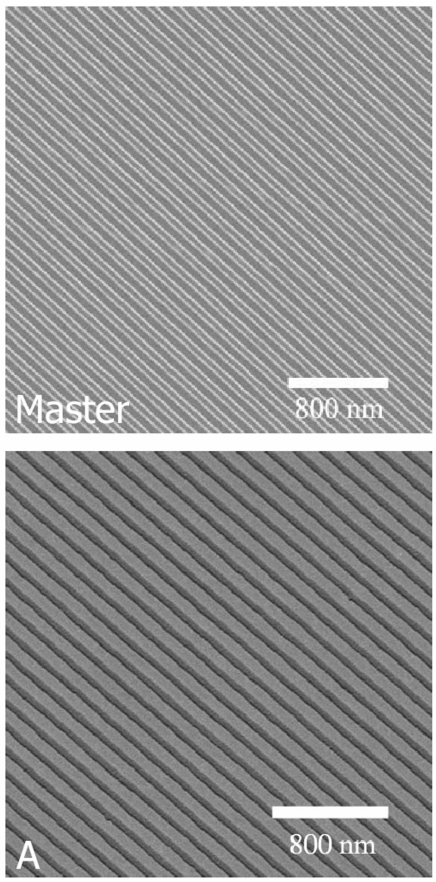

Figure 5.2 The nickel stamp master (top) created through electroplating a resist patterned using a Nanonex NIL system. The polycarbonate cell substrate A (bottom) created using the nickel master and NIL. Both images are viewed from top down.

Micro contact printing [26-28] was used to contact transfer a chemical pattern onto the substrate. Poly(dimethylsiloxane) (PDMS) (Dow Corning Sylgard® 184) stamps with the desired chemical micropatterns were swabbed with hexadecanethiol (HDT), allowed to dry, then brought into contact with the gold-coated substrate. Figure 5.1 shows the process. Both stamps and substrates had alignment marks to guide alignment of the raised mesas of the stamp to the mechanical topography of the substrate. Three types of substrates were fabricated by varying the chemical pattern that was

overlaid onto the nanoscale topography. Substrate A had a uniform chemical pattern on the topography, substrate B had a chemical pattern of 10 μm diameter dots on the topography, and substrate C had a chemical pattern of 10 μm wide lanes that ran perpendicular to the nanogrooves of the topography. A substrate of smooth polycarbonate with uniform chemistry served as a control. For all trials, each substrate type was replicated 4 times. To characterize the μCP chemical patterning technique, printed substrates were etched in KCN to remove gold not protected by the HDT. The resulting substrate had HDT-functionalized gold lanes where the stamp inked the substrate spaced by titanium areas that were not chemically printed. Figure 5.3 shows SEM images of the resultant etched substrates, providing a clear illustration of the result of the combined topography and chemical patterning technique.

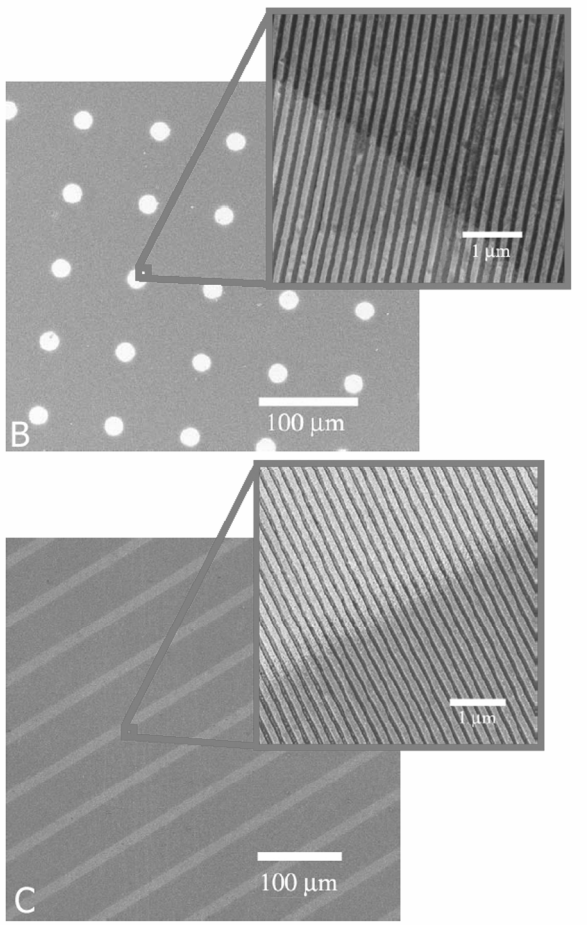

Figure 5.3 μCP creates chemical patterns of lanes and dots on the cell substrates independent of the underlying nanoscale topography.

For cell culture substrates, HDT-terminated patterns were stamped, then the bare gold areas not printed were derivatized with a tri(ethylene glycol)-terminated alkanethiol (EG_3-thiol). Samples were incubated in a 10 μg/mL solution of fibronectin to coat the HDT-printed areas with this bioadhesive protein. The non-fouling properties of the EG_3-thiol prevented protein adsorption and these regions remained resistant to cell adhesion. This resulted in substrates with a chemical pattern of fibronectin-coated HDT areas spaced by non-fouling EG_3-thiol domains. MC3T3-E1 osteoblast-like cells were plated at 350 cells/mm^2, cultured at 37º C in humidified 5% CO_2 in media consisting of 10%

fetal bovine serum and antibiotics in alpha-MEM for 24 hours. They were then fixed and prepared for either SEM or IF microscope observation.

5.3 Results and Discussion

Cells were analyzed for alignment and morphology of overall cell body and small cellular protrusions or filopodia using SEM. Substrate topography integrity was also evaluated after the culturing and fixing processes. Selective IF staining allowed optical microscopy of fibronectin to outline the printed chemical patterns and any fibronectin secreted or recruited by the cells, DNA to show the nuclei of the cells, and actin to show the cells cytoskeletons.

Unpatterned control samples showed typical, randomly oriented cell morphology with no dominant elongation direction and cytoskeletons extending radially from the nuclei. Figure 5.4 shows IF stained cells on the control sample. When cells were presented with the nanogrooves and uniform chemistry of substrate A, marked alignment and orientation along the grooves was observed. This agrees with other groups reporting cellular alignment on nanogrooves [11, 12]. Figure 5.4 shows IF stained cells on A. The cell bodies and nuclei were aligned with the nanogrooves. Predominantly, the cytoskeleton extended from the nuclei to the far ends of the cell body parallel to the nanogrooves. Cytoskeleton extension orthogonal to the nanogrooves was minimal in comparison. Figure 5.5 shows SEM images of the cells on A confirming overall cell body alignment to the nanogrooves. Small filopodia extended in all directions, regardless of groove orientation, while large cell protrusions were seen parallel to the nanogrooves.

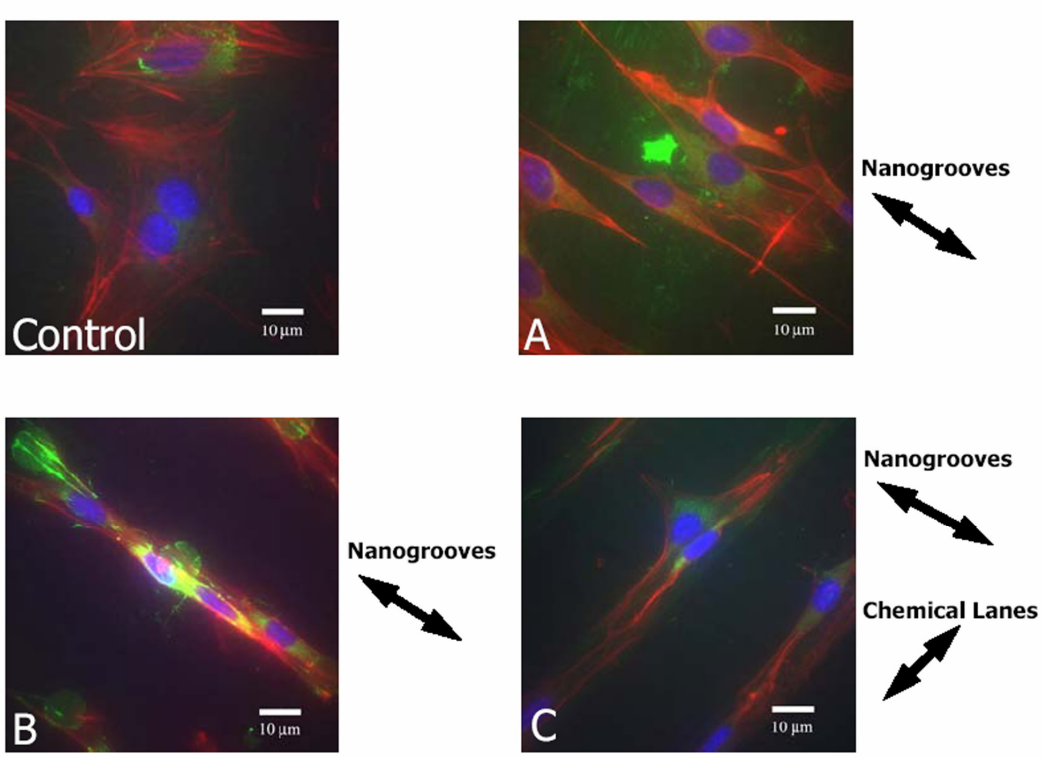

Figure 5.4 IF staining shows nuclei in blue, fibronectin in green and actin cytoskeleton in red. Cells align in the direction of the nanogrooves on substrates A and B. Overall, cells align to the chemical lanes on substrate C and are orthogonal to the nanogrooves. However, small extensions of the cells on substrate C align parallel to the nanogrooves where no chemical pattern is present.

Cells cultured on B showed results similar to A, regardless of the chemical pattern of fibronectin dots. Figure 5.4 shows the IF stained cells aligning to the nanogrooves with cell bodies and nuclei clearly aligned to the grooves and actin cytoskeletons extended predominantly parallel to the nanogrooves. Although cells were found preferentially on the fibronectin dots, they extended outside the dots into the EG_3-thiol protected non-fouling area. Figure 5.5 shows filopodia extended in various directions, larger cell extensions strictly aligned to the nanogrooves, and cell extensions protruded beyond the fibronectin dots. This result was contrary to previous work where microprinted fibronectin dots of the same size and shape restricted cell shape and attachment location on a smooth substrate [17] with no cell extension into the non-

fouling area. For B, the nanogrooves influenced the alignment and morphology of the cells to a greater extent than the fibronectin dots.

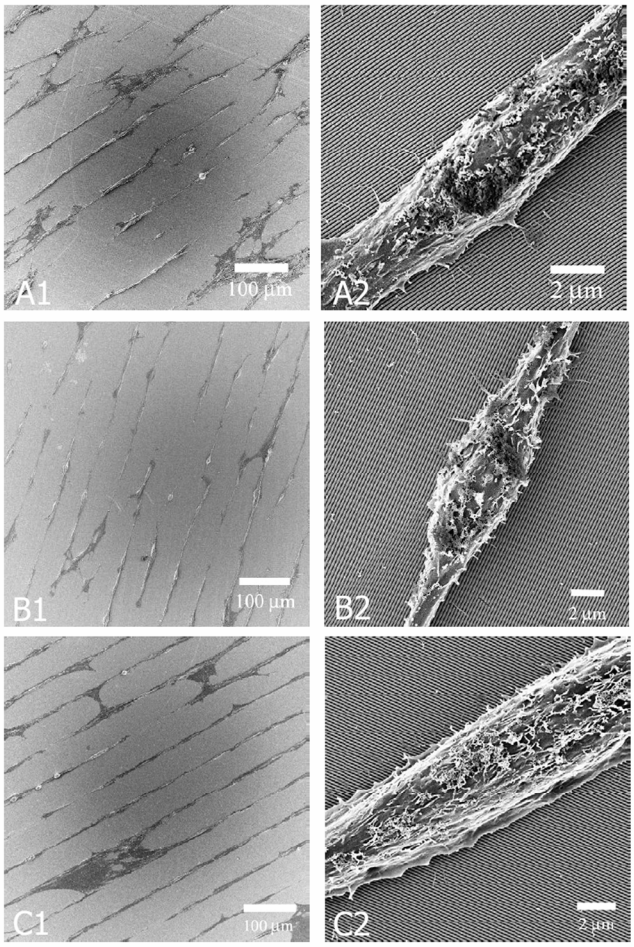

Figure 5.5 Osteoblast-like cells on substrate types A and B align and elongate along the nanogrooves. Substrate B exhibits preferential attachment of osteoblast-like cells to the fibronectin dots. However, osteoblasts on substrate type C align and elongate along the chemical lanes instead of the orthogonal nanogrooves.

Substrate C elicited a remarkably different cellular response as shown in Figure 5.4 and Figure 5.5. While cells aligned to nanogrooves on the other substrates, cells clearly aligned to the fibronectin lanes on C. This is in agreement with previous work where cells aligned to chemical lanes rather than mechanical grooves [24]. Cell bodies, nuclei, and overall cytoskeletons aligned to the fibronectin lanes. Cell attachment was

highly preferential to the lanes, however some bridging of lanes occurred as can be seen in Figure 5.5 where cells crossed the non-fouling areas. Figure 5.4 shows a cell that extended into the non-fouling area parallel to the nanogrooves. Since it was next to another cell, the extension into the non-fouling area may be induced by the restricted spreading area with the nanogrooves guiding the direction of the extension. This phenomena was observed in other locations, typically where the spreading area was limited. Figure 5.6 shows cells extended beyond the chemically patterned area into the non-fouling area. Cell alignment modulated from the chemical lanes to the nanogrooves once cell extension proceeded beyond the chemical lanes. For substrate C, the chemical lanes influenced alignment and morphology of the cells to a greater extent than the nanogrooves. However, nanogroove influence was not absent as indicated by bridging and some directed cell extension into the non-fouling area.

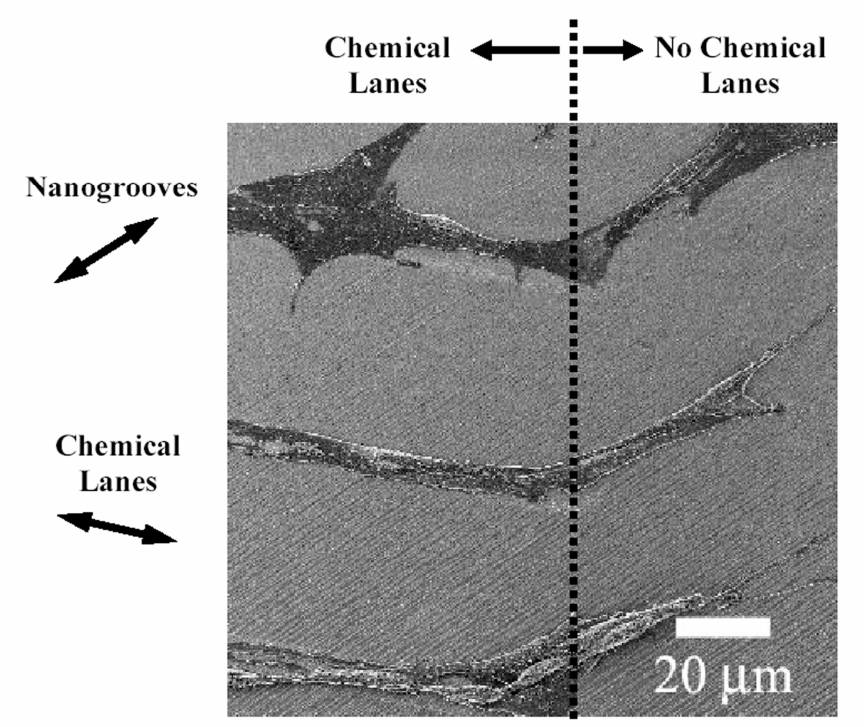

Figure 5.6 Osteoblast-like cells preferentially align to the chemical lanes, but where the lanes end the cells align to the nanogrooves.

5.4 Conclusion

This chapter reports cell culture substrates fabricated by combining NIL-formed mechanical nanotopography with μCP overlaid chemical micropatterns. Cells cultured on the substrates showed varying alignment and elongation due to pattern geometry and continuity. Nanotopography influenced cell alignment on substrates with nanogrooves overlaid with either uniform chemistry or fibronectin dots. Chemical patterns determined cellular alignment on substrates with nanotopography overlaid with continuous fibronectin lanes.

The technique presented here enables scaleable fabrication of cell culture substrates with well-defined nanotopography and micropatterned chemical domains. This highly scaleable approach allows for the large sample sizes needed for quantitative biological data collection, clinical trials, and eventually large scale production. These substrates facilitate further studies of the relative impact of nanoscale topography and microscale chemical patterns on cell morphology and function.

5.5 References

[1] Curtis A, Wilkinson C. Topographical Control of Cells. Biomaterials. 1997 Dec;18(24):1573-83.

[2] Jung DR, Kapur R, Adams T, Giuliano KA, Mrksich M, Craighead HG, et al. Topographical and physicochemical modification of material surface to enable patterning of living cells. Critical Reviews in Biotechnology. 2001;21(2):111-54.

[3] Flemming RG, Murphy CJ, Abrams GA, Goodman SL, Nealey PF. Effects of synthetic micro- and nano-structured surfaces on cell behavior. Biomaterials. 1999 Mar;20(6):573-88.

[4] Weiss P. Experinments on cell and Axon Orientation in Vitro. Journal of Experimental Zoology. 1945;100(3):353-86.

[5] Baac HW, Lee JH, Seo JM, Park TH, Chung H, Lee SD, et al. Submicron-scale topographical control of cell growth using holographic surface relief grating. Materials Science & Engineering C-Biomimetic and Supramolecular Systems. 2004 Jan;24(1-2):209-12.

[6] Motlagh D, Senyo SE, Desai TA, Russell B. Microtextured substrata alter gene expression, protein localization and the shape of cardiac myocytes. Biomaterials. 2003 Jun;24(14):2463-76.

[7] Wang JHC, Grood ES, Florer J, Wenstrup R. Alignment and proliferation of MC3T3-E1 osteoblasts in microgrooved silicone substrata subjected to cyclic stretching. Journal of Biomechanics. 2000;33:729-35.

[8] Schmidt J, von Recum AF. Macrophage response to microtextured silicone. Biomaterials. 1992;13:1059-69.

[9] Charest JL, Bryant LE, Garcia AJ, King WP. Hot embossing for micropatterned cell substrates. Biomaterials. 2004;25(19):4767-75.

[10] Mata A, Boehm C, Fleischman A, Muschler G, Roy S. Analysis of connective tissue progenitor cell behavior on polydimethylsiloxane smooth and channel micro-textures. Biomedical Microdevices. 2002;4:267-75.

[11] Yim KF, Reano RM, Pang SW, Yee AF, Chen CS, Leong KW. Nanopattern-induced changes in morphology and motility of smooth muscle cells. Biomaterials. 2005;26:5405-13.

[12] Teixeira AI, Abrams GA, Bertics PJ, Murphy CJ, Nealey PF. Epithelial contact guidance on well-defined micro- and nanostructured substrates. Journal of Cell Science. 2003 May 15;116(10):1881-92.

[13] van Kooten TG, von Recum AF. Cell adhesion to textured silicone surfaces: The influence of time of adhesion and texture on focal contact and fibronectin fibril formation. Tissue Engineering. 1999 Jun;5(3):223-40.

[14] Dalby MJ, Gadegaard N, Riehle MO, Wilkinson CDW, Curtis ASG. Investigating filopodia sensing using arrays of defined nano-pits down to 35 nm diameter in size. International Journal of Biochemistry & Cell Biology. 2004 Oct;36(10):2005-15.

[15] Walboomers XF, Croes HJE, Ginsel LA, Jansen JA. Contact guidance of rat fibroblasts on various implant materials. Journal of Biomedical Materials Research. 1999 Nov;47(2):204-12.

[16] Zinger O, Zhao G, Schwartz Z, Simpson J, Wieland M, Landolt D, et al. Differential regulation of osteoblasts by substrate microstructural features. Biomaterials. 2005;26:1837-47.

[17] Gallant ND, Capadona JR, Frazier AB, Collard DM, Garcia AJ. Micropatterned surfaces for analyzing cell adhesion strengthening Langmuir. 2002 2002;18:5579-84.

[18] Chen CS, Mrksich M, Huang S, Whitesides GM, Ingber DE. Micropatterned surfaces for control of cell shape, position, and function. Biotechnology Progress. 1998 May-Jun;14(3):356-63.

[19] Mrksich M, Dike LE, Tien J, Ingber DE, Whitesides GM. Using Microcontact Printing to Pattern the Attachment of Mammalian Cells to Self-Assembled Monolayers of Alkanethiolates on Transparent Films of Gold and Silver. Experimental Cell Research. 1997;235:305-13.

[20] Bhatia SN, Yarmush ML, Toner M. Controlling cell interactions by micropatterning in co-cultures: hepatocytes and 3T3 fibroblasts. Journal of Biomedical Materials Research. 1997 1997/02//;34(2):189-99.

[21] Revzin A, Tompkins RG, Toner M. Surface Engineering with Poly(ethlyne glycol) Photolithography to Create High-Density Cell Arrays on Glass. Langmuir. 2003;19:9855-62.

[22] Miller C, Jeftinija S, Mallapragada S. Synergistic effects of physical and chemical guidance cues on neurite alignment and outgrowth on biodegradable polymer substrates. Tissue Engineering. 2002 Jun;8(3):367-78.

[23] Mrksich M, Chen CS, Xia Y, Dike LE, Ingber DE, Whitesides GM. Controlling cell attachment on contoured surfaces with self-assembled monolayers of alkanethiolates on gold. ProcNatlAcadSciUSA. 1996;93(20):10775-8.

[24] Britland S, Perridge C, Denyer M, Morgan H, Curtis A, Wilkinson C. Morphogenetic guidance cues can interact synergistically and hierarchically in steering nerve cell growth. Experimental Biology Online. 1996;1(2).

[25] Chou SY, Krauss PR, Renstrom PJ. Imprint lithography with 25-nanometer resolution. Science. 1996 Apr 5;272(5258):85-7.

[26] Xia Y, Whitesides G. Soft Lithography. Annual Review of Materials Science. 1998;28:153-84.

[27] Mrksich M. Tailored substrates for studies of attached cell culture. Cellular and Molecular Life Sciences. 1998 Jul;54(7):653-62.

[28] Whitesides GM, Ostuni E, Takayama S, Jiang X, Ingber DE. Soft lithography in biology and biochemistry. 2001 2001///;3:335-73.

[29] Dike LE, Chen CS, Mrksich M, Tien J, Whitesides GM, Ingber DE. Geometric Control of Switching Between Growth, Apoptosis, and Differentiation during Angiogenesis using Micropatterned Substrates. In Vitro Cell Developmental Biology - Animal. 1999;35:441-8.

CHAPTER 6

MYOBLAST ALIGNMENT AND DIFFERENTIATION ON CELL CULTURE SUBSTRATES WITH MICROSCALE TOPOGRAPHY AND MODEL CHEMISTRIES

This chapter analyzes the alignment and differentiation of myoblast cells adherent to surfaces having model chemistries and microtopographical patterns. The patterns strongly influenced cellular alignment but did not modulate expression of differentiation marker proteins in either primary or C2C12 myoblasts. Topographic patterns consisted of embossed ridges and grooves or arrays of holes, with feature sizes ranging from 5 – 75 μm. The topographic surfaces were prepared with a uniform self-assembled monolayer that presented CH_3 molecules for fibronectin adsorption. The myoblast cell models were cultured in differentiation conditions on the substrates. For both cell models, cells aligned to grooves, with groove width modulating orientation, and preferentially orientated parallel to rows of holes. None of the patterns significantly modulated cell density or differentiation as examined through sarcomeric myosin and acetylcholine receptor expression. The results indicate that for the specific configuration examined, microscale topography modulates myoblast alignment, but does not have significant impact on cell density or differentiation.

6.1 Introduction

A deep understanding of the complex interface between cells and a biomaterial surface is required for the engineering of biomaterial interfaces. The cell-surface interface of a biomaterial influences cellular response through various surface properties including surface topography [1], chemistry [2], and chemical patterns [3]. Topography in particular influences and modulates cell function as indicated by altered morphologies and alignments of cells on topographically patterned substrates with microscale [4, 5] and nanoscale [6-8] features.

The influence of surface topography on cell behavior may reach beyond morphological changes to encompass higher-order functions such as differentiation. For instance, osteoblasts cultured on rough surfaces possessed higher levels of bone marker production than those cultured on smooth substrates [9]. In addition, chemically etched microtopographies, composed of 10, 30, or 60 μm diameter pits along with overlaid acid etched roughness, modulated bone marker production [10] as did anisotropically etched grooves in silicon of depths 3, 10, and 30 μm [11]. Adding 5, 10, or 50 μm wide grooves to composite material cell substrates resulted in modest differences in osteogenic markers as compared to smooth substrates [12], although the patterning method may have resulted in altered surface chemistry. In addition, topographic patterns have influenced bonelike formations in an in vivo model [13]. Phenotypic marker modulation by surface mechanical features is not specific to bone-forming cells. Neurons cultured on polystyrene substrates expressed upregulated marker levels on substrates with 16 μm wide grooves as compared to smooth substrates [14]. In contradiction to evidence of

topographical influence of differentiation, molded polymer substrates with 2 μm and 50 μm parallel grooves failed to significantly influence osteogenic marker message levels [15]. Not all evidence affirms conclusive topographical influence on cell differentiation, indicating further characterization of the phenomena is required.

Surface chemistry also significantly affects cell function [16] including adhesion [17] and in particular differentiation. Surface chemistry has modulated differentiation in various cellular systems including epithelial cells [2], myoblasts [18, 19], and most notably osteoblasts [20]. The effects of surface chemistry on cell function are usually associated with differences in protein adsorption or activity [20, 21]. Since surface chemistry significantly influences differentiation of cells, topographically patterned substrates for cell differentiation studies should present characterized chemistry in order to isolate effects to those influenced by topography.

Thorough evaluation of topographical influence of cells necessitates cell substrates with a wide array of topographic features and feature sizes. Predominantly, topographic features of cell substrates are either linear, such as grooves and ridges, or non-linear such as pits or holes [1]. Previous studies of differentiation of cells on topography typically were limited to either linear [14, 22] or non-linear [10] features. One study did explore differentiation on both linear and non-linear features, although feature sizes were limited to either 5, 10, or 50 μm [12] as opposed to many feature sizes spanning a wide range. Since cellular response has been shown to vary with feature size [23, 24], it is critical to screen a wide range and array of feature sizes to fully characterize cellular response. As noted earlier, previous studies of differentiation of cells on topography used a few, discrete patterns which may not have fully spanned the possible

topographies of influence. Choosing a wide range of patterns, with many levels within the range, would provide a more complete analysis of topographical influence. Incorporating high-throughput analysis techniques would further enable rapid screening of a wide range of topographies and their influence on cell differentiation.

This work examines the influence of topography on alignment and differentiation of cells, while maintaining controlled surface chemistry through the use of a previously characterized SAM model chemical layer. The approach uses two well-characterized myoblast cell models with an objective quantification of differentiation coupled with a high-throughput (HT) substrate with a wide array of surface topographical patterns.

6.2 Materials and Methods

6.2.1 Reagents

Cell culture reagents, human plasma FN, and Dulbecco's phosphate-buffered saline (PBS: 137 mM NaCl, 2.7 mM KCl, 4.3 mM $Na_2HPO_4 \cdot 7H_2O$, 1.5 mM KH_2PO_4, 0.9 mM $CaCl_2 \cdot 2H_2O$, 1.0 mM $MgCl_2 \cdot 6H_2O$, pH 7.4), rhodamine-conjugated bungarotoxin, and insulin-transferrin-selenium-X were obtained from Invitrogen (Carlsband, CA). Fetal bovine and horse sera were supplied by Hyclone (Logan, UT). Monoclonal MF20 (specific for sarcomeric myosin) antibodies were purchased from the Developmental Studies Hybridoma Bank (Iowa City, IA). Biotinylated anti-mouse IgG antibody was purchased from Jackson ImmunoResearch (West Grove, PA), while FITC-conjugated anti-biotin and rabbit polyclonal anti-FN antibodies were obtained from Sigma-Aldrich (St. Louis, MO). Ethidium homodimer-2, Alexa Fluor 488-conjugated anti-rabbit IgG, and rhodamine conjugated α-bungarotoxin were obtained from Molecular

Probes (Eugene, OR). Research grade 0.5 mm thick polycarbonate sheet was sourced from Goodfellow (Devon, PA).

6.2.2 Fabrication of Substrate Topography

Hot-embossing was used to create substrate topography [25]. Briefly, silicon master wafers were fabricated through standard optical lithographic patterning followed by anisotropic deep-reactive ion etching. Feature sizes ranged from 5 – 75 μm, and masters were oxidized and soaked in buffered oxide etch to remove scalloping from the etch process. Each 100 mm wafer contained 16 replicas of the high-throughput substrate pattern. The patterned side of the silicon master was placed in contact with a polycarbonate blank, then loaded into a force and temperature controlled press. Under light load, temperature was increased to 300 C, then the load was increased to 130 kN and maintained for 20 minutes. After cooling, the load was released, and the substrate was separated from the silicon master. To enable chemical functionalization of the surface, 10 nm of titanium and 20 nm of gold were evaporated onto the surface at a base pressure of 2 x 10-6 Torr and deposition rate of 0.5 Å/s. The evaporation process was characterized to prevent melting of the polymer such that the topographic features were not altered in the process.

6.2.3 Substrate Surface Chemistry Preparation

Self-assembled monolayers presenting CH_3 groups were used to present a well-defined chemistry [26]. Briefly, cell substrates were immersed in a 1.0 mM solution of

hexadecanethiol in absolute ethanol for 15 s, then rinsed three times in 95% ethanol. After rinsing in sterilized water 3 times, and phosphate buffered saline (PBS) 3 times, samples were incubated in a 20 μg/mL solution of human plasma fibronectin for 30 minutes at room temperature. Non-specific binding was blocked with a 1% bovine serum albumin solution in PBS for 1 hour. Loosely bound protein was eluted in PBS overnight.

6.2.4 Cell Culture

Primary myoblasts were harvested and cultured according to the protocol in [27] in accordance with IACUC-approved protocols using tissue culture dishes coated in 0.01% type I collagen, growth media (GM) composed of Ham's F10 nutrient mixture supplemented with 20% fetal bovine serum (FBS), 2.5 ng/mL bFGF, and 1% penicillin-streptomycin. C2C12 myoblasts were subcultured according the protocol in [19] using standard tissue culture dishes and GM composed of Dulbecco's Modified Eagle Medium supplemented with 20% FBS, and 1% penicillin-streptomycin. Both cell types were passaged at 50% confluency using standard passaging techniques.

Cells were seeded on substrates in 12 well dishes using their respective GM, allowed to adhere for 6 hours, then the GM was exchanged with a fusion media (FM) which consisted of DMEM supplemented with 1% insulin-transferrin-selenium-X and 1% penicillin-streptomycin. Primary myoblasts cultured for 48 hours in FM before fixing while C2C12 myoblasts were cultured for 96 hours. Negative controls remained in GM for the entire culture time.

6.2.5 Cell Fixation and Staining

Cells were fixed and immunostained for sarcomeric myosin as an indicator of differentiation. Cell cultures were fixed in 70% ethanol/37% formaldehyde/glacial acetic acid (20:2:1) then blocked in 5% horse serum in PBS for 1 h. Samples were sequentially incubated in 2 mg/ml MF-20 mouse antibody, 5 mg/ml biotinylated anti-mouse IgG secondary antibody, and 10 mg/ml FITC-conjugated anti-biotin antibody. Cell nuclei were counter-stained with 200 nM ethidium homodimer-2.

As a second marker of differentiation, cells were stained using rhodamine-conjugated bungarotoxin venom to label acetylcholine receptors [28]. Cells were rinsed in PBS, fixed in 3.7% formaldehyde, then incubated in .1% Triton X-100, 2% horse serum, and 2% BSA in PBS. Cells were then incubated in 2 μg/mL rhodamine-conjugated bungarotoxin for 1 hour, and counterstained with Hoechst DNA stain.

Previous work characterized the SAMs as well as the quantity and the activity of the adsorbed fibronectin [26]. To verify the fibronectin layer did not adsorb preferentially to either ridges or grooves, substrates coated in fibronectin were fixed in 3.7% formaldehyde, blocked in BSA, then sequentially incubated in 2.5 μg/mL rabbit anti-FN antibody, and 5 μg/mL AlexaFluor 488 conjugated anti-rabbit for one hour each. Immunofluorescent microscopy was used to inspect the samples for similar fluorescence intensity of immunolabeled protein on ridges versus grooves.

6.2.6 Image Analysis and Statistics

Cell images were taken with an inverted fluorescence microscope and processed using Image Pro software. Quantitative data consisted of cell nuclear major axis angle (with respect to sample topography) and percentage of cells expressing sarcomeric myosin. Statistical differences were obtained through analysis of variance with a subsequent Tukey HSD multiple comparisons test to compare pairs of means. A significance level of 0.05 was used to determine significant differences unless otherwise noted. The results are from 5 independent replications of the HT substrate.

6.3 Results

6.3.1 Topographically patterned HT substrate with well-defined surface chemistry

Hot-embossing created a polycarbonate substrate possessing well-defined topographic features consistent over many replications. Figure 6.1 shows a schematic of the HT substrate with representative SEMs. The HT substrate contained 35 distinct fields, with features uniform within each field. Since the HT substrate fit into a single well of a 12-well dish, uniform culture conditions were assured across all fields. In addition, the precise array of distinct topographically patterned fields lent itself to automated high-throughput analysis of cell morphology and protein expression. Patterns were either (i) holes in an orthogonal array where the pitch was twice the diameter of the holes, (ii) grooves and ridges where groove width was equal to ridge width, or (iii) a smooth surface which served as an internal control. Characteristic feature sizes, diameter

for holes or width for grooves, ranged from 5 – 75 µm, with 17 distinct feature sizes. Feature dimensions were analyzed via SEM inspection before and after evaporative metal coating, and groove and hole depth was verified via AFM to be 5.1 µm.

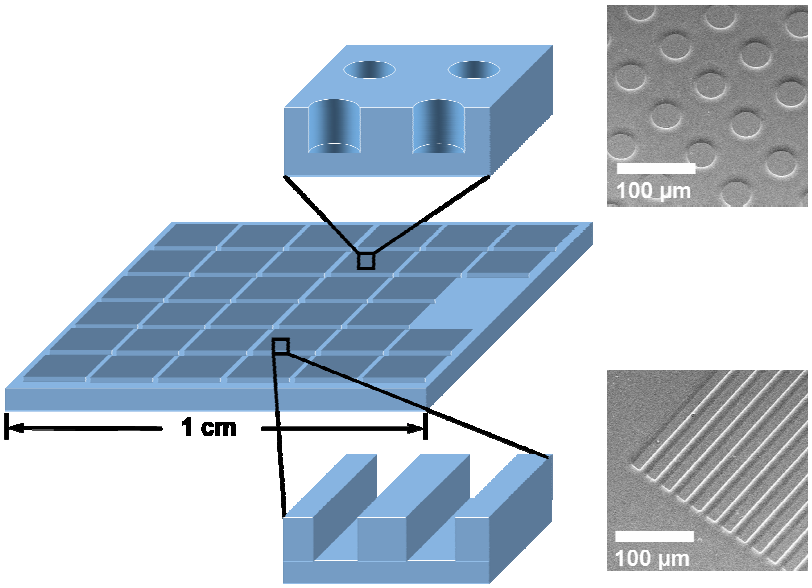

Figure 6.1 The high-throughput (HT) substrate contained hole and groove patterns. Patterns are uniform within each field, but vary within the entire substrate. Patterns are either holes or grooves with diameters or groove widths ranging from 5 – 75 µm. A smooth area serves as an internal control surface.

Figure 6.2 shows an SEM image of one field of the HT substrate after the metal evaporation step. Although the underlying SAM, fibronectin adsorption process, and resultant surface have been well characterized on smooth surfaces [26], substrates were further evaluated for consistency of the fibronectin layer across the topography. Immunostaining for fibronectin, as shown in Figure 6.2, revealed similar intensities of fibronectin on both ridges and grooves throughout the substrate.

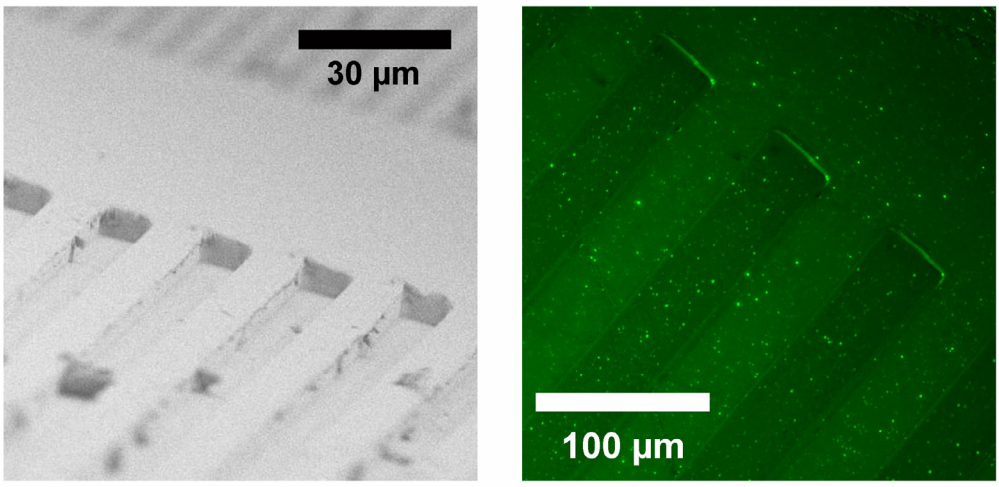

Figure 6.2 Hot-embossing and SAM techniques create substrates with well-defined topography and uniform chemistry. Left: An SEM of the gold coated HT substrate shows groove shape with their depth of 5 µm verified via AFM. Right: An IF image of immunostained fibronectin adsorbed to the SAM on the HT substrate. Fibronectin quantity does not appear significantly different on ridges as compared to grooves.

6.3.2 Alignment of primary and C2C12 myoblasts

Quantitative analysis of alignment of myoblasts revealed a strong influence of the topographic features on cellular alignment. Cell nuclear alignment served as a robust metric to judge overall cell body alignment as previously demonstrated [7, 29]. Nuclear alignment angles were measured with respect to the grooves, oriented nominally at 0°, and cell angles ranged from 0 - 90°. Figure 6.3 shows immunostained primary myoblasts and corresponding histograms of alignment angles from all 5 replicates of the experiment for a characteristic feature size of 10 µm. As expected, cells on smooth substrates exhibited a uniform distribution of alignment angles. Interestingly, cells on hole topographies showed a distribution of alignment angles with small peaks at both 0° and 90°. These angles correspond with the orientation of the rows and columns of holes on the substrate. Cells were seen bridging some smaller holes, typically less than 25 µm, but

preferentially remained on the raised spaces in between the holes. Cells on groove topographies exhibited a strong alignment to the grooves, with almost no cells aligning perpendicularly. Most cells on all substrates exhibited an elongated morphology, as expected for a differentiated myoblast. Figure 6.3 shows data only for primary myoblasts. C2C12 myoblasts behaved similarly.

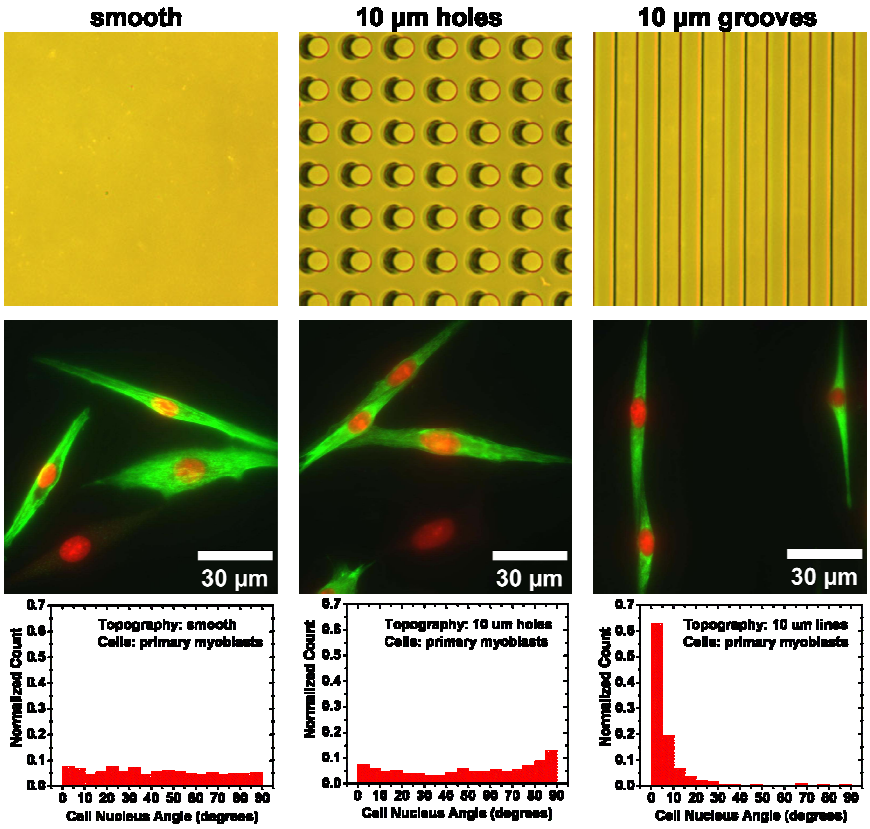

Figure 6.3 Cellular orientation is influenced by surface topography. Immunostaining of sarcomeric myosin and nuclei, along with histograms of cell alignment angles taken over 5 samples show alignment of myoblasts. Cells orient randomly on smooth substrates, orient with a preference for horizontal and vertical directions on substrates with holes, and align parallel to grooves.

Topography influenced cell alignment in a pattern feature shape-dependent manner and modulated alignment on linear patterns in a pattern feature size-dependent manner. Figure 6.4 shows a summary of the percentage of myoblasts aligning to the

grooves. Cells with alignment angles of less than 10° were counted as aligned. All hole patterns had similar levels of alignment as the control. In contrast, all groove widths exhibited significantly higher alignment than either hole patterns or control for primary myoblasts, while groove widths of 5, 10, and 25 μm exhibited significantly higher alignment than hole patterns or control for C2C12 myoblasts. In addition, alignment peaked at 10 μm for both primary and C2C12 myoblasts. Qualitatively, both cell types exhibited similar trends for fraction of aligned cells versus groove width, with primary myoblasts exhibiting higher alignment than C2C12 myoblasts for all groove widths.

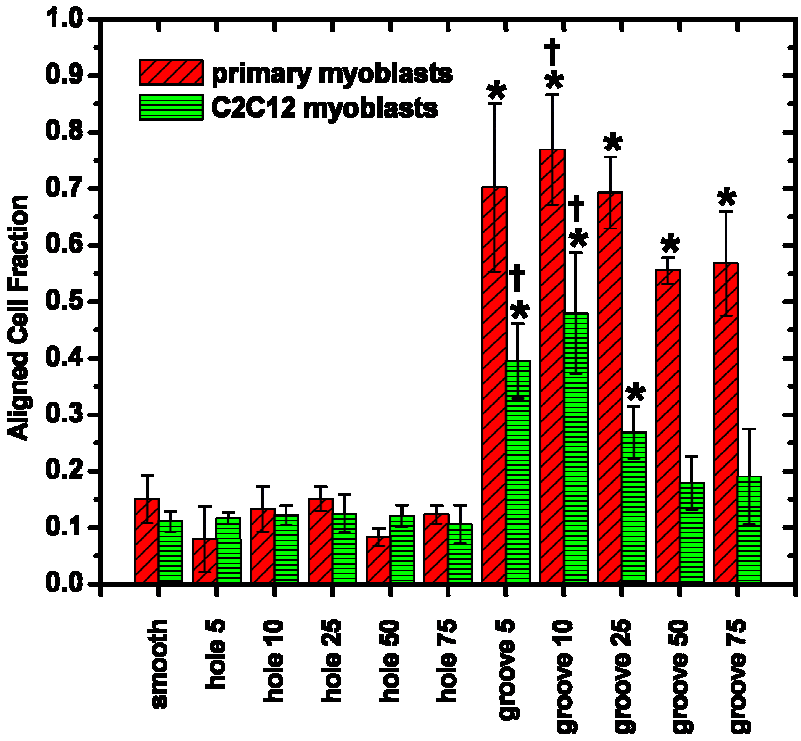

Figure 6.4 Grooves significantly influence myoblast alignment. Cells aligned within 10° of the grooves were counted as aligned, with alignment quantified for 5 independent replicas of the substrate. Cells aligned dependent on feature shape and size, (means ± stdev, P <0.05, * vs smooth and hole, † vs groove 50 and groove 75).

6.3.3 Myogenic differentiation on topographical patterns

We examined sarcomeric myosin expression as a marker of myogenic differentiation to evaluate the effects of well-defined topography on differentiation. In contrast to cellular alignment processes, topography combined with a uniform, well-controlled model surface chemistry did not significantly influence either cell numbers or sarcomeric myosin expression in either primary or C2C12 myoblasts. Figure 6.5 shows cell densities and fraction of cells expressing sarcomeric myosin with representative images of the immunostained sarcomeric myosin. Each field was scored for total cells and percentage of cells expressing sarcomeric myosin, and averages were taken over 5 sample replicates. Cells cultured in GM as a negative control showed negligible fractions of cells expressing sarcomeric myosin. Since proximity factors, such as the amount of cell-cell contact and available spreading area, have been shown to influence cell function [30, 31], and cell density may modulate these proximity factors, differences in cell density could influence cell function. We did not observe any differences in cell numbers as a function of topography, indicating effects of the topography do not act through these proximity factors and are limited to cell-material interactions.

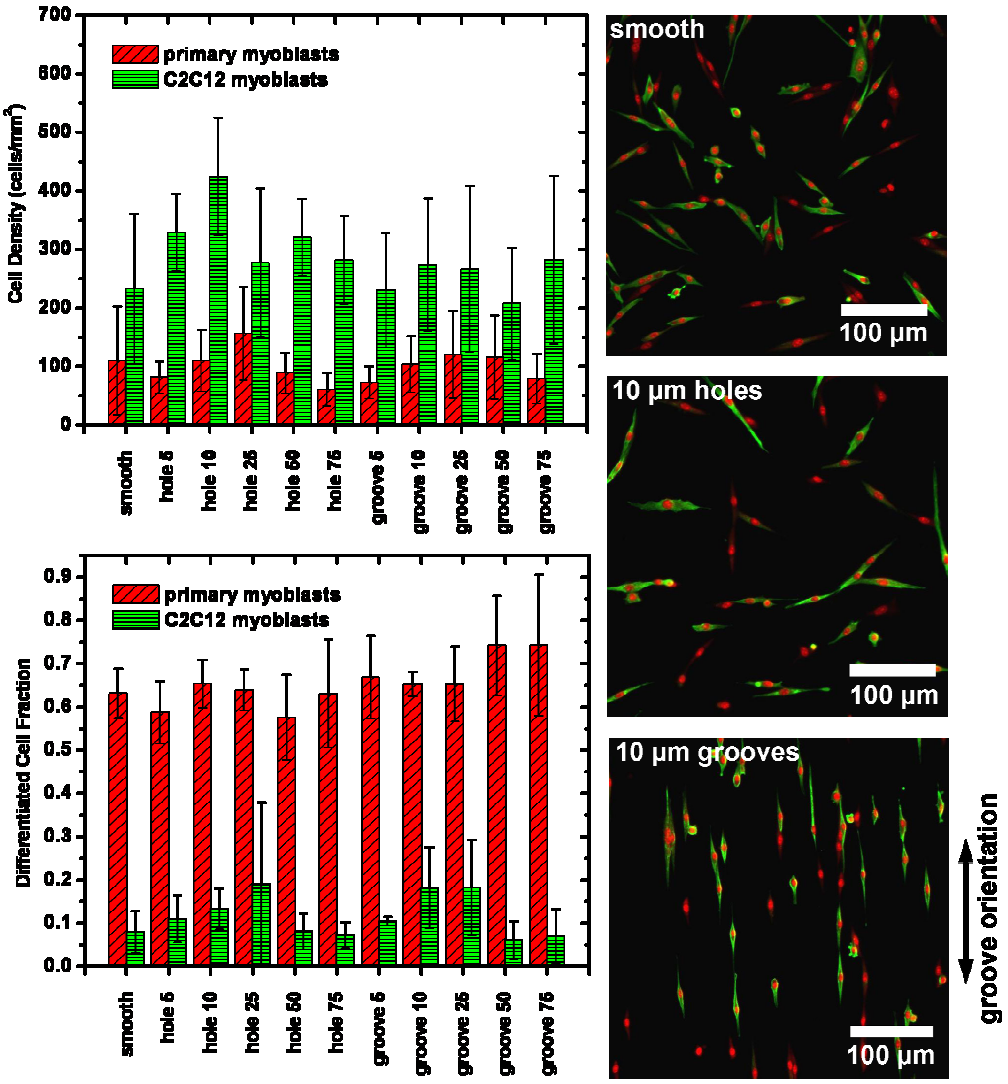

Figure 6.5 Topography does not significantly modulate myoblast density or differentiation. Cell density and percentage of cells expressing sarcomeric myosin was quantified for both primary and C2C12 myoblasts on the HT substrate for 5 independent replicas of the HT substrate. Primary myoblasts showed significantly higher differentiation levels over C2C12 myoblasts.

As an additional metric of differentiation, primary myoblasts were cultured as described above, then stained for acetylcholine receptors using a rhodamine-conjugated bungarotoxin. Bungarotoxin selectively binds to acetylcholine receptors [28]. A negative control sample of primary myoblasts kept in GM showed negligible levels of staining for the acetylcholine receptor. Acetylcholine receptor expression was similar for control substrates and topographically patterned substrates as shown in Figure 6.6.

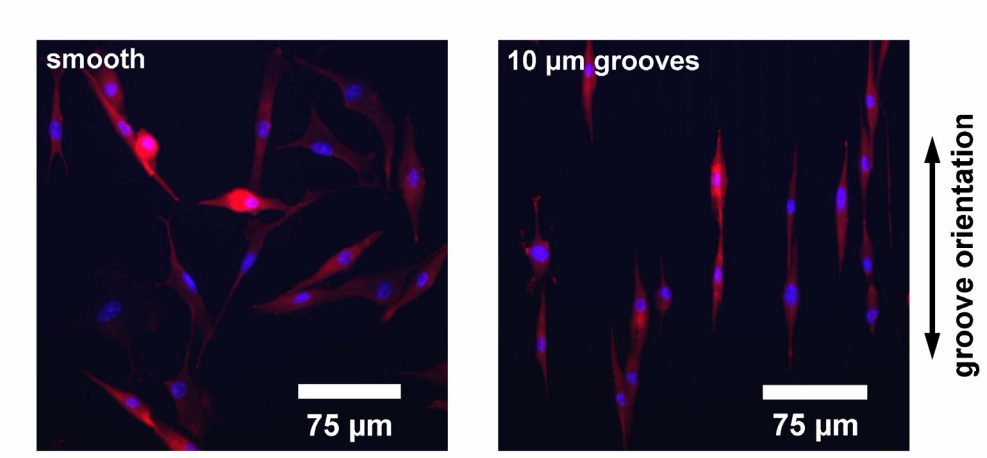

Figure 6.6 Acetylcholine receptor expression is not influenced by topography. Primary myoblasts were labeled with rhodamine-conjugated bungarotoxin which binds specifically to acetylcholine receptors and counterstained with Hoechst. Acetylcholine expression was similar for smooth and grooved substrates.

6.4 Discussion

Substrate topography of groove width ranging from 5-75 µm strongly influenced myoblast alignment. This alignment response agrees well with previous studies of cell-topography interactions [4] including recently documented findings [6, 7, 32] and a myoblast specific study [33]. Specifically, alignment depended on groove width, with increased alignment on narrower groove widths, consistent with previous reports [24]. For C2C12 myoblasts, the groove widths of 50 µm and 75 µm did not elicit significantly stronger alignment than a smooth control substrate. This may indicate that a large spacing of grooves reduces the number of interactions of cells with substrate discontinuities to a point where insignificant alignment occurs. The apparent upper alignment limit to feature size did not occur with the primary myoblasts as alignment levels were significantly higher for all groove widths.

In addition to alignment in response to microgrooves, myoblasts exhibited preferential polarization directions on substrates with holes. Due to the orthogonal array of holes, directions of minimal obstructions were oriented at 0° and 90°, and peaks of alignment angles at these orientations were noted in histograms of alignment angle data. The peaks were noted for several hole sizes with a significantly larger fraction of cells orienting between 80° and 90° on 5 μm holes than on the smooth control surface. Topographic features have restricted cell extension and migration regardless of whether the features are recessed or protruding [34]. Here, myoblast extension was restricted by the pattern of holes, resulting in cellular extension predominantly directed between rows of holes where minimal obstructions were present. This phenomena is similar to what has been described as 'gap guidance' [35], but in this case the features are recessed into the substrate rather than protruding from the substrate.

In general, alignment was stronger for primary myoblasts as opposed to C2C12 myoblasts whether due to contact guidance or gap guidance. In addition, a larger percentage of primary myoblasts differentiated, as measured through sarcomeric myosin expression, than the C2C12 myoblasts. As primary myoblasts had both higher alignment and differentiation levels than the C2C12 myoblasts, polarization of myoblasts during myogenesis may lead to more cells aligning to the grooves. Myoblasts polarized under differentiation conditions on smooth control areas at a similar level as those on grooved areas indicating that grooved topography does not necessarily induce polarization. However, grooves clearly guided the direction of polarization, and higher levels of differentiated cells could have led to more aligned cells.

Restriction of cellular extension direction by the patterned topography did not result in changes in differentiation as indicated by sarcomeric myosin or acetylcholine receptor expression. Cellular extension has been restricted by chemical patterns [36] and topographical patterns [23]. On chemical patterns, restricting cell extension and consequent spreading has resulted in altering levels of differentiation markers of cells cultured on them [37] as well as altered amounts of bound receptors [38] with a dependency on spread cell area. In this chapter, although topography limited cellular extension direction, differentiation remained uninfluenced suggesting the impact of early cell-spreading events on differentiation was minimal. Chemical patterns differ from topographic ones in that the area of cell contact with the substrate is altered significantly by chemical patterns. The topographic features did not limit the area for cellular extension and consequent area of cell contact remained unrestricted. In addition, the model chemical surface provided consistent spatial ligand distribution. Therefore it is unlikely that the amount of ligand bound by the cells changed significantly due to the topographic patterns. Topography may impact differentiation if features were designed such that they restricted cell extension and spreading to the point where the spread cell area was altered, thereby resulting in a change in amount of ligand-bound receptors.

Myogenic differentiation represents a particularly useful model to evaluate the effects of surface properties on cell function as it is a well characterized process [39] and has been used in studying the influence of surface properties on cellular differentiation in the past [18, 19]. Previous work has speculated that alignment of myoblasts into parallel arrays may influence differentiation of myoblasts [33]. Here, although the alignment of myoblasts to the topography resulted in parallel arrays of myoblasts, no significant

differences were seen in expression of myogenic markers, indicating that morphological changes do not necessarily modify phenotypic expression. In addition, although the topography did not significantly impact sarcomeric myosin expression up to the 96 hour culture time, it may be possible that longer culture time may result in modulation of sarcomeric myosin or other markers by the topography. The lack of differentiation response to topography was demonstrated in this work with two cell types, primary myoblasts [27] and a C2C12 myogenic cell line [40, 41], suggesting that these results are not specific to one cell model. However, not all cell types respond the same, as indicated by osteogenic marker differences due to surface roughness [9] or combinations of surface roughness and topography [10]. Modulation of differentiation by topography may be phenotype specific, or may be limited to specific topographical patterning methods that may induce changes in surface properties other than topography.

6.5 Conclusions

We fabricated high-throughput substrates for analysis of cells cultured on various shapes and sizes of topographic features. Model chemistries presented via SAMs provided an independently controlled, previously characterized, and uniform surface chemistry overlaid onto the topography to minimize surface chemistry effects on the cells. We demonstrated strong alignment to ridges and grooves with a dependence on groove width for both primary and C2C12 myoblasts. In addition, selective orientation of myoblasts was achieved through limitation of cell extension and migration due to obstruction by topographic holes. Myogenesis, as observed through sarcomeric myosin

and acetylcholine receptor expression, was not significantly influenced by the topography. The findings here provide insight into cell-material interactions and provide guidance for design of materials-based regulation of cellular function.

6.6 Acknowledgements

The authors would like to thank Charles A. Gersbach and Kristin E. Michael for insightful advice, Timothy A. Petrie for sample metallization, and Grace K. Pavlath for donation of myoblasts.

6.7 References

[1] Flemming RG, Murphy CJ, Abrams GA, Goodman SL, Nealey PF. Effects of synthetic micro- and nano-structured surfaces on cell behavior. Biomaterials. 1999 Mar;20(6):573-88.

[2] Allen LT, Fox EJP, Blute I, Kelly ZD, Rochev Y, Keenan AK, et al. Interaction of soft condensed materials with living cells: Phenotype/transcriptome correlations for the hydrophobic effect. PNAS. 2003 May 27, 2003;100(11):6331-6.

[3] McBeath R, Pirone DM, Nelson CM, Bhadriraju K, Chen CS. Cell Shape, Cytoskeletal Tension, and RhoA Regulate Stem Cell Lineage Commitment. Developmental Cell. 2004;6(4):483-95.

[4] Curtis A, Wilkinson C. Topographical Control of Cells. Biomaterials. 1997 Dec;18(24):1573-83.

[5] Jung DR, Kapur R, Adams T, Giuliano KA, Mrksich M, Craighead HG, et al. Topographical and physicochemical modification of material surface to enable patterning of living cells. Critical Reviews in Biotechnology. 2001;21(2):111-54.

[6] Teixeira AI, McKie GA, Foley JD, Bertics PJ, Nealey PF, Murphy CJ. The effect of environmental factors on the response of human corneal epithelial cells to nanoscale substrate topography. Biomaterials. 2006;27(21):3945.

[7] Charest J, Eliason M, Talin A, Simmons B, Garcia A, King W. Polymer cell culture substrates with combined nanotopographical patterns and micropatterned chemical domains. Journal of Vacuum Science & Technology B. 2005;23(6):3011-4.

[8] Johansson F, Carlberg P, Danielsen N, Montelius L, Kanje M. Axonal outgrowth on nano-imprinted patterns. Biomaterials. 2006;27(8):1251.

[9] Lossdorfer S, Schwartz Z, Wang L, Lohmann CH, turner JD, Wieland M, et al. Microrough implant surface topographies increase osteogenesis by reducing osteoclast formation and activity. Journal of Biomedical Materials Research. 2004;70A:361-9.

[10] Zinger O, Zhao G, Schwartz Z, Simpson J, Wieland M, Landolt D, et al. Differential regulation of osteoblasts by substrate microstructural features. Biomaterials. 2005;26:1837-47.

[11] Perizzolo D, Lacefield WR, Brunette DM. Interaction between topography and coating in the formation of bone nodules in culture for hydroxyapatite- and titanium-coated micromachined surfaces. Journal of Biomedical Materials Research. 2001 Sep 15;56(4):494-503.

[12] Rea SM, Brooks RA, Best SM, Kokubo T, Bonfield W. Proliferation and differentiation of osteoblast-like cells on apatite-wollastonite/polyethylene composites. Biomaterials. 2004;25:4503-12.

[13] Chehroudi B, McDonnell D, Brunette DM. The effects of micromachined surfaces on formation of bonelike tissue on subcutaneous implants as assessed by radiography and computer image processing. Journal of Biomedical Materials Research. 1997 Mar 5;34(3):279-90.

[14] Recknor JB, Sakaguchi DS, Mallapragada SK. Directed growth and selective differentiation of neural progenitor cells on micropatterned polymer substrates. Biomaterials. 2006;27(22):4098.

[15] Matsuzaka K, Yoshinari M, Shimono M, Inoue T. Effects of multigrooved surfaces on osteoblast-like cells *in vitro*: Scanning electron microscopic observation and mRNA expression of osteopontin and osteocalcin. Journal of Biomedical Materials Research Part A. 2004;68A(2):227-34.

[16] Brodbeck W, Patel J, Voskerician G, Christenson E, Shive M, Nakayama Y, et al. Biomaterial adherent macrophage apoptosis is increased by hydrophilic and anionic substrates *in vivo*. Proceedings of the National Academy of Science. 2002;99(16):10287-92.

[17] Shen M, Horbett TA. The effects of surface chemistry and adsorbed proteins on monocyte/macrophage adhesion to chemically modified polystyrene surfaces. J Biomed Mater Res. 2001 2001/12/05/;57(3):336-45.

[18] Garcia AJ, Vega MD, Boettiger D. Modulation of Cell Proliferatoin and Differentiation through Substrate-dependent Changes in Fibronectin Conformation. Molecular Biology of the Cell. 1999;10:785-98.

[19] Lan MA, Gersbach CA, Michael KE, Keselowsky BG, Garcia AJ. Myoblast proliferation and differentiation on fibronectin-coated self assembled monolayers presenting different surface chemistries. Biomaterials. 2005 Aug;26(22):4523-31.

[20] Keselowsky BG, Collard DM, Garcia AJ. Integrin binding specificity regulates biomaterial surface chemistry effects on cell differentiation. Proceedings of the National Academy of Science. 2005 April 26, 2005;102(17):5953-7.

[21] Keselowsky BG, Collard DM, Garcia AJ. Surface chemistry modulates focal adhesion composition and signaling through changes in integrin binding. Biomaterials. 2004 Dec;25(28):5947-54.

[22] K. Matsuzaka MYMSTI. Effects of multigrooved surfaces on osteoblast-like cells *in vitro*: Scanning electron microscopic observation and mRNA expression of osteopontin and osteocalcin. Journal of Biomedical Materials Research Part A. 2004;68A(2):227-34.

[23] Teixeira AI, Abrams GA, Bertics PJ, Murphy CJ, Nealey PF. Epithelial contact guidance on well-defined micro- and nanostructured substrates. Journal of Cell Science. 2003 May 15;116(10):1881-92.

[24] Clark P, Connolly P, Curtis ASG, Dow JAT, Wilkinson CDW. Topographical Control of Cell Behavior 2. Multiple Grooved Substrata. Development. 1990 Apr;108(4):635-44.

[25] Charest JL, Bryant LE, Garcia AJ, King WP. Hot embossing for micropatterned cell substrates. Biomaterials. 2004;25(19):4767-75.

[26] Keselowsky BG, Collard DM, Garcia AJ. Surface chemistry modulates fibronectin conformation and directs integrin binding and specificity to control cell adhesion. Journal of Biomedical Materials Research Part A. 2003 Aug 1;66A(2):247-59.

[27] Rando TA, Blau HM. Primary mouse myoblast purification, characterization, and transplantation for cell-mediated gene therapy. J Cell Biol. 1994 June 1, 1994;125(6):1275-87.

[28] McCann CM, Bracamontes J, Steinbach JH, Sanes JR. The cholinergic antagonist {alpha}-bungarotoxin also binds and blocks a subset of GABA receptors. PNAS. 2006 March 28, 2006;103(13):5149-54.

[29] Charest JL, Eliason MT, Garcia AJ, King WP. Combined microscale mechanical topography and chemical patterns on polymer cell culture substrates. Biomaterials. 2006;27(11):2487.

[30] Nelson CM, Pirone DM, Tan JL, Chen CS. Vascular Endothelial-Cadherin Regulates Cytoskeletal Tension, Cell Spreading, and Focal Adhesions by Stimulating RhoA. Mol Biol Cell. 2004 June 1, 2004;15(6):2943-53.

[31] McBeath R, Chen CS. Regulation of human mesenchymal stem cell differentiation by cell adhesion. Molecular Biology of the Cell. 2002 Nov;13:121A-A.

[32] Diehl KA, Foley JD, Nealey PF, Murphy CJ. Nanoscale topography modulates corneal epithelial cell migration. Journal of Biomedical Materials Research A. 2005 December 1, 2005;75(3):603-11.

[33] Evans DJR, Britland S, Wigmore PM. Differential response of fetal and neonatal myoblasts to topographical guidance cues in vitro. Development Genes Evolution. 1999;209:438-42.

[34] Clark P, Connolly P, Curtis AS, Dow JA, Wilkinson CD. Topographical control of cell behaviour. I. Simple step cues. Development. 1987 March 1, 1987;99(3):439-48.

[35] Hamilton DW, Brunette DM. "Gap guidance" of fibroblasts and epithelial cells by discontinuous edged surfaces. Experimental Cell Research. 2005;309(2):429-37.

[36] Parker KK, Brock AL, Brangwynne C, Mannix RJ, Wang N, Ostuni E, et al. Directional control of lamellipodia extension by constraining cell shape and orienting cell tractional forces. FASEB J. 2002 August 1, 2002;16(10):1195-204.

[37] Dike LE, Chen CS, Mrksich M, Tien J, Whitesides GM, Ingber DE. Geometric Control of Switching Between Growth, Apoptosis, and Differentiation during Angiogenesis using Micropatterned Substrates. In Vitro Cell Developmental Biology - Animal. 1999;35:441-8.

[38] Gallant ND, Michael KE, Garcia AJ. Cell Adhesion Strengthening: Contributions of Adhesive Area, Integrin Binding, and Focal Adhesion Assembly. Mol Biol Cell. 2005 September 1, 2005;16(9):4329-40.

[39] Sabourin LA, Rudnicki MA. The molecular regulation of myogenesis. Clinical Genetics. 2000;57:16-25.

[40] Yaffe D, Saxel O. Serial passaging and differentiation of myogenic cells isolated from dystrophic mouse muscle. 1977;270(5639):725-7.

[41] Blau HM, Webster C. Isolation and characterization of human muscle cells. Proceedings of the National Academy of Science. 1981;78:5623-7.

CHAPTER 7

THE INFLUENCE OF CHEMICAL SURFACE PATTERNING ON KERATINOCYTE CELL-CELL CONTACT AND DIFFERENTIATION

This chapter analyzes the differentiation of primary human keratinocytes cultured on chemically micropatterned substrates. The substrates provide a model environment to evaluate the effect of cell-cell contact on keratinocyte expression of the differentiation marker involucrin. In addition, the micropatterned substrates provide control of the cell-material interface and show potential to regulate the quantity of cell-cell contact to discrete, user-defined levels. The substrate presented "bowtie"-shaped micropatterns with available cell-spreading areas of 75-1600 μm^2 and discrete levels of intended cell-cell contact of low contact, high contact, and no contact. Keratinocytes cultured on the bowtie patterns exhibited localization of E-cadherin at the cell-cell interface, with discrete interface length controlled by bowtie pattern dimensions for well spread cells. The fraction of involucrin expressing keratinocytes was significantly higher for cells cultured on patterns permitting contact as compared to those on patterns that prevented cell-cell contact. Available cell spreading area did not significantly alter keratinocyte expression of involucrin.

7.1 Introduction

Interfaces between cells and their surroundings, including extra-cellular matrix (ECM), biomaterial surfaces, and other cells, serve as a complex communication network influencing cellular fate [1, 2] and host response to biomaterials [3]. Chemical patterning of the cell-material interface provides means to control cellular interactions with its surroundings. Chemical surface patterning has regulated cell-material interactions thereby impacting cellular alignment to material features [4], cell adhesion strength [5], and differentiation [6]. Recently, chemical patterning of the cell-material interface has controlled cell-cell interaction through precise isolation of cell pairs and restriction of cell spreading area, resulting in changes to focal adhesion formation [7] and proliferation [8]. Control of cell-cell contact through chemical patterning may influence differentiation, although this area remains as yet unexplored.

Epidermal keratinocytes provide a well-characterized cell model where differentiated cells develop cell-cell junctions [9], suggesting that cell-cell contact plays an inherent role in the differentiation process. Keratinocytes form cell-cell adherens junctions through various transmembrane proteins including those of the classical cadherin family such as E-cadherin and P-cadherin. Keratinocytes lacking E-cadherin, a common cell-cell junction protein, exhibited down-regulated markers of differentiation *in vivo* [10]. Inhibition of both E-cadherin and P-cadherin with antibodies resulted in reduction of differentiation markers *in vitro*, however inhibition of only E-cadherin increased some differentiation markers [11], indicating that the influence of cell-cell contact on differentiation may involve multiple junction proteins requiring a broader

inhibition of contact mechanisms to attenuate differentiation. Keratinocytes expressed increasing levels of differentiation markers as a function of increasing cell-cell contact due to the cells reaching confluency [12]. Since both cell-cell contact and cell density increase with confluency, these differentiation results may arise from a combination of the two parameters. Chemical patterning to regulate cell-cell contact could be used to decouple the effects of cell density and cell-cell contact, while providing broad inhibition of cell-cell interaction.

Differentiation of keratinocytes is marked by upregulation of various proteins including involucrin. Involucrin is an envelope protein deposited on the inner surface of the plasma membrane by epidermal keratinocytes as they progress from the basal to the spinous layer [13]. Keratinocytes have expressed involucrin *in vitro* after 16 hours in differentiation conditions [14], indicating that it can serve as an early marker of differentiation. In addition, involucrin is associated with epidermal cells exiting the cell cycle and entering a terminal differentiation state [15]. Keratin 10 serves as another marker of keratinocyte differentiation. Keratin 10 is a protein that forms intermediate filaments and is expressed by epidermal cells in the suprabasal layer during differentiation [16].

This chapter investigates the effects of cell-cell contact on keratinocyte expression of involucrin and keratin 10 by employing a micropatterned cell substrate as an *in vitro* model environment. Micro-contact printed bowtie-shaped islands coordinate cell location to regulate cell-cell contact while preserving consistent cell density. In addition, available cell-spreading area is controlled to maintain a consistent cell-material interface thereby decoupling the effects of cell-material and cell-cell interactions.

7.2 Materials and Methods

7.2.1 Micro-contact printing of substrates

Cell substrates consisted of 0.5 mm thick polycarbonate samples, embossed with a polished silicon wafer to ensure consistent roughness, and coated in 10 nm of titanium and 20 nm of gold. Micro-contact printing (μCP) [17] was applied to pattern microscale bowtie-shaped chemical domains onto the substrate surface using polydimethylsiloxane (PDMS) stamps (Figure 7.1). The PDMS stamps were made by pouring Sylgard 184 and 186 in a 5:1 ratio into microfabricated molds, purging air in a vacuum, and curing according to the manufacturer's specifications. Before μCP, PDMS stamps were cleaned by sonicating in 70% ethanol and drying under nitrogen. Stamps were swabbed with hexadecanethiol (HDT), dried under nitrogen, and pressed onto the gold-coated substrate under a 50 g mass. Remaining bare gold areas were derivatized with a tri(ethylene glycol)-terminated alkanethiol (EG3-thiol) for 4 hours. Samples were sequentially rinsed 3 times each in 95% ethanol, sterile deionized water, and phosphate buffered saline (PBS). The substrates were incubated in 10 μg/mL fibronectin-like protein polymer (F-5022, Sigma-Aldrich) for 15 minutes to promote cell adhesion, incubated in PBS overnight, then rinsed 3 times in PBS immediately before seeding. The resulting substrate had μCP areas of HDT monolayers coated in fibronectin-like polymer, while the remaining areas were covered in EG3-thiol monolayers which prevent protein

adsorption and hence remained resistant to cell adhesion. To characterize the printing process, bowtie patterns were μCP as above, then coated in 20 μg/ml fibronectin for 30 minutes and rinsed in PBS. Fibronectin coated samples were then fixed in 3.7% Para formaldehyde, sequentially incubated in rabbit polyclonal anti-fibronectin (Sigma-Aldrich) and AlexaFluor 488-conjugated anti-rabbit IgG antibody (Invitrogen Corporation).

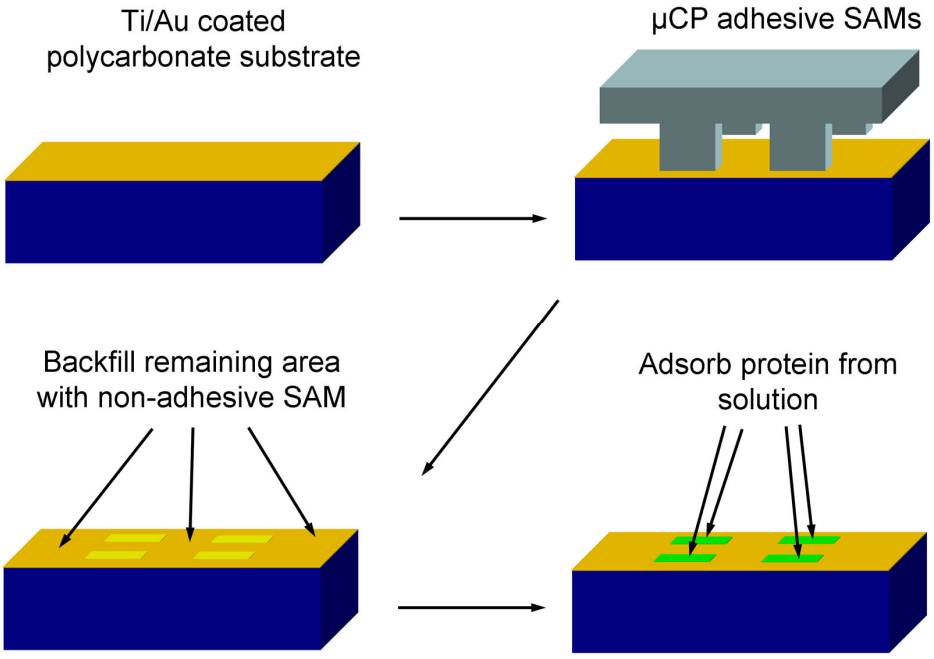

Figure 7.1 Cell substrate fabrication. Smooth polycarbonate samples were coated in 10 nm Ti and 20 nm Au followed by μCP of bowtie-shaped adhesive areas with adhesive methyl-terminated SAMs. Remaining areas were backfilled with non-adhesive tri(ethylene glycol)-terminated SAMs. Subsequent adsorption of protein from solution resulted in protein-coated bowtie patterns surrounded by non-adhesive spaces.

7.2.2 Cell Culture

Normal human keratinocytes (NHKs) isolated from neonatal foreskin (Emory Skin Disease Research Center) were cultured in keratinocyte growth medium (KGM, Cambrex Corp., East Rutherford, NJ). Keratinocytes at passage 4 or less were seeded in KGM media with 0.05 mM calcium (low calcium) onto the patterned substrates at 140

cells/mm^2. After 24 hours of culture, media was switched to KGM media containing 0.5 mM calcium (high calcium) to induce differentiation. Samples were cultured for 48 hours in high calcium KGM media before analysis.

7.2.3 Cell Fixation and Staining

After the appropriate culture time, cells were fixed either for Immunofluoresence microscopy (IF) or scanning electron microscopy (SEM). For IF, samples were rinsed twice in cold PBS, incubated in cold methanol for 20 minutes, and allowed to air dry. To stain cell-cell junctions, samples were sequentially incubated in mouse IgG2a anti-E-cadherin antibody (BD Transduction Laboratories) for 1 hour and AlexaFluor 488-conjugated anti-mouse IgG antibody (Invitrogen Corporation). To stain for the markers of differentiation, involucrin and keratin 10, samples were incubated in either rabbit anti-involucrin H-120 (Santa Cruz Biotechnology, Santa Cruz, CA) or mouse anti-keratin 10 Ab-2 (Lab Vision Corporation, Fremont, CA), and subsequently incubated in either AlexaFluor 488-conjugated anti-mouse IgG antibody or AlexaFluor 594-conjugated anti-rabbit IgG antibody (Invitrogen Corporation). All IF samples were counterstained with Hoechst DNA stain for 1 hour, rinsed, and then mounted to slides. A Nikon E600 epifluorescence microscope equipped with a Spot RT low light camera and ImagePro was used to collect and analyze all IF cell images.

For scanning electron microscopy, samples were rinsed in cold PBS, fixed in 2.5% gluteraldehyde in PBS for 30 min, then dried in graded ethanol solutions of 70%, 90%, and 100% twice each for 15 minutes. Samples were then immersed in HMDS

twice for 30 minutes, and allowed to dry overnight before sputter-coating with gold. Samples were examined in a LEO 1530 scanning electron microscope.

7.2.4 Image analysis and statistics

To quantify the fraction of differentiated cells, substrates were examined through IF. Patterns were scored only if proper patterning occurred, with once cell localized to each half of the bowtie pattern. The fraction of cells expressing a particular marker protein was calculated for each of 5 samples. Averages were compared with Tukey HSD using SYSTAT software.

7.3 Results

7.3.1 Chemical bowtie pattern substrate

The resulting bowtie substrate stamp presented 15 distinct fields, each with several hundred replicates of a given bowtie pattern. Figure 7.2 shows the layout of the bowtie stamp and examples of the pattern types. The surface area of one half of a bowtie pattern was 75, 100, 625, 900, or 1600 μm^2. The bowtie pattern was designed to permit one cell to attach to each half of the bowtie, with the cells spreading towards each other and forming a cell-cell contact interface at the narrow section of the bowtie. For each given surface area the halves of the bowtie pattern were configured to promote 3 levels of cell-cell contact. *Low contact* bowties possessed a narrow contact area between the two halves, *high contact* bowties possessed a contact area over twice the width of the low contact area, and bowties with *no contact* had each half separated by a distance of 35 μm.

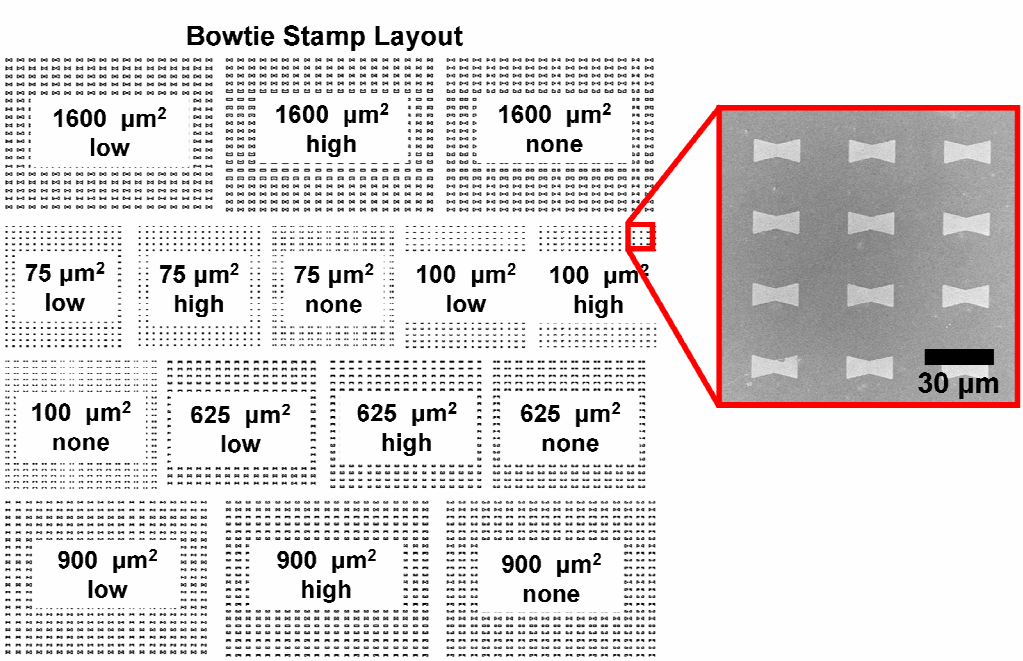

Figure 7.2 Layout of bowtie stamp shows distinct fields of bowtie patterns with half-bowtie areas and contact levels indicated. Inset image is a printed and etched substrate to show fidelity and shape of the bowtie patterns.

Pattern transfer from PDMS stamp to substrate resulted in good fidelity of features and accurate replication of the patterns. Figure 7.3 shows samples of fields within the stamp and corresponding features printed by them. Each half of the bowtie provided an area for a single cell to spread, where the non-adhesive spaces in between suppressed protein and cell adhesion in order to restrict cells to the patterns.

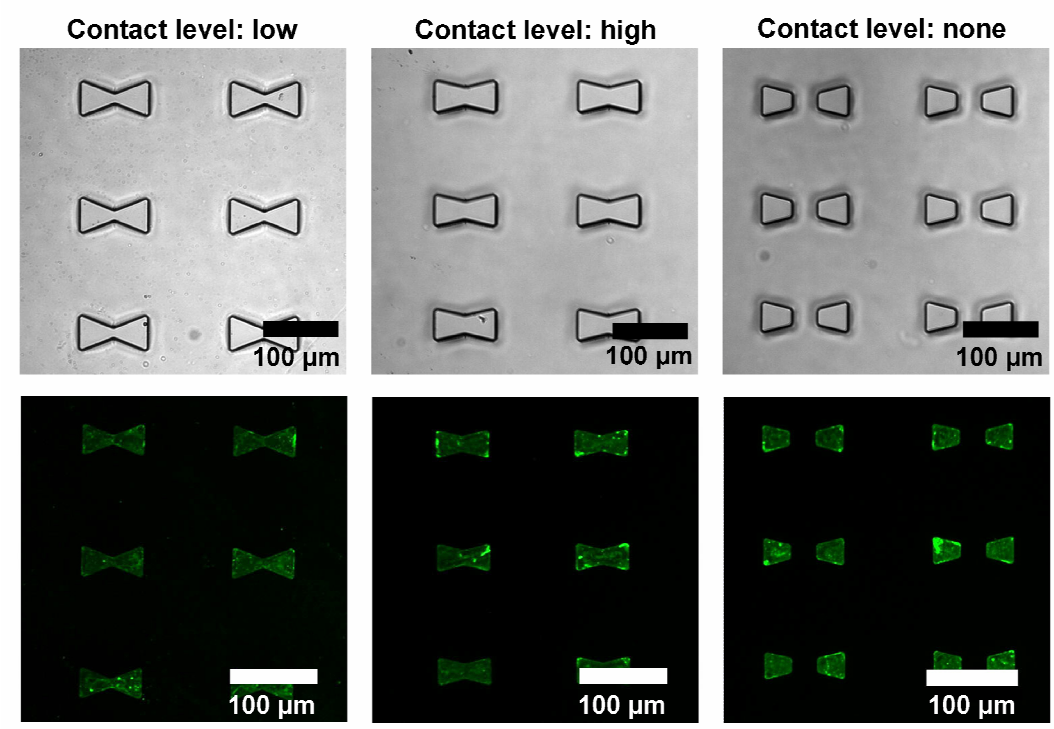

Figure 7.3 Top: PDMS stamps possessed raised bowtie patterns with discrete levels of contact and a range of half-bowtie surface areas 75-1600 µm^2. Bottom: Green IF-stained fibronectin indicates the printed areas on the substrate where protein readily adsorbs. Dark spaces of ethylene glycol SAMs in between patterns do not adsorb significant amounts of protein.

7.3.2 Bowtie pattern influence of cell-cell contact

Optimization of cell seeding density was performed in order to attain the maximum number of properly populated patterns. Patterns with only one cell adherent to each half of the bowtie were considered properly populated. Replicates of the bowtie substrate were each seeded at a different cell density. Low densities resulted in few of the patterns populated with cells, with the number of cells per pattern increasing with seeding density. Proper population of patterns was also a function of pattern size, as larger patterns required lower seeding densities to prevent overpopulation of the patterns. The optimal seeding density resulted in the properly populated patterns of 75, 100, and 625 µm^2.

In general, cell adhesion was restricted to bowtie patterns with very few cells bridging the non-adhesive domains. Patterns with half-bowtie areas of 75, 100, and 625 μm^2 often possessed only one adherent cell on each half, while the larger patterns of 900 and 1600 μm^2 often had more than one cell on each half of the bowtie.

E-cadherin staining demonstrated localized concentration of this junction protein at the cell-cell contact region. Figure 7.4 shows cells cultured on bowtie patterns, as well as a control sample consisting of a confluent layer of keratinocytes cultured on unpatterned protein, stained for E-cadherin and nuclei. Bowtie patterns designed for no contact prevented any cell-cell contact between cells while both low and high contact patterns permitted cell-cell junctions to form. In this way, the bowtie patterns controlled cell-cell contact to configurations of either absence or presence of contact. Control sample keratinocytes possessed cell-cell interfaces typical of keratinocytes cultured in high-calcium media [18], whereas keratinocytes on bowtie patterns possessed cell-cell interfaces localized between the two cells.

A fraction of bowtie patterns displayed discrete levels of cell-cell contact dependent on pattern size. For 75 and 100 μm^2 patterns, cells displayed clear interfaces as indicated by the E-cadherin staining in Figure 7.4, but the interfaces varied in length and shape, and the amount of cell-cell contact was not well-controlled. The patterns presenting areas greater than 625 μm^2 did provide discrete levels of control in cases where cells appeared well spread and possessed a flattened morphology. Several 625 μm^2 patterns possessed cells which formed a straight interface across the narrowest portion of the bowtie, thereby restricting the interface length to the width of the narrow portion of the bowtie. Figure 7.4 shows two examples where the cell-cell interface was

restricted to a low level of contact (lower left image) and high level of contact (lower center image). Although some 625 μm^2 patterns controlled cell-cell interfaces, others showed uncontrolled interfaces (lower right image) similar to those seen in the 75 and 100 μm^2 patterns.

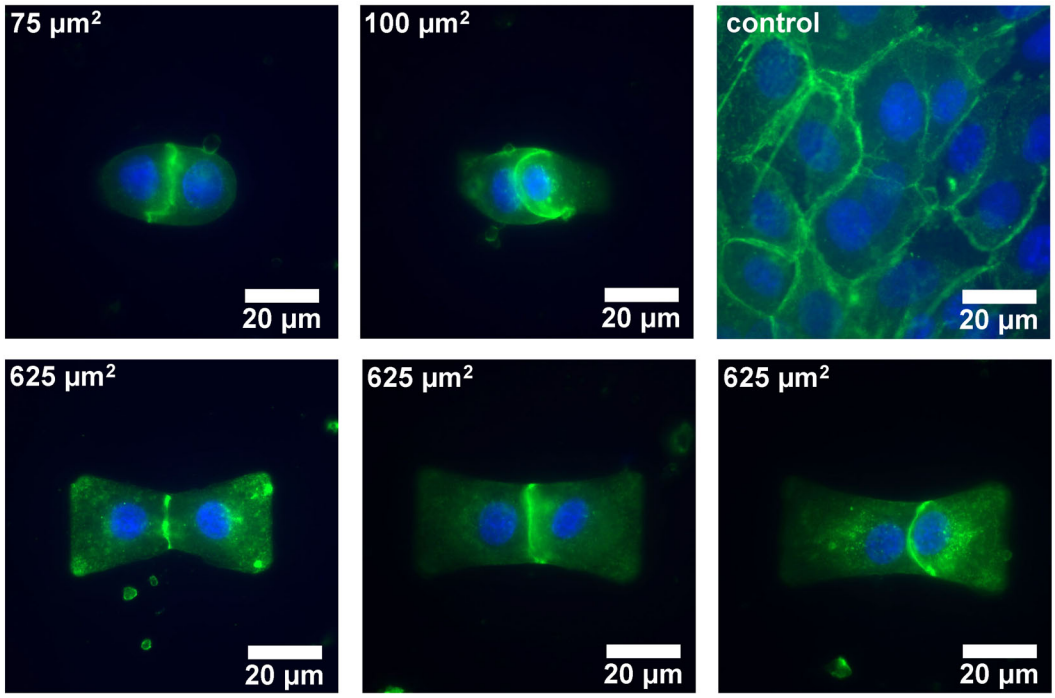

Figure 7.4 Keratinocytes stained for E-cadherin in green and counterstained blue. Both 75 and 100 μm^2 patterns resulted in clear cell-cell contact areas, with uncontrolled interfaces. The 625 μm^2 patterns also resulted in clear cell-cell contact areas, with some patterns exhibiting well-controlled cell interfaces for both low and high contact patterns, as well as uncontrolled interfaces.

Examination of 3-D cell morphology by SEM revealed rounded morphologies for cells adherent to bowtie patterns. Figure 7.5 shows SEM images of cells on bowtie patterns. Cells remained somewhat rounded on most patterns, with spherical morphologies found on no-contact bowtie patterns. On 75 and 100 μm^2 patterns, cells remained rounded in all cases observed with minimal flattening at the edges of the patterns. In contrast, cells on 625 μm^2 patterns had significant flattened areas at the edge of the patterns, and cells on 900 and 1600 μm^2 patterns often had completely flat and spread morphologies.

In general, rounded morphology and restricted spreading resulted in irregular cell-cell interfaces. Figure 7.5 shows samples of cell-cell interfaces which possessed a variety of morphologies including a straight interface region between the two cells in A and an angled interface region in B. Since the interface region protruded from the substrate, interface control via the chemical pattern was diminished resulting in irregular cell-cell interfaces. Patterns with areas greater than 625 μm^2 patterns promoted more cell spreading which reduce protrusion of the interface region from the substrate, resulting in increased control of the cell-cell interface by the chemical patterns. Cell protrusion was present on most 625 μm^2 patterns, and the resulting cell-cell interfaces were often irregular as shown by the arrow in C of Figure 7.5. However, a few well-spread cells on larger patterns appeared to have interfaces which did not protrude significantly from the substrate. The interfaces of the well-spread cells were limited in height to that of the flattened cell, and limited in width by the chemical patterning, resulting in a controlled amount of cell-cell contact.

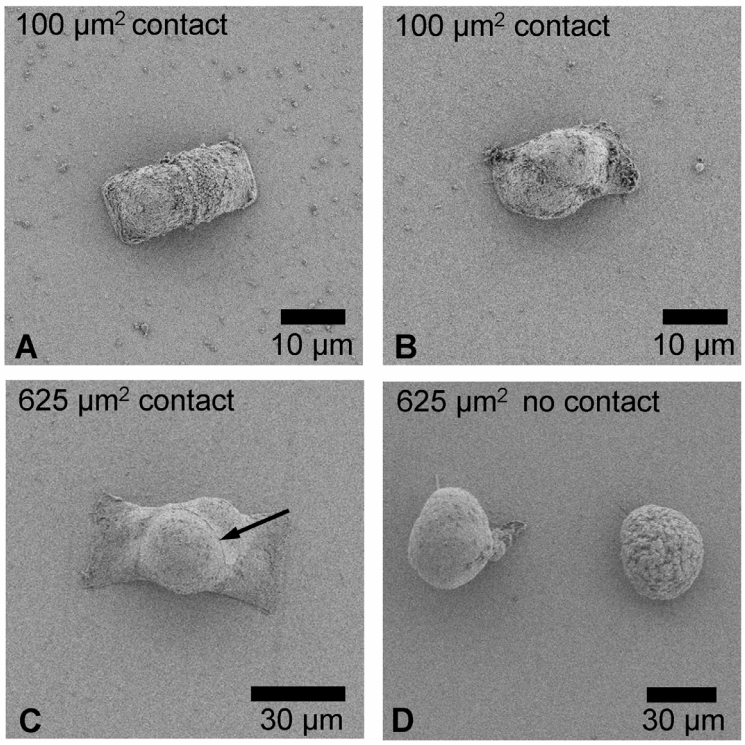

Figure 7.5 Cells displayed a rounded morphology on most patterns. On 75 and 100 μm^2 contact patterns, cells remained rounded with interfaces possessing a variety of morphologies including straight (upper left) and angled (upper right). Cells on 625 μm^2 patterns tended to flatten and spread more, although the interface area was often still rounded resulting in uncontrolled interfaces in some cases. Cells on patterns with no contact were typically spherical for most pattern sizes (lower right).

7.3.3 Cell-cell contact and expression of differentiation markers

The relative differentiation rates of patterned cells were observed through expression of the epidermal spinous layer differentiation markers involucrin and keratin 10. Figure 7.6 shows keratinocytes on bowtie patterns labeled for E-cadherin cell-cell junctions and involucrin. For cells in contact, nearly all cells exhibited E-cadherin localized to the cell-cell interface with a fraction of the cells simultaneously expressing involucrin. Figure 7.6 shows examples of patterns where both cells expressed involucrin as shown for the 100 μm^2 pattern, and where only one of the cells expressed involucrin as shown for the 625 μm^2 example. Although both scenarios were common for cells in

contact, expression of involucrin occurred in both cells more often than a single cell for all pattern sizes.

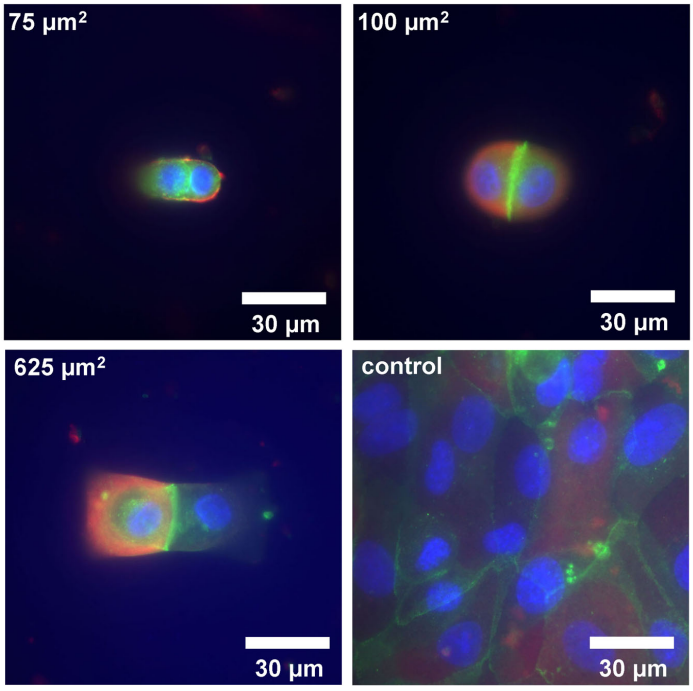

Figure 7.6 Keratinocytes IF-stained red for involucrin, green for E-cadherin, and blue for DNA. Cells simultaneously displayed concentrations of E-cadherin at the cell-cell interface and expressed involucrin.

To quantify the influence of the bowtie patterns on differentiation, staining was performed for both involucrin and keratin 10. Analysis of both marker proteins provided a clear signal, which enabled IF observation and evaluation of the fraction of cells expressing the markers. Figure 7.7 shows examples of cells on bowtie patterns labeled for involucrin, keratin 10, and nuclei for several pattern sizes. Since significant numbers of cells did not exhibit discrete levels of either *low contact* or *high contact*, patterned cells on both types of patterns were grouped into the *contact* category and compared to cells without any contact grouped in the *no-contact* category. A low fraction of keratinocytes expressed keratin 10 after 48 hours in differentiation conditions, thus it did not serve as a quantifiable indicator of differentiation. Involucrin appeared uniform

throughout a cell, as expected for the envelope protein [9] and was expressed by at least 25% of cells for all samples, pattern sizes, and shapes.

Involucrin expression was scored only for cells with one cell nuclei located on each half of the bowtie pattern to ensure cell-cell contact occurred between only two cells for patterns permitting contact and cell-cell contact was prevented for patterns with no contact. Patterns with areas larger than 625 μm^2 resulted in greater than 2 cells per pattern and were therefore not scored. Cells on the 75 and 100 μm^2 patterns appeared rounded, whereas cells on the 625 μm^2 patterns appeared more spread, confirming results of the SEM analysis. For the 3 pattern sizes, most cells appeared to spread to cover the available area, which would indicate regulation of cell-substrate contact area.

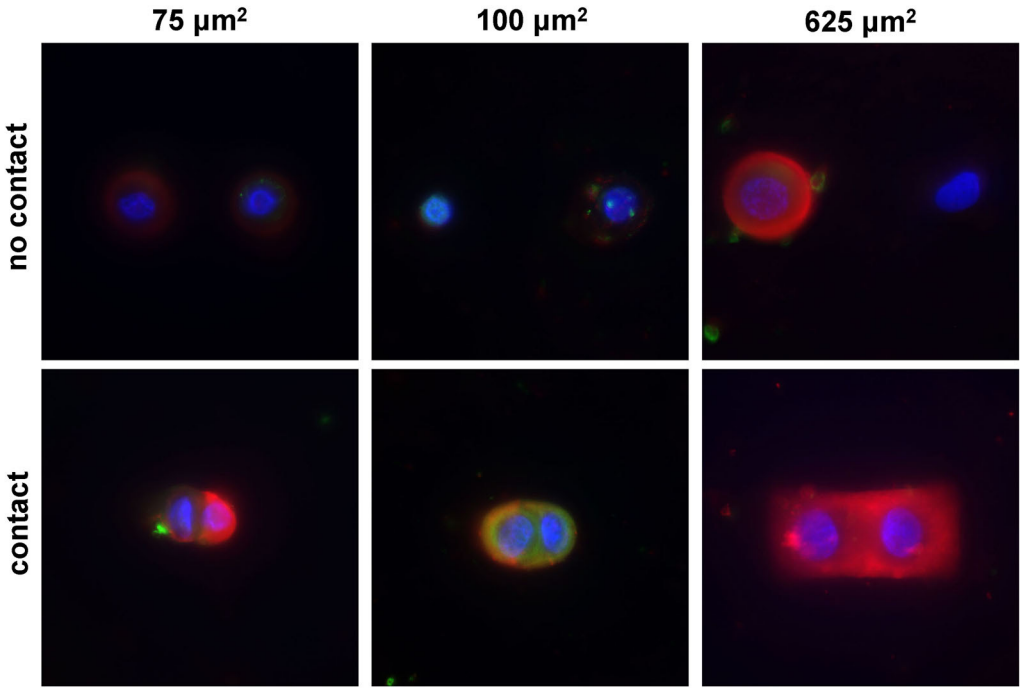

Figure 7.7 Keratinocytes immunolabeled red for involucrin, green for keratin 10, and blue for nuclei after 48 hour culture in differentiation conditions. Cells on 75 and 100 μm^2 patterns remained rounded in morphology, while cells on 625 μm^2 patterns spread and conformed to the pattern to a greater extent.

Patterns promoting contact resulted in a higher fraction of cells expressing involucrin. Figure 7.8 shows quantitative data comparing involucrin expression for cells

in contact and no-contact patterns for 3 pattern sizes. The fraction of cells expressing involucrin was significantly higher on patterns permitting cell-cell contact than on patterns preventing cell-cell contact for all pattern sizes. In contrast, pattern size did not significantly influence involucrin expression.

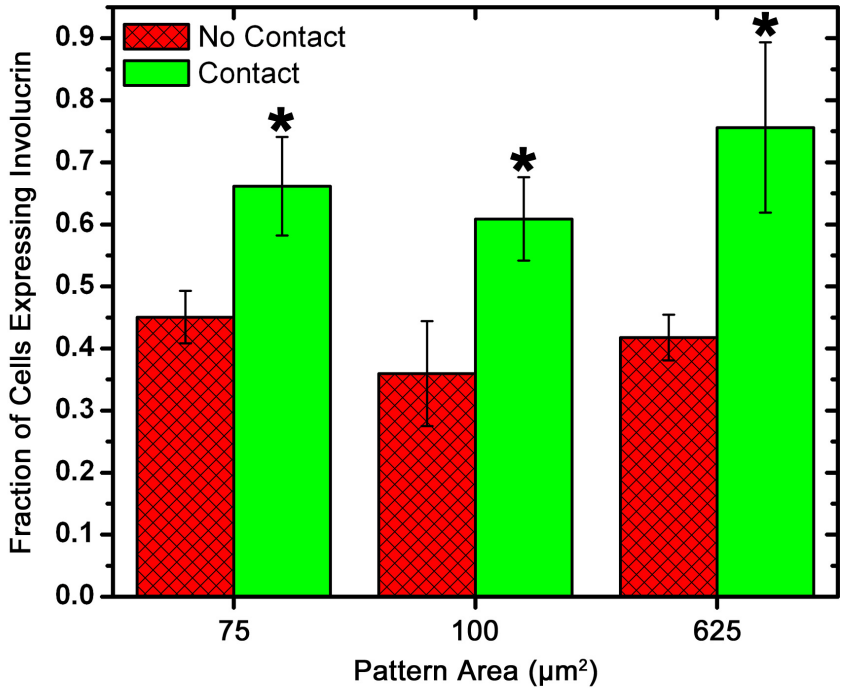

Figure 7.8 Cells on patterns permitting cell-cell contact express involucrin more often than cells on patterns preventing cell-cell contact. Data is from 5 replicates of the bowtie pattern substrate (means ± stdev, P <0.02, * contact vs. no contact within one pattern size).

7.4 Discussion

In this study, a micropatterned *in vitro* cell model regulating cell-cell contact and cell-material interaction shows a significant dependence of keratinocyte involucrin expression on micropattern configuration. Thus, the model provides a means to study

effects of cell-cell contact between isolated pairs of cells in a well-controlled environment.

This model provides a robust method to control the cell-material interface for cells isolated to the patterns by controlling available cell-spreading area and the adhesive molecule present at the cell-surface interface within the patterns. Patterns that restrict cell-spreading area alter quantity of bound integrins dependent on pattern size [5], which in turn has effects on cell function. Specifically, inhibition of keratinocyte terminal differentiation has resulted from binding of fibronectin to β1 integrins [19]. Here, cell spreading is restricted as indicated by the rounded morphology of cells adherent to the patterns. A rounded morphology results from restricted cell spreading [20], and indicates full occupation of the pattern by the cell. In this way, the pattern size determines the quantity of cell-material contact. In addition, the model patterns consisted of a layer of RGD adhesive motif-presenting protein-like polymer adsorbed to a controlled chemical model layer. The uniform model layer, in conjunction with the uniformly applied protein-like polymer, provides a chemical interface consistent across the various pattern sizes and shapes.

The micropatterns controlled cell-cell interfaces by either permitting or preventing cell-cell contact. Cells on both *low contact* and *high contact* patterns displayed distinct localization of E-cadherin between cells indicating a cell-cell functional interface. The *no-contact* patterns prevented all cell contact, with a distinct gap between cells devoid of any cellular extensions. Furthermore, the patterns showed potential to control the level of cell-cell contact on patterns where the cell-cell interface occupied the narrow portion of the bowtie as in the lower left images in Figure 7.1. In

this configuration, the width of the narrow portion of the bowtie served to limit the length of the cell-cell interface, thereby permitting a user to control interface lengths via bowtie pattern design. Localization of the cell-cell interface to the bowtie narrow region occurred for patterns with significantly spread cells. Cells spread significantly on patterns 625 μm^2 or larger, with very flat cell morphologies present on the 900 and 1600 μm^2 patterns. This dependence of cell spreading on pattern size could be exploited by optimizing pattern size for a given cell model to ensure patterns large enough to encourage spreading, yet small enough to discourage adhesion of more than two cells per bowtie. However, responses to patterns are cell-type specific, therefore characterization and evaluation is necessary for each particular cell model of interest.

For the various pattern sizes studied, keratinocyte differentiation as measured by involucrin expression did not depend on pattern size. This finding suggests that cell shape/morphology does not regulate early differentiation steps in this cell type. In contrast, cells have altered expression of differentiation markers dependent on pattern size [6] and corresponding cell shape resulting from modulation of pattern size [21]. Data from this study differs since pattern surface areas which ranged from 75-625 μm^2, where other studies used pattern surface areas which ranged from 1024-10000 μm^2 [6] and 400-10000 μm^2 [21]. In addition previous studies did not incorporate cell-cell contact as a factor, therefore cell-cell contact might have dominated influence of differentiation thereby masking effects of cell spreading area.

Effects of the cell-cell contact control via bowtie patterns may have had some influence on keratinocyte proliferation. Mammary epithelial cells have shown higher proliferation rates on patterns permitting cell-cell contact [8] and available cell spreading

area of patterns has shown significant influence on cell proliferation [22]. In this work, although influence of cell-cell contact on proliferation was not specifically studied, available cell spreading area was well-controlled in order to limit its effects on proliferation. However, media containing high calcium treatment, as used in this work, results in abrogation of cell proliferation of keratinocytes [23] indicating that cell proliferation was probably quite limited for cells used in this study. In addition, cells expressing involucrin are committed to differentiation and therefore not likely to proliferate [15], indicating that proliferation of involucrin positive cells was not likely to significantly confound the data presented here. Ongoing and future work will evaluate effects of the patterns on keratinocyte proliferation and apoptosis to specifically address this issue.

7.5 Conclusions

A cell substrate consisting of μCP domains of model chemistry coated in cell adhesive protein-like polymer provided an *in vitro* model system to study cell-cell contact effects on keratinocyte differentiation. The model system consisted of bowtie patterns that either permitted or prevented cell-cell contact in addition to providing controlled available cell spreading areas. In addition, the system showed potential to regulate the cell-cell interface to control the amount of cell-cell contact through user design of bowtie pattern dimensions. A study of primary human keratinocytes on the model substrates indicated influence of the patterns on differentiation. Higher fractions of cells expressed involucrin on patterns permitting contact as compared to cells on patterns which

prevented contact, independent of pattern size. These results show the ability to control both cell-material and cell-cell interactions through micropatterned cell-material interfaces, enabling further control of biologically influential parameters within an *in vitro* model.

7.6 Acknowledgements

The authors would like to thank Andrew P. Kowalczyk for gracious donation of keratinocytes and laboratory support and Jean Marie Jennings for assistance in keratinocyte culture.

7.7 References

[1] Keselowsky BG, Collard DM, Garcia AJ. Integrin binding specificity regulates biomaterial surface chemistry effects on cell differentiation. Proceedings of the National Academy of Science. 2005 April 26, 2005;102(17):5953-7.

[2] Allen LT, Fox EJP, Blute I, Kelly ZD, Rochev Y, Keenan AK, et al. Interaction of soft condensed materials with living cells: Phenotype/transcriptome correlations for the hydrophobic effect. Proceedings of the National Academy of Science. 2003 May 27, 2003;100(11):6331-6.

[3] Shen M, Pan YV, Wagner MS, Hauch KD, Castner DG, Ratner BD, et al. Inhibition of monocyte adhesion and fibrinogen adsorption on glow discharge plasma deposited tetraethylene glycol dimethyl ether. J Biomater Sci Polym Ed. 2001;12(9):961-78.

[4] Charest JL, Eliason MT, Garcia AJ, King WP. Combined microscale mechanical topography and chemical patterns on polymer cell culture substrates. Biomaterials. 2006;27(11):2487.

[5] Gallant ND, Michael KE, Garcia AJ. Cell Adhesion Strengthening: Contributions of Adhesive Area, Integrin Binding, and Focal Adhesion Assembly. Mol Biol Cell. 2005 September 1, 2005;16(9):4329-40.

[6] McBeath R, Pirone DM, Nelson CM, Bhadriraju K, Chen CS. Cell Shape, Cytoskeletal Tension, and RhoA Regulate Stem Cell Lineage Commitment. Developmental Cell. 2004;6(4):483-95.

[7] Nelson CM, Pirone DM, Tan JL, Chen CS. Vascular Endothelial-Cadherin Regulates Cytoskeletal Tension, Cell Spreading, and Focal Adhesions by Stimulating RhoA. Mol Biol Cell. 2004 June 1, 2004;15(6):2943-53.

[8] Liu WF, Nelson CM, Pirone DM, Chen CS. E-cadherin engagement stimulates proliferation via Rac1. J Cell Biol. 2006 May 8, 2006;173(3):431-41.

[9] Fuchs E. Epidermal Differentiation - The Bare Essentials. JCell Biol J1 - JCB. 1990 Dec;111(6):2807-14.

[10] Young P, Boussadia O, Halfter H, Grose R, Berger P, Leone DP, et al. E-cadherin controls adherens junctions in the epidermis and the renewal of hair follicles. EMBO J. 2003 Nov;22(21):5723-33.

[11] Hines MD, Jin HC, Wheelock MJ, Jensen PJ. Inhibition of cadherin function differentially affects markers of terminal differentiation in cultured human keratinocytes. Journal of Cell Science. 1999 Dec;112(24):4569-79.

[12] Kolly C, Suter MM, Muller EJ. Proliferation, cell cycle exit, and onset of terminal differentiation in cultured keratinocytes: Pre-programmed pathways in control of c-Myc and Notch1 prevail over extracellular calcium signals. Journal of Investigative Dermatology. 2005 May;124(5):1014-25.

[13] Rice RH, Green H. Presence in human epidermal cells of a soluble protein precursor of the cross-linked envelope activation of the cross-linking by calcium-ions. Cell. 1979;18(3):681-94.

[14] Kawabata H, Kawahara K, Kanekura T, Araya N, Daitoku H, Hatta M, et al. Possible role of transcriptional coactivator P/CAF and nuclear acetylation in calcium-induced keratinocyte differentiation. JBiolChem. 2002 Mar;277(10):8099-105.

[15] Watt FM. Selective migration of terminally differentiating cells from the basal layer of cultured human epidermis. J Cell Biol. 1984 January 1, 1984;98(1):16-21.

[16] Eichner R, Sun TT, Aebi U. The role of keratin subfamilies and keratin pairs in the formation of human epidermal intermediate filaments. J Cell Biol. 1986 May 1, 1986;102(5):1767-77.

[17] Singhvi R, Kumar A, Lopez GP, Stephanopoulos GN, Wang DIC, Whitesides GM, et al. Engineering Cell-Shape and Function. Science. 1994 Apr 29;264(5159):696-8.

[18] Le TL, Yap AS, Stow JL. Recycling of E-Cadherin: A Potential Mechanism for Regulating Cadherin Dynamics. J Cell Biol. 1999 July 12, 1999;146(1):219-32.

[19] Watt FM. Stem cell fate and patterning in mammalian epidermis. CurrOpinGenetDev. 2001 Aug;11(4):410-7.

[20] Gallant ND, Capadona JR, Frazier AB, Collard DM, Garcia AJ. Micropatterned surfaces for analyzing cell adhesion strengthening Langmuir. 2002 2002;18:5579-84.

[21] Thomas CH, Collier JH, Sfeir CS, Healy KE. Engineering gene expression and protein synthesis by modulation of nuclear shape. 2002 2002/02/19/;99(4):1972-7.

[22] Chen CS, Mrksich M, Huang S, Whitesides G, Ingber DE. Geometric control of cell life and death. 1997;276:1425-8.

[23] Tu CL, Chang WH, Bikle DD. The extracellular calcium-sensing receptor is required for calcium-induced differentiation in human keratinocytes. JBiolChem. 2001 Nov;276(44):41079-85.

CHAPTER 8

SUMMARY AND RECOMMENDATIONS

8.1 Summary

This work presented fabrication of topographically and chemically patterned cell substrates and characterization of cellular response to micro- and nano-patterned cell-material interfaces. This work furthers the understanding of the cell-surface interface by contributing high-throughput methods to independently pattern topography and chemistry, and establishing significant effects of micropatterned model environments on cell function.

To fabricate precise, repeatable topographic features on cell substrates, hot-embossing imprint lithography was used to create microscale topographical features in polymer in a high-throughput fashion. Hot-embossing improved upon previous cell substrate fabrication techniques by expanding material selection beyond glass, silicon, and polymers requiring curing. Embossed feature sizes on cell substrates ranged from 100 nm through 75 μm in a variety of pattern configurations and shapes. The study of osteoblasts cultured on the embossed topographic patterns indicated morphological cellular response including alignment and elongation of cell bodies, and alignment of nuclei, and focal adhesions.

The combination of hot-embossing and micro-contact printing resulted in a method to independently form topographical and chemical patterns on cell substrates, while avoiding cleanroom processing of the substrates. After embossing of the

topography, the substrates were coated in gold, then micro-contact printed (μCP) with a hexadecanethiol (HDT) monolayer and backfilled with ethylene glycol (EG_3) monolayers. The specific manner by which the patterning methods were combined enabled fibronectin lanes with geometries independent of the underlying topographical patterns. Thus, lanes 10 μm wide spaced by either 10, 20, 50, or 100 μm were printed orthogonally to the 8 μm wide grooves and 16 μm wide mesas. The resulting analysis of osteoblast alignment on the substrates provided insight into the relative influence of the patterning methods on cellular alignment. For all configurations analyzed, the grooves dominated the alignment mechanism. Although cells remained restricted to fibronectin lanes on a smooth substrate, when fibronectin lanes were presented simultaneously with orthogonal grooves cells often bridged up to 50 μm of non-adhesive spaces in order to align to the grooves. Substrates with fibronectin lanes orthogonal to the grooves did result in reduced alignment to the grooves as compared to a grooved substrate with no lanes.

In a similar fashion, either rows of 10 μm diameter fibronectin dots or 10 μm wide fibronectin lanes spaced by EG_3 monolayers, were printed orthogonally over a uniform topography of 100 nm wide ridges and grooves. In contrast to the previous study, osteoblasts aligned to the fibronectin lanes rather than the 100 nm grooves. Here the fibronectin lanes were continuous and of a much larger width than the grooves. When presented with the discontinuous 10 μm dot pattern overlaid onto the 100 nm grooves, the cells aligned to the grooves and extended beyond the dots into the non-adhesive areas. Thus, the relative influence of topography and chemical patterns on cellular alignment may depend on continuity of patterns and pattern feature size. The

combination of hot-embossing and micro-contact printing enables rapid fabrication of user-defined patterns to further characterize the relative influence of and interplay between the two pattern types for a given cell model.

Topographical patterns, used in conjunction with a chemical model layer, provided a model to examine the expression of a differentiation marker by and alignment of myoblasts in the presence of a wide variety of topographies. Hot-embossing topographically patterned a polycarbonate substrate with multiple fields of patterns. The patterns were uniform within each field, but varied across the substrate and consisted of 5-75 μm diameter holes and 5-75 μm wide grooves. The substrate was coated in gold, derivatized with a HDT monolayer, and coated in fibronectin to present a characterized chemistry to adherent cells. Primary and C2C12 myoblasts aligned to grooves in a groove-width dependent manner, while significant alignment did not occur on the patterns of holes or a smooth control pattern. None of the patterns modulated cell density or expression of the differentiation marker sarcomeric myosin. This model improves upon studies of cell differentiation on topography as the chemical model layer ensures a characterized chemical interface applied independently of the topographical patterns.

Finally, patterning the cell-surface interface was used to control cell-cell contact. Micro-contact printing generated adhesive bowtie-shaped patterns spaced by EG_3 monolayers on a smooth substrate. Keratinocytes adhered to the bowties in pairs on patterns with surface areas of 75, 100, and 625 μm^2, with developed cell-cell contact areas between them as indicated by E-cadherin staining. For well-spread cells, the cell-cell interface often occurred at the narrow part of the bowtie pattern and was thus regulated by the pattern geometry. For most cells, a lack of spreading led to a rounded

morphology and a consequently irregular cell-cell interface. Cells appeared to occupy the entire surface area of the patterns, indicating that the cell-material contact area was well-controlled by the patterns. Patterns permitting cell-cell contact resulted in a higher fraction of involucrin expressing cells than patterns preventing cell-cell contact, independent of surface area of the patterns. The bowtie pattern model showed potential to regulate cell-cell contact to discrete levels, and would provide a method to modulate cell-cell contact while presenting consistent cell-spreading area and cell density.

Cell-surface interface patterning techniques presented here have enabled rapid fabrication of topography, controlled topography independently of chemistry and chemical patterns, and shown potential to regulate cell-cell interfaces with significant influence on cellular function.

8.2 Future Recommendations

This work presents development and application of advanced fabrication techniques to pattern cell-surface interfaces with demonstrated significant influence on cellular function. The techniques control both topographical and chemical features independently to provide a user-definable model interface for study of cellular function. Future study of cellular function in vitro will require additional development of the combined topographical and chemical patterning process and increased functionality of the substrates.

8.2.1 Development of combined topographical and chemical patterning

Two areas of development provide opportunities to refine combined topographical and chemical patterning of cell substrates. First, the ability of the μCP stamp to contact and successfully pattern recessed topography is limited. Modeling of elastomeric stamp deformation predicts print quality as a function of stamp parameters for flat substrates [1], however the added complexity of stamp deformation to a topographically patterned substrate is yet to be examined. The modeling of stamp deformation to topographical features would provide a guide to develop successful patterning parameters. Since sub-100 nm topographical features may be desirable for cell culture substrates, modeling must include the behavior of elastomeric materials and their ability to conform to the topography in the nanoscale regime. The modeling may discover practical and fundamental limits for continuous chemical patterning over topography. Second, applying a uniform coating of protein over topographic patterns may be limited as recessed feature sizes approach those of protein molecules. Understanding protein solution wetting to micro- and nano-scale features would provide insight into the feasibility of protein adsorption to complex topographic surfaces.

8.2.2 Increased functionality of patterned substrates

Increased functionality of the substrates would improve analysis throughput and provide opportunities to not only observe but control or trigger higher-order cell-surface interactions. Substrates with a high percentage of successful cell-pattern attachment would improve analysis throughput by assuring a suitable population of cells for analysis

on each substrate. To increase the yield of the cell-pattern attachment, dielectrophoretic retention could be employed to guide cells to patterns. Trapping potentials of 5V or less have successfully trapped single cells without significantly impacting cell health [2]. This could not only improve the yield of simple patterning, but enable complicated patterning strategies where multiple cells or cell types are positioned precisely on one pattern.

Increased functionality of substrates can also lead to higher-order cell-surface interactions. Substrate design can incorporate specific probes co-located with chemical or topographical patterns that encourage cell attachment. Probe interaction could be electrical, chemical, or mechanical in order to characterize cellular response to various stimuli. Electrical stimulation could trigger response of muscle or nerve cell for observation, while electrical sensing would permit feedback of cell response to other stimuli. Local delivery of treatments or analysis reagents to specific cells via microfluidic channels would provide a means to perform multiple assays within one substrate. Mechanical sensing could be performed with a piezoresistive flexible substrate chemically patterned to isolate cell attachment.

8.3 References

[1] Sharp KG, Blackman GS, Glassmaker NJ, Jagota A, Hui CY. Effect of stamp deformation on the quality of microcontact printing: Theory and experiment. Langmuir. 2004 Jul;20(15):6430-8.

[2] Gray DS, Tan JL, Voldman J, Chen CS. Dielectrophoretic registration of living cells to a microelectrode array. Biosensors and Bioelectronics. 2004;19(12):1765-74.